In Situ Structure and Function Analysis
of Nitrifying/Denitrifying Biofilms

Dissertation

zur Erlangung des Grades eines

Doktors der Naturwissenschaften

- Dr. rer. nat. -

dem Fachbereich Biologie/Chemie der

Universität Bremen

vorgelegt von

Andreas Schramm

Bremen

Dezember 1998

Die vorliegende Arbeit wurde in der Zeit von Januar 1996 bis Dezember 1998
am Lehrstuhl für Mikrobiologie der Technischen Universität München
und am Max-Planck-Institut für Marine Mikrobiologie in Bremen angefertigt.

1. Gutachter: Prof. Dr. Bo Barker Jørgensen
2. Gutachter: Priv.-Doz. Dr. Rudolf Amann

Tag des Promotionskolloquiums:　17. 12. 1998

für Doris und Anne

VORWORT

Die vorliegende Dissertation befaßt sich mit Untersuchungen zur Nitrifikation in Biofilmen sowie zur Denitrifikation in Belebtschlammflocken. Beide Systeme werden häufig in der Abwasserreinigung eingesetzt. Neue Einblicke in ihre Strukturen und Funktionen - so das Ziel dieser mehr auf Grundlagenforschung ausgerichteten Arbeit - sollten zu einem besseren Verständnis der an der Stickstoffentfernung beteiligten Prozesse beitragen, was langfristig auch zu einer stabileren und effizienteren Abwasserreinigung führen könnte.

Die Ergebnisse des experimentellen Teiles wurden in sechs englischsprachigen Manuskripten zusammengefaßt (Chapter 2-7). Die ersten drei sind bereits in einer internationalen Fachzeitschrift veröffentlicht, ein weiteres ist eingereicht, und die beiden letzten werden zur Publikation vorbereitet. Der Zusammenhang der Einzelteile und ihr Bezug zum Hauptthema wird in der Einleitung (Chapter 1) und in der Zusammenfassung deutlich gemacht, erschließt sich aber auch (so hoffe ich) beim Lesen der einzelnen Artikel.

Ganz herzlich möchte ich mich bei Rudi Amann bedanken, der diese Arbeit ermöglichte und betreute, mir alle Freiheiten ließ und stets für anregende Diskussionen zur Verfügung stand. Bo Barker Jørgensen danke ich für die Übernahme des Erstgutachtens und für alle Unterstützung am MPI Bremen. Karl-Heinz Schleifer und Niels Peter Revsbech brachten mich - noch zu Zeiten der Diplomarbeit - auf den wissenschaftlichen Weg, und Michi Wagner bzw. Lars Hauer Larsen, Niels B. Ramsing und Lars B.Pedersen zeigten mir erste methodische Schritte und weckten die Begeisterung für Mikroben und Mikrosensoren. Ihnen allen herzlichen Dank! Einen besonderen Anteil an dieser Arbeit hatte Dirk de Beer mit seinem Know-how über Biofilme und LIX-Elektroden (die mir so manche schlaflose Nacht brachten und teilweise den letzten Nerv raubten: „Tu NIX mit LIX!"). Er war immer wieder mit neuen Ideen, Anregungen und tatkräftiger Unterstützung an den verschiedensten Projekten beteiligt.

Für angenehme und ertragreiche Aufenthalte an der Universität Aarhus (Dept. of Microbial Ecology), der Universität Amsterdam (Dept. of Chemical Engineering) und am Prague Institute of Chemical Technology (Dept. of Water Technology and Environmental Engineering) danke ich ganz herzlich Niels Peter Revsbech, Simon Ottengraf und Jiri Wanner, sowie allen Mitarbeitern an den dortigen Instituten. Außerdem möchte ich mich bei all meinen Co-Autoren für die hervorragende Zusammenarbeit bedanken.
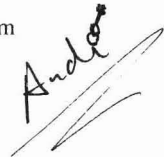
CONTENTS

Chapter 1

GENERAL INTRODUCTION

In Situ Structure and Function Analysis of Biofilms
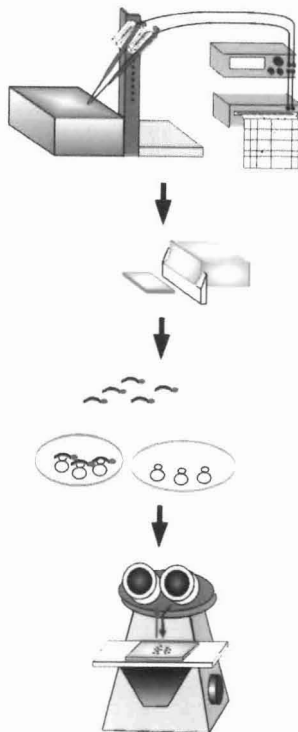
1

Front page:

Flow chart of "*In situ* structure and function analysis of biofilms". Individual steps are: microsensor measurements, cryosectioning of the fixed, embedded biofilm, fluorescence *in situ* hybridization (FISH) with oligonucleotide probes, and microscopic detection of the respective microorganisms. Figure by Niels B. Ramsing and A. Schramm

In Situ Structure and Function Analysis of Biofilms

Dipl.-Biol. Andreas Schramm, Priv.-Doz. Dr. Rudolf Amann

Nachwuchsgruppe Molekulare Ökologie
Max-Planck-Institut für Marine Mikrobiologie
Celsiusstrasse 1
28359 Bremen

Abstract

In situ structure and function analyses are prerequisites for both understanding the complex network of microbial populations and processes inside biofilms, and manipulating the structure and function of biofilm reactors. Modern microbial ecology can provide the tools for such investigations: Microsensors are minimally invasive instruments to measure gradients of many important metabolites and parameters with high spatial resolution. The gradients can also be used to evaluate the zonation and rates of the measured processes. Fluorescence *in situ* hybridization with rRNA-targeted oligonucleotide probes allows the identification, localization, and quantification of microorganisms directly in the biofilm. Furthermore, the application of the rRNA approach can circumvent the bias inherent in cultivation dependent studies, and therefore lead to a more realistic picture of the composition of a microbial community. The combined application of these two *in situ* techniques bears great potential for new and exciting insights into the structure and function of biofilms.

1   Introduction

What can microbial ecology offer to the study of biotechnological processes such as biological wastewater treatment? The function of a wastewater treatment plant is determined by the activities and interactions of its microbial community. Thus, as engineers try to adjust process parameters in order to optimize a plant, microbial ecologists may assist in providing information on the identity of microorganisms responsible for specific activities, on interactions between cells of the same or different populations, and in analyzing the influence of changing environmental conditions. In the long run, reactors could by this interdisciplinary approach be designed specifically to meet the requirements of the targeted microbial community.

However, the ecological investigation of those complex ecosystems such as activated sludge or biofilms is still in its infancy. Classical approaches, e.g., the isolation of microorganisms or physico-chemical bulk measurements usually do not lead to a comprehensive picture of the microbial community nor can they resolve coupled processes in flocs, aggregates, or biofilms. These habitats are highly stratified systems with steep physico-chemical gradients and organisms adapted to sequential transformations along those gradients. Therefore, sophisticated *in situ* techniques are necessary to identify microorganisms and measure activities at the place of their occurrence or, in other words, to analyze structure and function of biofilms on a microscale.

2   Biofilms

Biofilms are defined as surface attached accumulations of microbial cells encased in extracellular polymeric substances (EPS) [5]. In nature, they can be found at almost any surface exposed to water, ranging in thickness between a few cell layers to a few centimeters. In many aquatic systems the majority of microbial conversions takes place in biofilms covering sediments, rocks, or plants [13]. In biotechnology, biofilm reactors are increasingly used for wastewater treatment and bioremediation processes, or by the pharmaceutical and fermentation industry. Biofilm reactors are advantageous for some processes because the biomass is immobilized and thus retained in the reactor. Thereby, relatively high concentrations of biomass can be achieved even of microorganisms with low specific growth rates, like methanogens or nitrifiers.

2.1   Biofilm structure

The compartments of biofilm systems are the biofilm that colonizes a surface (the substratum), the diffusion boundary layer, and the bulk liquid. The bottom part of the biofilm is usually an uniform, dense base film, which is firmly adhered to the substratum by EPS; it is often covered with a more heterogeneous, fluffy surface film, consisting of cell clusters, EPS, and interstitial voids in contact with the bulk liquid [18], [42], [64]. Occasionally, streamers protrude into the bulk liquid and move in the flow. Whether the biofilm structure is dominated by the homogeneous base film (Fig. 1A), cell clusters and voids (Fig. 1B), or streamers, may be determined by factors like growth rate [68], substrate concentration [72], shear stress [69], grazing, and cell surface properties [13].
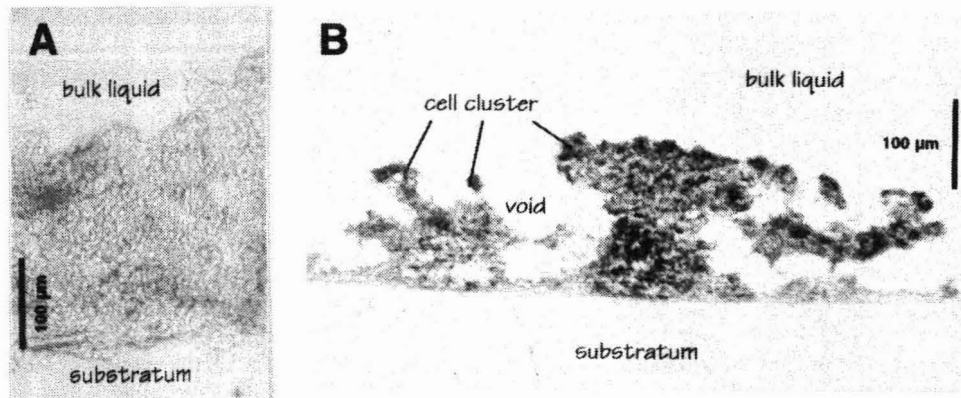
Fig.1.   Physical structure (A) of a compact nitrifying biofilm and (B) of an aerobic, heterotrophic biofilm. Note the voids between the cell clusters.

In addition to its physical structure, the community structure of biofilms is of special interest. This encompasses the composition of the microbial community and its spatial arrangements, which both determine cell to cell interactions that might largely modulate the physiological properties of a biofilm.

2.2   Biofilm function

The physical structure of a biofilm directly determines its transport mechanisms. Most biofilms are characterized by mass transfer resistance: a diffusive boundary layer (DBL) is created by viscous forces around the biofilm surface and separates the biofilm matrix from the turbulent bulk liquid. Solutes are only transported by molecular diffusion in the DBL and in the biofilm matrix, and therefore steep gradients occur [29]. The chemical conditions inside a

biofilm are thus very different from the bulk water conditions, often leading to substrate limitations. On the other hand, processes such as denitrification, sulfate reduction, or methanogenesis can be found in the deeper, anaerobic zones of the biofilm, or in anaerobic micro-niches. Sequential conversions such as coupled nitrification - denitrification [63] or sulfate reduction - sulfide oxidation [34] often take place on a micrometer scale at oxic-anoxic interfaces. In general, microorganisms and processes are extremely compressed in biofilms. Measurements of the chemical gradients are needed to characterize the microenvironments, to understand the internal conversions, and to relate them to the microorganisms inhabiting certain zones in a biofilm.

It should be kept in mind, however, that liquid flow in voids will play an important role for mass transfer in biofilms with a more open structure and at higher flow velocity. Advective transport of solutes is much more efficient than diffusion and can considerably increase fluxes [17].

As much as the structure of the microbial community is determined by environmental conditions prevailing inside the biofilm, microorganisms by their activities create their own microenvironments. The results are highly stratified communities, where microbiologically mediated elemental cycles (e.g. N- or S-cycle) occur on a submillimeter scale. Nitrogen transformations, for example, can be initiated by aerobic mineralization of organic matter and the consequent release of ammonium. Ammonium can be either assimilated or sequentially oxidized via nitrite to nitrate, which again can be reduced in the anaerobic part of the biofilm to dinitrogen gas or ammonium. In such a biofilm, aerobic heterotrophs, ammonia- and nitrite-oxidizers, and nitrate-reducing bacteria would coexist in a competitive, syntrophical, or commensal way. Detailed investigation of such interactions is the key for the understanding and manipulation of biofilm function.

A further important property of biofilms is the protection of microorganisms against hazardous influences. The immobilization of cells, and the production of EPS not only alleviates common environmental shocks (e.g. sudden pH or substrate changes) but also provides resistance against some inhibitory substances (e.g. antibiotics or xenobiotics) [7].

2.3 Aggregates and flocs

In an extended definition, bacterial aggregates or flocs, both commonly used for biotechnological processes, can be seen as kind of "mobilized" biofilms. Although not attached to a substratum, they share most other characteristics with typical biofilms: they consist of clusters of cells embedded in EPS, sometimes including voids and a very irregular surface (e.g. activated sludge flocs), they usually are surrounded by a DBL that allows only diffusional transport of solutes, and they often develop steep chemical gradients and spatially distinct microenvironments [15], [21], [38], [39], [50]. Therefore, the same high resolution *in situ* techniques are needed for the structure and function analysis of aggregates or flocs as are needed for biofilm investigations.

3 Microsensors

The determination of microenvironments and *in situ* activities inside biofilms requires tools with high spatial and temporal resolution and minimum disturbance of the sample, i.e. negligible change of its physical structure and negligible consumption of the analyte. Microsensors with tip diameters of 1 - 30 µm have thus been developed and applied in microbial mats and biofilms to measure O_2 (Fig. 2), pH, CO_2, H_2, H_2S, S^{2-}, NH_4^+, NO_2^-, NO_3^-, N_2O, CH_4, $HClO$, Ca^{2+}, glucose, photosynthesis, light, temperature, and diffusivity or flow (reviewed in [36], [56]). From these measurements microenvironments can be defined and the zonation and rates of processes can be estimated.

3.1 Measuring principles

Microsensors rely on either electrochemical or optical principles [36]. The electrochemical sensors can be divided in three groups: amperometric, potentiometric, and biosensors.

silver guard
cathode

silicone
membrane

glass pipette

measuring cathode
(gold-plated platinum)
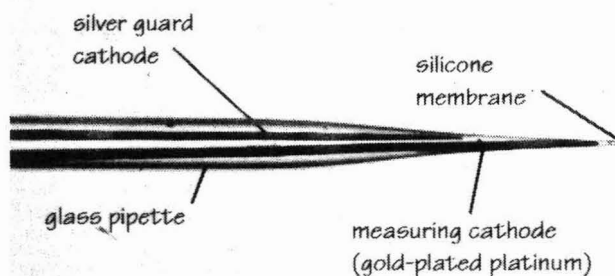
Fig. 2.
Amperometric oxygen
microsensor with a tip
diameter of 5 μm

Amperometric sensors detect the current caused by electrochemical reactions of the analyte at the sensor tip. A potential difference between the sensing electrode and the reference drives the reaction, and the current, measured by a sensitive picoamperemeter, is proportional to the analyte concentration [58]. Examples of this principle are the Clark-type O_2 microsensor [53], the combined O_2/N_2O microsensor [54], and sensors for HClO [16], H_2 [24], and H_2S [28].

Potentiometric sensors detect an electrical potential difference generated by a charge separation of ions across a membrane. This ion-selective membrane can be either special glass as for the pH electrode (a miniaturized commercial pH electrode [67]), or a liquid ion exchanger (LIX) as for LIX microsensors. LIX microsensors can be made very small (1 μm), but often suffer from a short lifetime and a low selectivity of the membrane [58]. Examples are LIX sensors for NH_4^+ [20], NO_3^- [19], [27], and NO_2^- [14]. A CO_2 microsensor can be constructed with an internal LIX pH-sensor [12]

Microbiosensors combine biological catalysts (i.e. enzymes or whole cells) with electrochemical sensors. The first example was a glucose microsensor based on immobilized glucose oxidase [8]. Recently, CH_4 and NO_3^- biosensors were described, both consisting of bacteria (methanotrophs or denitrifiers) immobilized in front of a conventional amperometric microsensor for O_2 or N_2O, respectively [11, 37].

Fiber-optical microsensors (micro-optodes) are either used to directly measure light distribution in a sample [35], or contain an indicator chemistry at the fiber tip, that changes its luminescence or absorption in response to an analyte. O_2 [32], pH [33], and temperature [31] optodes have been developed based on that principle.

3.2 Application to biofilms

Microsensor studies in biofilms have addressed respiration, photosynthesis, and oxygen transfer [6], [18], [25], [26], nitrification and denitrification [9], [10], [21], [47], [55], sulfate reduction and sulfide oxidation [34], and methanogenesis [38]. It is beyond the scope of this article to summarize the results of more than ten years of microsensor research. However, there is a common trend that should be emphasized: most of the measured processes occur in narrow zones of 50 - 300 μm, often in close coupling to each other.

4 Molecular Techniques

Methods to analyze the populations relevant in biofilms must meet at least two requirements: firstly to reveal a comprehensive picture of the community structure, i.e. of the identity and abundance of its members, and secondly to detect their spatial arrangements inside the biofilm. Both criteria are not fully addressed by cultivation-based classical microbiology.

Therefore, during the past decade techniques were adapted from molecular biology for the cultivation-independent, phylogenetic identification and *in situ* detection of individual microbial cells (reviewed in [1], [3], [60]).

4.1 Phylogeny and its impact on microbial ecology

The starting point for this development was the revolutionary change in bacterial systematics during the 1980s. By comparative 16S rRNA sequence analysis, Carl Woese and coworkers established for the first time a framework for the identification of bacteria based not on their morphology and on physiological tests but on their evolutionary history (phylogeny) [73]. rRNA molecules (5S, 16S, and 23S rRNA) are polynucleotides (~ 120, 1500, and 3000 bases long, respectively), that are integral constituents of the ribosome. Because of their functional constancy, their universal distribution, and because they possess regions of different degrees of conservation, rRNAs are excellent molecules for discerning evolutionary relationships among organisms. Databases have been initiated for rRNA sequences [22], [40], [65], now encompassing over 10,000 16S rRNA sequences for comparison. Diagnostic sequence regions can be found specific for different taxonomic units ranging from the domain to the species level. Besides the reliable identification of isolated microorganisms or extracted rRNA (see below), two further characteristics of rRNAs offer even more possibilities for microbial ecology. (i) rRNAs are naturally amplified in living cells (1,000 - 10,000 copies). This makes them easy and sensitive to assay, and gives the opportunity to identify single bacteria by fluorescent oligonucleotide hybridization (Fig. 3). (ii) The amount of rRNA in individual cells is proportional to their general metabolic activity [59]. In principle, it is thus possible to estimate the activity of single cells after fluorescent oligonucleotide hybridization [23].

4.2 The rRNA approach

Population analysis based on 16S rRNA omitting cultivation was applied to natural microbial communities, and now is referred to as the rRNA approach [48], [49]. Total DNA is extracted from an environmental sample, followed by the PCR-amplification of the almost full length 16S rDNA, and a clone library of these rDNA fragments is constructed. The 16S rRNA genes out of the clones are sequenced and compared with databases to yield information about the identity or relatedness of new sequences. Oligonucleotide probes (i.e. short pieces of DNA, labeled with a radiotracer or a fluorescent dye) can be designed to specifically target the retrieved sequences. Finally, the populations behind this sequences are detected by oligonucleotide probing of intact fixed cells, most commonly by fluorescence *in situ* hybridization (FISH), where the fluorescent label of the probes is visualized by epifluorescence microscopy [3]. Due to the single-cell resolution of this method, quantification as well as the analysis of the spatial distribution of populations is possible.

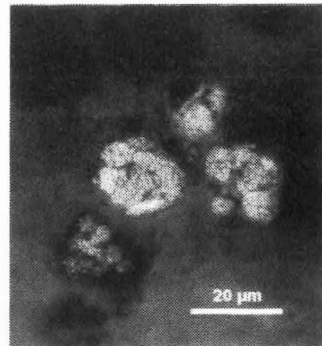Fig. 3. Confocal microscopic image of FISH targeting
    Nitrosospira sp. in a nitrifying biofilm

By application of probes with different specificity, labeled with three different fluorescent dyes, the simultaneous detection of up to seven distinct populations was shown [2]. For more detailed insights, 3D-analysis using confocal laser scanning microscopy and image analysis can be performed [70].

4.3 Application to biofilms

In biofilms, various studies involving FISH have been undertaken. They encompass investigations of laboratory model systems (e.g. [66]) as well as of rather complex "natural" biofilms (e.g. [71]). A population analysis on the subclass level was performed in drinking water biofilms [30], [41] and in a membrane-bound biofilm [57]. Populations of sulfate-reducing bacteria [4] and nitrifying bacteria [43] could be visualized in laboratory and bioreactor films. A set of probes was used to identify *Paracoccus* sp. in biofilms of a denitrifying sand filter [46]. For assaying metabolic activity and 3D-distribution of individual cells in biofilms, intense use was made of confocal laser scanning microscopy and image analysis [44], [45], [51]. For application of FISH to activated sludge flocs and aggregates ("mobilized biofilms", section 2.3), see [3], [60], and references therein.

5 Combined Approaches

Microsensor measurements and molecular techniques on their own were shown to yield valuable and exciting information. Their combination for *in situ* studies in biofilms, aggregates, or flocs is the logical consequence of the advantages and limitations of the two methods and offers great potential for the most detailed insights into function and structure of these systems. In the first combined investigation, studying a photosynthetically active trickling filter biofilm, Niels Ramsing and coworkers could relate microprofiles of oxygen and sulfide to the occurrence of sulfate reducing bacteria (SRB) as detected by FISH [52]. Distribution and activity of SRB were regulated by the photosynthetically controlled oxygen penetration depth.

FISH focusing on nitrifying biofilms showed that ammonia- and nitrite-oxidizing bacteria formed dense clusters in close vicinity to each other. Their nitrifying activity was confirmed by microsensor measurements, which revealed high activities in narrow zones of ca. 100 µm, correlating to the maximum abundance of nitrifiers. Different nitrifying communities were observed, most likely dependent on the trophic conditions of the biofilm system. They encompassed a *Nitrosomonas-Nitrobacter* association in an ammonia- and nitrite-rich environment [63], a *Nitrosospira-Nitrospira* association in an autotrophic, nitrogen-poor system [61], [62], and a complex community of various species of ammonia- and nitrite-oxidizers during the succession of a membrane-bound nitrifying/denitrifying biofilm (this thesis, Chapter 6).

Fig. 4. Detection of *Nitrobacter* sp. by FISH (red cluster) correlated to oxygen and nitrate profiles measured with microsensors (adapted from [63])
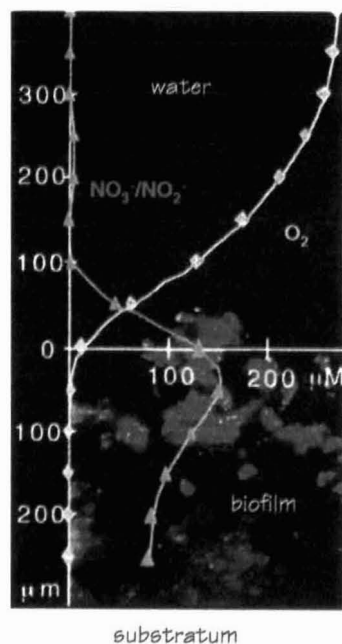
In conclusion, unlike ten years ago, the tools for extended *in situ* investigations are available. What matters now is to apply them in a clever way to increase our basic understanding of community structures and activities of biofilms, and of the factors controlling them.

6 Acknowledgment

7 References

[1] Amann, R., F.O. Glöckner, and A. Neef. 1997. Modern methods in subsurface microbiology: in situ identification of microorganisms with nucleic acid probes. *FEMS Microbiol. Rev.* **20**:191-200.

[2] Amann, R., J. Snaidr, M. Wagner, W. Ludwig, and K.-H. Schleifer. 1996. In situ visualization of high genetic diversity in a natural microbial community. *J.Bacteriol.* **178**:3496-3500.

[3] Amann, R.I., W. Ludwig, and K.H. Schleifer. 1995. Phylogenetic identification and in situ detection of individual microbial cells without cultivation. *Microb.Rev.* **59**:143-169.

[4] Amann, R.I., J. Stromley, R. Devereux, R. Key, and D.A. Stahl. 1992. Molecular and microscopic identification of sulfate-reducing bacteria in multispecies biofilms. *Appl.Environ.Microbiol.* **58**:614-623.

[5] Characklis, W.G., and P.A. Wilderer. 1989. *Structure and Function of Biofilms.* John Wiley & Sons Ltd., Chichester.

[6] Chen, Y.S., and H.R. Bungay. 1981. Microelectrode studies of oxygen transfer in trickling filter slimes. *Biotech.Bioeng.* **23**:781-792.

[7] Costerton, J.W., K.-J. Cheng, G.G. Geesey, T.I. Ladd, J.C. Nickel, M. Dasgupta, and T.J. Marrie. 1989. Bacterial biofilms in nature and disease. *Annu.Rev.Microbiol.* **41**:435-464.

[8] Cronenberg, C.C.H., H. Van Groen, D. de Beer, and J.C. van den Heuvel. 1991. Oxygen-independent glucose microsensor based on glucose oxidase. *An.Chim.Acta.* **242**:275-278.

[9] Dalsgaard, T., J. de Zwart, L.A. Robertson, J.G. Kuenen, and N.P. Revsbech. 1995. Nitrification, denitrification and growth in artificial *Thiosphaera pantotropha* biofilms as measured with a combined microsensor for oxygen and nitrous oxide. *FEMS Microbiol.Ecol.* **17**:137-148.

[10] Dalsgaard, T., and N.P. Revsbech. 1992. Regulating factors of denitrification in trickling filter biofilms as measured with the oxygen/nitrous oxide microsensor. *FEMS Microbiol.Ecol.* **101**:151-164.

[11] Damgaard, L.R., and N.P. Revsbech. 1997. A microscale biosensor for methane containing methanotrophic bacteria and an internal oxygen reservoir. *Anal.Chem.* **69**:2262-2267.

[12] de Beer, D., A. Glud, E. Epping, and M. Kühl. 1997. A fast responding CO_2 microelectrode for profiling sediments, microbial mats and biofilms. *Limnol.Oceanogr.* **42**:1590-1600.

[13] de Beer, D., and M. Kühl. Interfacial processes, gradients and metabolic activities in microbial mats and biofilms, Chapter 15 *in:* B. P. Boudreau and B. B. Jørgensen (ed.), The benthic boundary layer. Oxford University Press, Oxford. in press

[14] de Beer, D., A. Schramm, C.M. Santegoeds, and M. Kühl. 1997. A nitrite microsensor for profiling environmental biofilms. *Appl.Environ.Microbiol.* **63**:973-977.

[15] de Beer, D., A. Schramm, C.M. Santegoeds, and H.K. Nielsen. 1998. Anaerobic processes in activated sludge. *Wat.Sci.Tech.* **37**:605-608.

[16] de Beer, D., R. Srinivasam, and P.S. Stewart. 1994. Direct measurements of chlorine penetration into biofilms during disinfection. *Appl.Environ.Microbiol.* **60**:4339-4344.

[17] de Beer, D., and P. Stoodley. 1995. Relation between the structure of an aerobic biofilm and transport phenomena. *Wat.Sci.Tech.* **32**:11-18.

[18] de Beer, D., P. Stoodley, F. Roe, and Z. Lewandowski. 1994. Effects of biofilm structures on oxygen distribution and mass transport. *Biotech.Bioeng.* **43**:1131-1138.

[19] de Beer, D., and J.-P.R.A. Sweerts. 1989. Measurement of nitrate gradients with an ion-selective microelectrode. *An.Chim.Acta.* **219**:351-356.

[20] de Beer, D., and J.C. van den Heuvel. 1988. Response of ammonium-selective microelectrodes based on the neutral carrier nonactin. *Talanta.* **35**:728-730.

[21] de Beer, D., J.C. van den Heuvel, and S.P.P. Ottengraf. 1993. Microelectrode measurements of the activity distribution in nitrifying bacterial aggregates. *Appl.Environ.Microbiol.* **59**:573-579.

[22] De Rijk, P., Y. Van de Peer, and R. De Wachter. 1996. Database on the structure of large ribosomal subunit RNA. *Nucleic Acids Res.* **24**:92-97.

[23] DeLong, E.F., G.S. Wickham, and N.R. Pace. 1989. Phylogenetic stains: ribosomal RNA-based probes for the identification of single cells. *Science.* **243**:1360-1363.

[24] Ebert, A., and A. Brune. 1997. Hydrogen concentration profiles at the oxic-anoxic interface: A microsensor study of the hindgut of the wood-feeding lower termite *Reticulitermes flavipes* (Kollar). *Appl.Environ.Microbiol.* **63**:4039-4046.

[25] Glud, R.N., N.B. Ramsing, and N.P. Revsbech. 1992. Photosynthesis and photosynthesis-coupled respiration in natural biofilms quantified with oxygen microsensors. *J.Phycol.* **28**:51-60.

[26] Jensen, J., and N.P. Revsbech. 1989. Photosynthesis and respiration of a diatom biofilm cultured in a new gradient growth chamber. *FEMS Microbiol.Ecol.* **62**:29-38.

[27] Jensen, K., N.P. Revsbech, and L.P. Nielsen. 1993. Microscale distribution of nitrification activity in sediment determined with a shielded microsensor for nitrate. *Appl.Environ.Microbiol.* **59**:3287-3296.

[28] Jeroschewski, P., C. Steuckart, and M. Kühl. 1996. An amperometric microsensor for the determination of H_2S in aquatic environments. *Anal.Chem.* **68**:4351-4357.

[29] Jørgensen, B.B., and N.P. Revsbech. 1985. Diffusive boundary layers and the oxygen uptake of sediments and detritus. *Limnol.Oceanogr.* **30**:111-122.

[30] Kalmbach, S., W. Manz, and U. Szewyzk. 1997. Dynamics of biofilm formation in drinking water: phylogenetic affiliation and metabolic potential of single cells assessed by formazan reduction and in situ hybridization. *FEMS Microbiol.Ecol.* **22**:265-279.

[31] Klimant, I., M. Kühl, R.N. Glud, and G. Holst. 1997. Optical measurement of oxygen and temperature in microscale: strategies and biological applications. *Sensors and Actuators.* **B38-39**:29-37.

[32] Klimant, I., V. Meyer, and M. Kühl. 1995. Fiber-optic oxygen microsensors, a new tool in aquqtic biology. *Limnol.Oceanogr.* **40**:1159-1165.

[33] Kohls, O., I. Klimant, G. Holst, and M. Kühl. 1997. Development and comparison of pH microoptodes for use in marine systems. *Proc. SPIE.* **2978**:82-94.

[34] Kühl, M., and B.B. Jørgensen. 1992. Microsensor measurement of sulfate reduction and sulfide oxidation in compact microbial communities of aerobic biofilms. *Appl.Environ.Microbiol.* **58**:1164-1174.

[35] Kühl, M., C. Lassen, and B.B. Jørgensen. 1994. Optical properties of microbial mats: light measurements with fiber-optic microprobes, p. 149-167. *In:* L. J. Stal and P. Caumette (ed.), Microbial Mats: Structure, Development, and Environmental Significance. Springer Verlag, Berlin.

[36] Kühl, M., and N.P. Revsbech. Microsensors for the study of interfacial biogeochemical processes, Chapter 8 *in:* B. P. Boudreau and B. B. Jørgensen (ed.), The benthic boundary layer. Oxford University Press, Oxford. in press

[37] Larsen, L.H., T. Kjaer, and N.P. Revsbech. 1997. A microscale NO_3^- biosensor for environmental applications. *Anal.Chem.* **69**:3527-3531.

[38] Lens, P., D. de Beer, C. Cronenberg, S. Ottengraf, and W. Verstraete. 1995. The use of microsensors to determine population distributions in UASB aggregates. *Wat.Sci.Tech.* **31**:273-280.

[39] Lens, P.N., M.-P. De Poorter, C.C. Cronenberg, and W.H. Verstraete. 1995. Sulfate reducing and methane producing bacteria in aerobic wastewater treatment systems. *Wat.Res.* **29**:871-880.

[40] Maidak, B.L., G.J. Olsen, N. Larsen, R. Overbeek, M.J. McCaughey, and C.R. Woese. 1997. The RDP (ribosomal database project). *Nucleic Acids Res.* **25**:109-111.

[41] Manz, W., U. Szewzyk, P. Ericsson, R. Amann, K.-H. Schleifer, and T.-A. Stenström. 1993. In situ identification of bacteria in drinking water and adjoining biofilms by hybridization with 16S and 23S rRNA-directed fluorescent oligonucleotide probes. *Appl.Environ.Microbiol.* **59**:2293-2298.

[42] Massol-Deya, A., J. Whallon, R.F. Hickey, and J.M. Tiedje. 1995. Channel structure in aerobic biofilms of fixed-film reactors treating contaminated groundwater. *Appl.Environ.Microbiol.* **61**:769-777.

[43] Mobarry, B.K., M. Wagner, V. Urbain, B.E. Rittmann, and D.A. Stahl. 1996. Phylogenetic probes for analyzing abundance and spatial organization of nitrifying bacteria. *Appl.Environ.Microbiol.* **62**:2156-2162.

[44] Møller, S., C.S. Kristensen, L.K. Poulsen, J.M. Carstensen, and S. Molin. 1995. Bacterial growth on surfaces: automated image analysis for quantification of growth rate-related parameters. *Appl.Environ.Microbiol.* **61**:741-748.

[45] Møller, S., A.R. Pedersen, L.K. Poulsen, E. Arvin, and S. Molin. 1996. Activity and three-dimensional distribution of toluene-degrading *Pseudomonas putida* in a multispecies biofilm assessed by quantitative in situ hybridization and scanning confocal laser microscopy. *Appl.Environ.Microbiol.* **62**:4632-4640.

[46] Neef, A., A. Zaglauer, H. Meier, R. Amann, H. Lemmer, and K.-H. Schleifer. 1996. Population analysis in a denitrifying sand filter: conventional and in situ identification of *Paracoccus* spp. in methanol-fed biofims. *Appl.Environ.Microbiol.* **62**:4329-4339.

[47] Nielsen, L.P., P.B. Christensen, N.P. Revsbech, and J. Sørensen. 1990. Denitrification and oxygen respiration in biofilms studied with a microsensor for nitrous oxide and oxygen. *Microb.Ecol.* **19**:63-72.

[48] Olsen, G.J., D.J. Lane, S.J. Giovannoni, N.R. Pace, and D.A. Stahl. 1986. Microbial ecology and evolution: a ribosomal rRNA approach. *Annu.Rev.Microbiol.* **40**:337-365.

[49] Pace, N.R. 1996. New perspective on the natural microbial world: molecular microbial ecology. *ASM News.* **62**:463-470.

[50] Ploug, H., M. Kühl, B. Buchholz-Cleven, and B.B. Jørgensen. 1997. Anoxic aggregates - an ephemeral phenomenon in the pelagic environment? *Aquat.Microb.Ecol.* **13**:285-294.

[51] Poulsen, L.K., G. Ballard, and D.A. Stahl. 1993. Use of rRNA fluorescence in situ hybridization for measuring the activity of single cells in young and established biofilms. *Appl.Environ.Microbiol.* **59**.

[52] Ramsing, N.B., M. Kühl, and B.B. Jørgensen. 1993. Distribution of sulfate-reducing bacteria, O_2, and H_2S in photosynthetic biofilms determined by oligonucleotide probes and microelectrodes. *Appl.Environ.Microbiol.* **59**:3840-3849.

[53] Revsbech, N.P. 1989. An oxygen microelectrode with a guard cathode. *Limnol.Oceanogr.* **34**:474-478.

[54] Revsbech, N.P., P.B. Christensen, L.P. Nielsen, and J. Sørensen. 1988. A combined oxygen and nitrous oxide microsensor for denitrification studies. *Appl.Environ.Microbiol.* **54**:2245-2249.

[55] Revsbech, N.P., P.B. Christensen, L.P. Nielsen, and J. Sørensen. 1989. Denitrification in a trickling filter biofilm studied by a microsensor for oxygen and nitrous oxide. *Wat.Res.* **23**:867-871.

[56] Revsbech, N.P., and B.B. Jørgensen. 1986. Microelectrodes: their use in microbial ecology, p. 293-352. *In:* K. C. Marshall (ed.), Advances in Microbial Ecology, vol. 9. Plenum, New York.

[57] Rothemund, C., R. Amann, S. Klugbauer, W. Manz, C. Bieber, K.-H. Schleifer, and P. Wilderer. 1996. Microflora of 2,4-dichloropheoxyacetic acid degrading biofilms on gas permeable membranes. *Syst.Appl.Microbiol.* **19**:608-615.

[58] Santegoeds, C.M., A. Schramm, and D. de Beer. 1998. Microsensors as a tool to determine chemical microgradients and bacterial activity in wastewater biofilms and flocs. *Biodegradation* **9**:157-169

[59] Schaechter, M., O. Maaloe, and N.O. Kjeldgaard. 1958. Dependency on medium and temperature of cell size and chemical composition during balanced growth of *Salmonella typhimurium*. *J. Gen.Microbiol.* **19**:592-606.

[60] Schramm, A., and R. Amann. Nucleic acid based techniques for analyzing the diversity, structure, and dynamics of microbial communities in wastewater treatment. *In:* Rehm, H.-J., G. Reed, A. Pühler, and P. Stadler (ed.). Biotechnology, 2nd ed., Vol. 11a, Wiley-VCH, Weinheim. in press

[61] Schramm, A., D. de Beer, H. van den Heuvel, S. Ottengraf, and R. Amann. 1998. *In situ* structure/function studies in wastewater treatment systems. *Wat.Sci.Tech.* **37**:413-416.

[62] Schramm, A., D. De Beer, M. Wagner, and R. Amann. 1998. Identification and activity in situ of *Nitrosospira* and *Nitrospira* spp. as dominant populations in a nitrifying fluidized bed reactor. Appl. Environ. Microbiol. **64**: 3480-3485

[63] Schramm, A., L.H. Larsen, N.P. Revsbech, N.B. Ramsing, R. Amann, and K.-H. Schleifer. 1996. Structure and function of a nitrifying biofilm as determined by in situ hybridization and the use of microelectrodes. *Appl.Environ.Microbiol.* **62**:4641-4647.

[64] Stoodley, P., D. de Beer, and Z. Lewandowski. 1994. Liquid flow in biofilm systems. *Appl.Environ.Microbiol.* **60**:2711-2716.

[65] Strunk, O., O. Gross, B. Reichel, M. May, S. Hermann, N. Stuckmann, B. Nonhoff, M. Lenke, T. Ginhart, A. Vilbig, T. Ludwig, A. Bode, K.-H. Schleifer, and W. Ludwig. ARB: a software environment for sequence data. *http://www.mikro.biologie.tu-muenchen.de*. Department of Microbiology, Technische Universität München, Munich, Germany.

[66] Szewzyk, U., W. Manz, R. Amann, K.-H. Schleifer, and T.-A. Stenström. 1994. Growth and in situ detection of a pathogenic *Escherichia coli* in biofilms of a heterotrophic water-bacterium by use of 16S- and 23S-rRNA-directed fluorescent oligonucleotide probes. *FEMS Microbiol.Ecol.* **13**:169-176.

[67] Thomas, R.C. 1978. Ion-sensitive intracellular microelectrodes, how to make and use them. Academic Press, London.

[68] Tijhuis, L., B. Hijman, M.C.M. van Loosdrecht, and J.J. Heijnen. 1996. Influence of detachment, substrate loading and reactor scale on the formation of biofilms in airlift reactors. *Appl.Microbiol.Biotech.* **45**:7-17.

[69] van Loosdrecht, M.C.M., C. Picioreanu, and J.J. Heijnen. 1997. A more unifying hypothesis for biofilm structures. *FEMS Microbiol.Ecol.* **24**:181-183.

[70] Wagner, M., B. Assmus, A. Hartmann, P. Hutzler, and R. Amann. 1994. *In situ* analysis of microbial consortia in activated sludge using fluorescently labelled, rRNA-targeted oligonucleotide probes and confocal scanning laser microscopy. *Journal of Microscopy.* **176**:181-187.

[71] Wagner, M., G. Rath, H.-P. Koops, J. Flood, and R. Amann. 1996. *In situ* analysis of nitrifying bacteria in sewage treatment plants. *Wat.Sci.Tech.* **34**:237-244.

[72] Wimpenny, J.W.T., and R. Colasanti. 1997. A unifying hypothesis for the structure of microbial biofilms based on cellular automaton models. *FEMS Microbiol.Ecol.* **22**:1-16.

[73] Woese, C.R. 1987. Bacterial evolution. *Microb.Rev.* **51**:221-271.

Outline of the Experimental Work

A combined approach of microsensor analysis and molecular techniques as described in Chapter 1 was used for the experiments to obtain a better understanding of nitrification and nitrifying bacteria in biofilms. This combination of methods had been initiated by Ramsing and coworkers to study a sulfate reducing biofilm [1]. Ion-selective microsensors for ammonium and nitrate had been developed and applied to nitrifying aggregates [2] but failed in the analysis of biofilms. Oligonucleotide probes specific for nitrifying bacteria of the genus *Nitrosomonas* [3] and *Nitrobacter* [4] were available at the Technical University of Munich, and a biosensor for nitrate/nitrite was under construction at the University of Aarhus.

In Chapter 2 of this dissertation, the first application of the biosensor in combination with fluorescence *in situ* hybridization (FISH) using the nitrifier probes is described. A nitrifying biofilm from a trickling filter was investigated, in which a narrow nitrification zone could be correlated with the maximum abundance of *Nitrosomonas* sp. and *Nitrobacter* sp.. Furthermore, these ammonia- and nitrite-oxidizing bacteria were shown to form dense clusters in close vicinity to each other.

The obvious next step was to develop an ion-selective microsensor for nitrite and to improve the microsensors available for ammonium and nitrate thus facilitating their application in biofilms. This was a prerequisite to investigate in detail substrates and products of ammonia- and nitrite-oxidizing bacteria in biofilms, and is described in Chapter 3.
Chapter 4 demonstrates the value of combining two *in situ* techniques. Hitherto uncultured relatives of the nitrite-oxidizer *Nitrospira moscoviensis* were identified in nitrifying aggregates applying the full cycle rRNA approach [5]. DNA was recovered from the sample, a 16S rDNA clone library constructed, and selected clones were sequenced. The comparison with an rRNA data base revealed their phylogenetic affiliation with *Nitrospira*. Oligonucleotide probes were designed for the *in situ* detection of the respective organisms. The ability of these uncultured bacteria to oxidize nitrite, which had been derived from their phylogenetic position, could be proven by use of the new nitrite microsensor. The ammonia-oxidizers in the aggregates, identified as *Nitrosospira* sp. by FISH, again occurred in dense clusters and close to the nitrite-oxidizers.

This investigation was extended to the *in situ* analysis of the whole reactor, of which the nitrifying aggregates originated (Chapter 5). Nitrification rates were determined by microsensor measurements in aggregates from three sampling sites in the reactor, and the respective ammonia- and nitrite-oxidizing populations were quantified using FISH in combination with confocal laser scanning microscopy (CLSM) and image analysis. From these data, the specific ammonium- and nitrite-oxidation rates (per cell) could be estimated.

Additionally, microsensor measurements were performed under elevated substrate concentrations to evaluate the potential nitrifying activity and to derive some information on the substrate affinities of the uncultured nitrifiers. The results were compared with literature data of different nitrifying bacteria and discussed in an ecophysiological context. A hypothesis was constructed predicting that *Nitrosomonas europaea* and *Nitrobacter* sp. should dominate under high substrate conditions while *Nitrosospira* sp. and *Nitrospira* sp. might be better competitors in low substrate environments.

This hypothesis was tested in another biofilm that initially contained all four populations and was grown under high substrate concentrations. Abundance and spatial distribution of the different nitrifiers along gradients of oxygen and nitrite are described in Chapter 6.

Finally (Chapter 7), the principles of *in situ* structure and function analyses were applied to the investigation of activated sludge flocs, that might be regarded as mobilized biofilms. Microsensor measurements were performed to detect anoxic microniches, denitrification, or sulfate reduction in single activated sludge flocs. Incubation experiments with $^{15}NO_3^-$ and $^{35}SO_4^{2-}$ yielded independent control of the obtained results. Furthermore, 3D-floc structure and community structure of sulfate reducing bacteria were investigated using CLSM and FISH, respectively. Anoxic microniches and denitrification were found to be possible and detectable by microsensor measurements in aerated activated sludge. Apparently, the structure of the activated sludge flocs played an important role for the occurrence of this phenomenon. However, anoxia seemed to be rather the exception than the rule in conventional wastewater treatment plants, and sulfate reduction was fully absent.

References

[1]   Ramsing, N.B., Kühl, M. and Jørgensen, B.B. (1993)
       Appl. Environ. Microbiol. 59, 3840-3849.
[2]   de Beer, D., van den Heuvel, J.C. and Ottengraf, S.P.P. (1993)
       Appl. Environ. Microbiol 59, 573-579.
[3]   Wagner, M., Rath, G., Amann, R., Koops, H.-P. and Schleifer, K.-H. (1995)
       Syst. Appl. Microbiol. 18, 251-264.
[4]   Wagner, M., Rath, G., Koops, H.-P., Flood, J. and Amann, R. (1996)
       Wat. Sci. Technol. 34, 237-244.
[5]   Amann, R.I., Ludwig, W. and Schleifer, K.H. (1995) Microbiol. Rev. 59, 143-169.

Chapter 2

Structure and Function of a Nitrifying Biofilm as Determined by

In Situ Hybridization and the Use of Microelectrodes
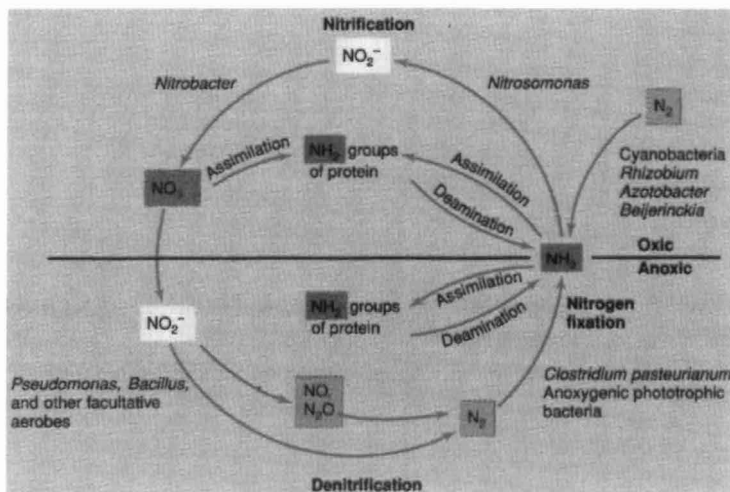
Front page:

The Nitrogen Cycle (from: Madigan, M.T., Martinko, J.M., and Parker, J. (1997) Brock Biology of Microorganisms, 8th edition, Prentice-Hall, New Jersey)
Note *Nitrosomonas* and *Nitrobacter* spp. as reference organisms for nitrification (on top)

Structure and Function of a Nitrifying Biofilm as Determined by In Situ Hybridization and the Use of Microelectrodes

ANDREAS SCHRAMM,[1] LARS HAUER LARSEN,[2] NIELS PETER REVSBECH,[2]
NIELS BIRGER RAMSING,[2] RUDOLF AMANN,[1]*
AND KARL-HEINZ SCHLEIFER[1]

*Technische Universität München, Lehrstuhl für Mikrobiologie, D-80290 Munich, Germany,[1]
and Department of Microbial Ecology, Institute of Biological Sciences,
University of Aarhus, DK-8000 Aarhus C, Denmark*

Microprofiles of O_2 and NO_3^- were measured in nitrifying biofilms from the trickling filter of an aquaculture water recirculation system. By use of a newly developed biosensor for NO_3^-, it was possible to avoid conventional interference from other ions. Nitrification was restricted to a narrow zone of 50 µm on the very top of the film. In the same biofilms, the vertical distributions of members of the lithoautotrophic ammonia-oxidizing genus *Nitrosomonas* and of the nitrite-oxidizing genus *Nitrobacter* were investigated by applying fluorescence in situ hybridization of whole fixed cells with 16S rRNA-targeted oligonucleotide probes in combination with confocal laser-scanning microscopy. Ammonia oxidizers formed a dense layer of cell clusters in the upper part of the biofilm, whereas the nitrite oxidizers showed less-dense aggregates in close vicinity to the *Nitrosomonas* clusters. Both species were not restricted to the oxic zone of the biofilm but were also detected in substantially lower numbers in the anoxic layers and even occasionally at the bottom of the biofilm.

Lithoautotrophic nitrification is a two-step process in which the combined action of ammonia- and nitrite-oxidizing bacteria results in the transformation of NH_3 to NO_3^- via NO_2^-. It can lead to significant loss of fertilizer nitrogen in soil and to nitrate pollution of groundwater and surface water (40). On the other hand, nitrification is the initial step of total nitrogen removal from sewage via denitrification. There, it is important to prevent eutrophication of receiving waters or at least—when denitrification fails—to avoid contamination of receiving waters with ammonium salts that are toxic to most fish species (38).

Increased attention has, therefore, been paid to the physiology and ecology of nitrifying bacteria during the last decade. The genera *Nitrosomonas* and *Nitrobacter* are still the two best-known catalysts of the two respective steps (7, 29), but recent studies of nitrification have resulted in the isolation of new species (e.g., see references 8 and 28), and the discovery of unexpected metabolic steps (for example, see references 9 and 39). Various techniques for the determination of nitrification rates, e.g., by using nitrification inhibitors (23), ^{15}N dilution techniques (27), or isotope pairing (46), have been developed. However, determination of the exact localization of nitrification and nitrifying bacteria remained difficult. Both the ammonia and the nitrite oxidizers are typical examples of fastidious bacteria. They are slowly growing bacteria and are difficult to enumerate by cultivation-dependent methods (5). Therefore, in situ identification methods have been evaluated. First, fluorescent-antibody techniques were used to detect and count nitrifiers microscopically (1, 6). However, because of the large serological diversity of ammonia oxidizers (6) and nonspecific bindings of fluorescent antibody to extracellular polymeric substances (48), these methods were not completely satisfying. More recently, progress in molecular ecology has enabled the

successful application of fluorescence in situ hybridization with 16S rRNA-targeted oligonucleotide probes in more complex environments as well (for a review, see reference 4). With this background, Wagner et al. could design a probe specific for halotolerant and halophilic members of the genus *Nitrosomonas* and successfully apply it to the detection of ammonia-oxidizing bacteria in activated sludge (51). Furthermore, two probes specific for all hitherto-sequenced species of *Nitrobacter* have been developed (52).

This introduction of a new, very powerful technique for in situ analysis of complex community structure coincided with the introduction of microelectrodes into the field of microbial ecology. These sensors make it possible today to monitor several metabolic reactions on a scale relevant for the study of stratified bacterial communities (for reviews, see references 43 and 45). For monitoring the nitrogen cycle, microsensors for nitrous oxide-oxygen (44), ammonia (15), and nitrate (14) have been developed and used for investigations in different habitats (12, 17, 24, 25, 36, 44). Despite an interference especially of HCO_3^- on the applied NO_3^- sensor, the work of Jensen et al. (24, 25) provides valuable information on the stratification of nitrifying activity and regulating effects of oxygen and ammonia. With a recently developed biosensor for nitrate (13, 31), it is, however, now possible to avoid the restrictions imposed by interfering ions.

In this study, we combined for the first time microprofiles of nitrification activity and data on the microdistribution of nitrifying bacteria in a biofilm. Fluorescent-oligonucleotide probing has already been applied to biofilm studies several times (e.g., see references 2 and 35). In a study of sulfate-reducing bacteria (SRB) in a trickling-filter biofilm, Ramsing et al. (41) had used this technique to relate the distribution of SRB to microprofiles of oxygen, sulfide, and pH. The present study was done with another trickling-filter biofilm treating the wastewater of an eel aquaculture. Growth of nitrifying bacteria was supported in this system by high concentrations of ammonia and stable temperatures of approximately 25°C. The relation between chemical gradients and the bacterial stratification is

---

* Corresponding author. Mailing address: Lehrstuhl für Mikrobiologie, Technische Universität München, Arcisstr. 16, D-80290 Munich, Germany. Phone: 49 89 2892 2373. Fax: +49 89 2892 2360. Electronic mail address: amann@mbitum2.biol.chemie.tu-muenchen.de.

TABLE 1. Probe sequences, target sites, and concentrations of formamide and NaCl in the hybridization or washing buffer, respectively, required for specific whole-cell in situ hybridization

Probe	Probe sequence	Target site (*Escherichia coli* rRNA positions)	% Formamide (hybridization buffer)	Concn of NaCl (washing buffer) (mM)
EUB338	5'-GCTGCCTCCCGTAGGAGT-3'	16S (338–355)	20	0.225
NEU23a	5'-CCCCTCTGCTGCACTCTA-3'	16S (653–670)	40	0.056
NIT2	5'-CGGGTTAGCGCACCGCCT-3'	16S (1433–1450)	40	0.056
NIT3	5'-CCTGTGCTCCATGCTCCG-3	16S (1030–1047)	40	0.056
CNIT3	5'-CCTGTGCTCCAGGCTCCG-3	Used as competitor together with NIT3		
NON338	5'-ACTCCTACGGGAGGCAGC-3'	Nonbinding control	20	0.225

described, and possible reasons for the occurrence of nitrifiers in the anaerobic zone are discussed.

MATERIALS AND METHODS

Biofilm samples. The biofilms were grown on plastic foils, placed in a vertical position in the bottom part of a trickling filter. The filter was installed inside the water cycle of an aquaculture producing eels (Rostved, Denmark). The water which drenched the biofilm permanently contained various but high concentrations of NH_4^+ (0.3 to 7 mM) and NO_3^- (27 to 39 mM); the values for NO_2^- and N_2O were 0.7 to 11 μM and 0.2 to 0.9 μM, respectively. The whole plant was located in a closed dark room which made it possible to maintain a stable temperature between 20 and 28°C. After 3 to 4 months, the biofilm had reached a thickness of approximately 200 μm. All of the analyses were performed after the foil pieces had been removed and brought to the laboratory submersed in in situ water.

Microelectrodes. Clark-type oxygen microelectrodes (42) with a 90% response time of less than 1 s and a negligible stirring sensitivity (<2%) were used to determine O_2 gradients at depth steps of 25 to 50 μm.

For measurements of NO_3^- profiles with a similar high resolution, a newly developed biosensor was used (13, 31). It was based on immobilized denitrifying bacteria (*Agrobacterium* sp.) which convert NO_3^- not to N_2 but only to N_2O. By placing the bacteria in a capillary in front of an electrochemical N_2O microsensor, the signal of the N_2O electrode was proportional to the concentration of NO_3^-. After optimization of its dimensions, the biosensor gave a linear response of from 0 to 300 μM NO_3^-, with 90% response times of approximately 20 s. The detection limit is approximately 3 μM NO_3^-. The only interfering substances were NO_2^- and N_2O, which were measured as NO_3^- and approximately 2× NO_3^-, respectively. It was, therefore, necessary to check the production of NO_2^- and N_2O by chemical analysis and the use of a previously described combined microsensor for O_2 and N_2O (12).

Measuring setup. Immediately after sampling, the biofilm was transferred to a covered aquarium with air-bubbled in situ water kept at room temperature (22°C), and O_2 profiles were measured as described previously (e.g., see reference 45). A two-point calibration of the electrodes was made with 100% O_2-saturated bulk water and the anoxic bottom of the film. The zero reading in the bottom of the biofilm was identical with the reading in N_2-bubbled water. Then, we changed the in situ water to air-bubbled tap water, and NH_4^+ was added to a concentration of 300 μM. We assumed that a new steady-state situation was reached after 10 min. The water exchange was necessary because of the very high concentrations of N compounds in the eel farm water. A background of approximately 30 mM NO_3^- would have been too high for accurate determination of concentration changes in the micromolar range because of nitrifying activity in the biofilm.

The NO_3^- profiles were measured in the same way as that for O_2, but a two-point calibration of the electrode in a corresponding aquatic medium containing no or 100 μM NO_3^-, respectively, was performed for every three or four profiles. To ensure equal temperature, the measuring setup served as a water bath for the calibration solutions.

Calibration of the N_2O sensor was done by adding certain amounts of N_2O-saturated water to the incubation water and using the values reported by Weiss and Price (53) for N_2O solubility.

Profiles of O_2 and NO_3^- were also recorded while the incubation water was only half-saturated with O_2. The O_2 concentration was adjusted by flushing the water with a 1:1 mixture of atmospheric air and N_2 and was controlled with an O_2 sensor. The incubation time under reduced O_2 was approximately 4 h.

During all measurements, microelectrodes were mounted on a computer-controlled, motor-driven micromanipulator (Märtzhäuser Wetzlar GmbH, Wetzlar, Germany), and the entry of the electrode tip in the biofilm was monitored with a dissection microscope. Data acquisition was done automatically by a custom-built program on a personal computer.

Calculations. Oxygen uptake was determined from the O_2 profiles as the flux, J, through the diffusive boundary layer (DBL), whereas the total rate of nitrification was calculated from the NO_3^- profiles as the complete flux, J, away from the layer of NO_3^- production. Net fluxes were calculated by Fick's first law of diffusion (26): $J = (\delta C(x)/\delta x) \cdot D_x(x) \cdot \Phi(x)$, where $C(x)$ is the concentration of the solute at the depth x, D_x is the apparent diffusion coefficient, and Φ is the porosity. We used table values of $2.24 \cdot 10^{-5}$ cm^2 s^{-1} (11) and $1.9 \cdot 10^{-5}$ cm^2 s^{-1} (32) for the diffusion coefficients of O_2 and NO_3^-, respectively, in water at 22°C. The diffusion coefficients in biofilms were assumed to be 40% lower than those in water, according to the measurements of $D_x \cdot \Phi$ performed by Revsbech et al. (44) and Glud et al. (22) with biofilms and microbial mats. Therefore, we used a value of $1.14 \cdot 10^{-5}$ cm^2 s^{-1} for $D_x \cdot \Phi$ of NO_3^- in the biofilm.

Chemical analysis. Water samples were taken from the trickling filter and from the measuring setup after the profiling to recalculate the NO_3^-/NO_2^- ratio. The samples were stored at −20°C until photospectrometrical analysis for NH_4^+, NO_2^-, and NO_3^- (10, 47, 49). For detection of N_2O, a Shimadzu GC-14A gas chromatograph equipped with an electron capture detector was used.

Biofilm fixation and cutting. Immediately after the microelectrode measurements, the biofilm samples were fixed in freshly prepared paraformaldehyde (4% in phosphate-buffered saline [PBS]) at 4°C for 1 h and were subsequently washed in PBS (3). Then, the middle of the sample was embedded in OCT compound (Tissue-Tek II; Miles, Elkhart, Ind.) and placed above evaporating liquid N_2 (41). When frozen, the biofilm was removed from the plastic foil by slightly bending the substratum. Subsequently, the biofilm was embedded from its bottom and frozen again. To prevent the samples from thawing, the last steps were performed in the cryostat (Dittes-Duspiva, Heidelberg, Germany) at −20°C. In this instrument, 10- to 20-μm-thick vertical cryosections were cut. The sections were placed in five of the six hybridization wells on gelatin-coated microscopic slides and immobilized by air drying and dehydrating with 50, 80, and 96% ethanol (3). The slides were then stored at room temperature for as long as several weeks.

Reference cells. Different mixtures of known bacterial strains were deposited on the last well of the microscopic slides and served as internal controls for hybridization efficiency. Mixtures of the following species were used: *Nitrosomonas eutropha* Nm57[1], *N. europaea* ATCC 25978[T]/Nm50[T], and *Nitrobacter* sp. (donated by G. Rath, Institut für Botanik, Abteilung Mikrobiologie, Universität Hamburg [as positive controls]) and *Comamonas testosteroni* DSM 50244[T] and *Bradyrhizobium japonicum* LMG 6138[T] (donated by M. Wagner, Lehrstuhl für Mikrobiologie, Technische Universität München [as negative controls]).

Oligonucleotide probes. The following rRNA-targeted oligonucleotides (for sequences and target sites, see Table 1) were used: (i) EUB338, a general probe complementary to a region of the 16S rRNA of all bacteria as a positive control of hybridization efficiency (3); (ii) NEU23a, a probe specific for a region of the 16S rRNA of some lithoautotrophic ammonia-oxidizing bacteria (including *N. europaea* and *N. eutropha*) as described recently by Wagner et al. (51); (iii) NIT2 and NIT3, probes specific for regions of the 16S rRNA of all hitherto-sequenced *Nitrobacter* strains (52); (iv) CNIT3, an unlabeled competitor to ensure the specificity of probe NIT3 when applied simultaneously (52); and (v) a negative-control probe, NON338, which is complementary to the probe EUB338 and, therefore, should be incapable of hybridization with rRNA of bacteria (34). The oligonucleotides were synthesized, labelled with the fluorescent dyes 5(6)-carboxy-fluorescein-N-hydroxysuccinimide ester (FLUOS; Boehringer Mannheim, Mannheim, Germany) and 5,(6)-carboxy-tetramethylrhodamine succinimidyl-ester (CT; Molecular Probes Inc., Eugene, Oreg.) and the hydrophilic sulphoindocyanine dye CY3 (monofunctional Cy3.29-OSu; Biological Detection Systems, Pittsburgh, Pa.) and purified as described previously (3, 51).

In situ hybridization. For whole-cell hybridization of biofilm sections, the protocol described by Manz et al. (34) was used. Formamide was added to the final concentrations listed in Table 1 to ensure optimal hybridization stringency. All hybridizations were performed at a temperature of 46°C and an incubation time of 3 h. A stringent washing step was performed at 48°C for 10 min in a buffer containing 20 mM Tris-HCl (pH 8.0), 0.01% sodium dodecyl sulfate, and NaCl at the concentrations listed in Table 1.

Microscopy. Biofilm sections were examined with an Axioplan epifluorescence microscope (Carl Zeiss, Oberkochen, Germany) with Zeiss filter sets 09 and 15 and filter set CY3-HQ (Chroma Technology Corp., Brattleboro, Vt.). Color micrographs were taken on Kodak Ektachrome P1600 color reversal film. Exposure times were 0.01 s for phase-contrast micrographs and 10 to 20 s for epifluorescence micrographs. A Zeiss LSM 410 confocal laser-scanning microscope (Carl Zeiss), equipped with an Ar-ion laser (488 nm) and an HeNe laser (543 nm), was used to record optical sections as described by Wagner et al. (50).
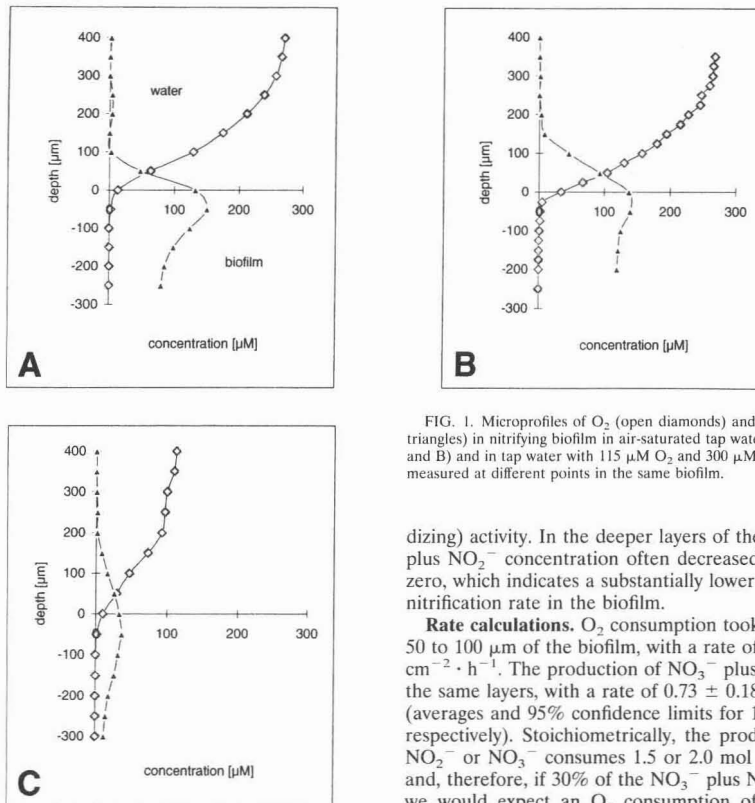
A

B

FIG. 1. Microprofiles of O_2 (open diamonds) and NO_3^- plus NO_2^- (filled triangles) in nitrifying biofilm in air-saturated tap water with 300 μM NH_4^+ (A and B) and in tap water with 115 μM O_2 and 300 μM NH_4^+ (C). Profiles were measured at different points in the same biofilm.

C

Image processing, depth profiles, and three-dimensional reconstructions were performed with the standard software delivered with the instrument.

RESULTS

Microgradients. All O_2 profiles measured with fully O_2-saturated water showed a decrease of O_2 within the DBL from 270 μM in the bulk water down to 20 to 60 μM on the biofilm surface. The thickness of the DBL varied between 150 and 250 μm because of a heterogeneous biofilm structure with protruding fluffy arms. O_2 penetrated approximately 100 μm into the biofilm, with fluctuations from 50 to 150 μm. Two representative depth profiles are shown in Fig. 1A and B.

To interpret the NO_3^- microprofiles, it should be kept in mind that both NO_2^- and N_2O are also detected by the biosensor. Therefore, NO_2^- was determined chemically together with NO_3^- from the bulk water after incubation and profiling. NO_2^- amounted to as much as 30% of the NO_3^- values. Because of this high percentage, the profiles should be considered as combined NO_3^- plus NO_2^- profiles. The measured N_2O profiles display a slight increase of N_2O from zero in the bulk water up to a maximum concentration of 4 μm at approximately 150 to 200 μm. The effect of N_2O was subtracted from the measured profiles, and the resulting combined NO_3^- plus NO_2^- profiles (Fig. 1) show a distinct peak just below the surface, indicating a high nitrifying (or at least ammonia-oxi-

dizing) activity. In the deeper layers of the biofilm, the NO_3^- plus NO_2^- concentration often decreased but never reached zero, which indicates a substantially lower denitrification than nitrification rate in the biofilm.

Rate calculations. O_2 consumption took place in the upper 50 to 100 μm of the biofilm, with a rate of 0.81 ± 0.13 μmol · $cm^{-2} · h^{-1}$. The production of NO_3^- plus NO_2^- appeared in the same layers, with a rate of 0.73 ± 0.18 μmol · $cm^{-2} · h^{-1}$ (averages and 95% confidence limits for 10 different profiles, respectively). Stoichiometrically, the production of 1 mol of NO_2^- or NO_3^- consumes 1.5 or 2.0 mol of O_2, respectively, and, therefore, if 30% of the NO_3^- plus NO_2^- pool is NO_2^-, we would expect an O_2 consumption of approximately 1.2 μmol · $cm^{-2} · h^{-1}$ only for nitrification. The discrepancy between the calculated O_2 demand for nitrification and the O_2 flux calculated from the O_2 profile will be discussed later. Denitrification in the layers below 150 μm ranged from 0 to 0.28 μmol · $cm^{-2} · h^{-1}$, with an average of 0.11 μmol · $cm^{-2} · h^{-1}$.

In situ water measurements. To check whether we changed the metabolism within the biofilm dramatically by substituting organic matter-containing in situ water with tap water plus nitrogen salts, we measured O_2 profiles before and after the substitution (data not shown). The depth penetration of O_2 did not change much, but a steeper concentration gradient in the DBL under in situ water (0.839 to 1.491 μmol · $cm^{-2} · h^{-1}$, with an average of 1.216 μmol · $cm^{-2} · h^{-1}$, compared with an average of 0.812 μmol · $cm^{-2} · h^{-1}$ under enriched tap water) indicated a decrease in heterotrophic activity. A shift in oxygen uptake by 30% would usually result in a substantial change in oxygen penetration, but the penetration in the applied biofilm was so shallow that the change was masked by temporal and spatial heterogeneity.

In situ detection of nitrifiers. An extremely dense layer of ammonia oxidizers could be detected with probe NEU23a throughout the aerobic part, and a few clusters were also found in deeper parts of the biofilm. They formed characteristic aggregates as described for *Nitrosomonas* species (33) and as seen before in other habitats (51, 52) (Fig. 2B). In addition, *Nitrobacter* sp. was detected in the biofilm. Reliable visualization required the simultaneous use of both probes NIT2 and

NIT3. The colonies were less dense than the *Nitrosomonas* clusters and occurred in lower numbers than the dominating ammonia oxidizers. The maximum of this nitrite-oxidizing population was in the aerobic nitrification zone, but some single cells and colonies still existed in the upper anoxic layers (at a depth of 100 to 200 μm) and even occasionally on the bottom of the film (Fig. 2D). In general, *Nitrobacter* colonies and cells were more evenly distributed than the ammonia oxidizers.

In the oxic zone, investigation by confocal laser-scanning microscopy (CLSM) revealed a close coexistence of ammonia and nitrite oxidizers, supporting a sequential metabolism from ammonia to nitrate (Fig. 2E).

Oxygen effect. Incubation with reduced O_2 concentration (115 μM) decreased both O_2 penetration and metabolic rates. The O_2 concentration reached levels of less than 20 μM on the biofilm surface and zero within 25 to 75 μm of depth. The total oxygen uptake was 0.35 ± 0.07 μmol $\cdot$ cm$^{-2} \cdot$ h^{-1}, whereas the production of NO_3^- plus NO_2^- decreased to 0.28 ± 0.14 μmol $\cdot$ cm$^{-2} \cdot$ h^{-1} (averages and 95% confidence limits for 10 different profiles, respectively). The main activity of nitrification was found at a depth of approximately 20 to 50 μm, and denitrification occurred in the deeper layers (100 to 200 μm), with an average rate of 0.10 μmol $\cdot$ cm$^{-2} \cdot$ h^{-1}. Again, the O_2 consumption was approximately 30% lower than that required for the measured nitrification rate (see Discussion). Representative profiles of O_2 and NO_3^- plus NO_2^-, respectively, are shown in Fig. 1C. As expected in a short-term experiment with slowly growing autotrophic nitrifiers, no change in their spatial distribution could be seen.

DISCUSSION

Microprofiles. It has long been difficult to obtain accurate microprofiles of nitrification. One of the problems of the LIX electrodes for NO_3^- used in the study described by Jensen et al. (24), was the interference of HCO_3^- (selectivity coefficient, 0.006) and, therefore, the need to perform measurements at artificial low alkalinities. However, the HCO_3^- production of biologically active biofilms and sediments does create steep concentration gradients within these systems. Thus, even with low concentrations of HCO_3^- in the overlying water, its biogenic accumulation resulted in inaccurate NO_3^- determination within the biofilm when the concentrations were less than approximately 25 μM (24). With the new biosensor, these problems were avoided, since the only agents interfering with the determination of NO_3^- are NO_2^- and N_2O. The additive determination of NO_3^- plus NO_2^- by the biosensor may be an advantage in some contexts. In the present investigation, it made it possible to determine the activity of NH_4^+ oxidation without having to consider how much of the intermediate NO_2^- was further oxidized to NO_3^-. For a detailed study of NO_2^- oxidation and the synergism between NH_4^+ and NO_2^- oxidizers, however, a microsensor for NO_2^- would be necessary. Such a microsensor was not available during this investigation.

The nitrifying activity of approximately 0.8 μmol $\cdot$ cm$^{-2} \cdot$ h^{-1} found in this study is very high compared with previous microsensor studies of nitrifying sediments (24) but is comparable to rates found at the surface of manure clumps in soil (37). The nitrifying layer in the investigated biofilm was only approximately 25 μm thick, indicating extremely high specific rates of approximately 30 μmol $\cdot$ cm$^{-3} \cdot$ h^{-1}. The manure-soil interface was analyzed by ^{15}N isotope techniques, and we do not know the exact thickness of the nitrifying layer in this system, but diffusion-reaction models indicated that the zone was very narrow. Such narrow zones with extremely high nitri-

fication activities are possible only when both NH_4^+ and O_2 are supplied to the active layers in adequate amounts. For oxygen, this is possible only by diffusion from a thoroughly mixed phase of overlying water to a superficial nitrification zone in the case of the biofilm or by gas phase diffusion in the case of the manure-soil system. It is difficult to obtain highly active pure cultures of nitrifying bacteria; however, judging from our environmental data, this must be due to unsuitable culture conditions.

The oxygen flux as calculated from the oxygen profile was too small to account for the nitrifying activity. A likely explanation is a local change in water current imposed by the microsensor. It has been shown that even microsensors with tips of a few micrometers cause such changes and that the diffusive boundary layer is eroded down to smaller thickness when a microsensor tip is inserted (21). Larger tips will result in a more vigorous erosion than thin tips, and since the biosensor was approximately 30 μm thick, compared with the 10-μm-thick oxygen microsensor, this could account for the observed discrepancy. The effect can actually be seen in Fig. 1, where near-constant water phase concentrations of NO_3^- were reached at approximately 100 to 150 μm above the biofilm, whereas the distance for oxygen was 200 to 300 μm. In future studies, it would be advisable to use microsensors of similar physical dimensions near the tip so that the data correspond to the same hydraulic regime.

Denitrification was heterogeneously distributed, but the rates were generally low. The concentration of NO_3^- plus NO_2^- was high throughout the anoxic layers of the biofilm; thus, the low level of activity is very likely due to a shortage of suitable organic electron donors. This argument is strongly supported by measuring denitrification at low oxygen concentrations; despite an increased anoxic zone and sufficient NO_3^- plus NO_2^- supply, the rate of denitrification remained the same. However, there is no doubt that the denitrification activity measured in our experiments was lower than that occurring in situ. This is a direct consequence of the substitution of the in situ water with tap water containing additional inorganic N salt, such that denitrifiers could use only organic compounds produced in the biofilm.

Stratification of nitrifiers. The dominance of chemolithoautotroph-nitrifying bacteria in the aerobic part of the biofilm is interesting, since they are considered to be poor competitors with heterotrophs (19). Reasons for a low level of competitiveness of the nitrifiers are high K_m values for oxygen compared with those for heterotrophs (16 μM for *Nitrosomonas* species and 62 μM for *Nitrobacter* species, but <1 μM for most of the heterotrophs) and slow growth (5). Obviously, there was a limited supply of easily degradable organic matter, whereas NH_4^+ was close to the optimum concentration of 2 to 10 mM (7, 29). Furthermore, the moderate and constant temperatures of the eel farm trickling filter at approximately 25°C supported the nitrifying bacteria, which are known to be especially bad competitors at cold temperatures.

It is obvious that oxygen is the limiting factor for both nitrification activity and abundance of the nitrifying population, since oxygen penetration, high rates of nitrification, and high numbers of nitrifiers are well correlated in the upper 50 μm of the biofilm. Although oxygen was present down to 100 μm, its concentration reached the K_m values of nitrifiers and therefore became limiting. In contrast, no depletion of NH_4^+ is expected in situ at substrate concentrations of a few micromolar, and even in the experimental setup, saturation with NH_4^+ is most likely, but this should be confirmed in future studies by additional use of an NH_4^+ microsensor.

As previously reported from other anaerobic environments
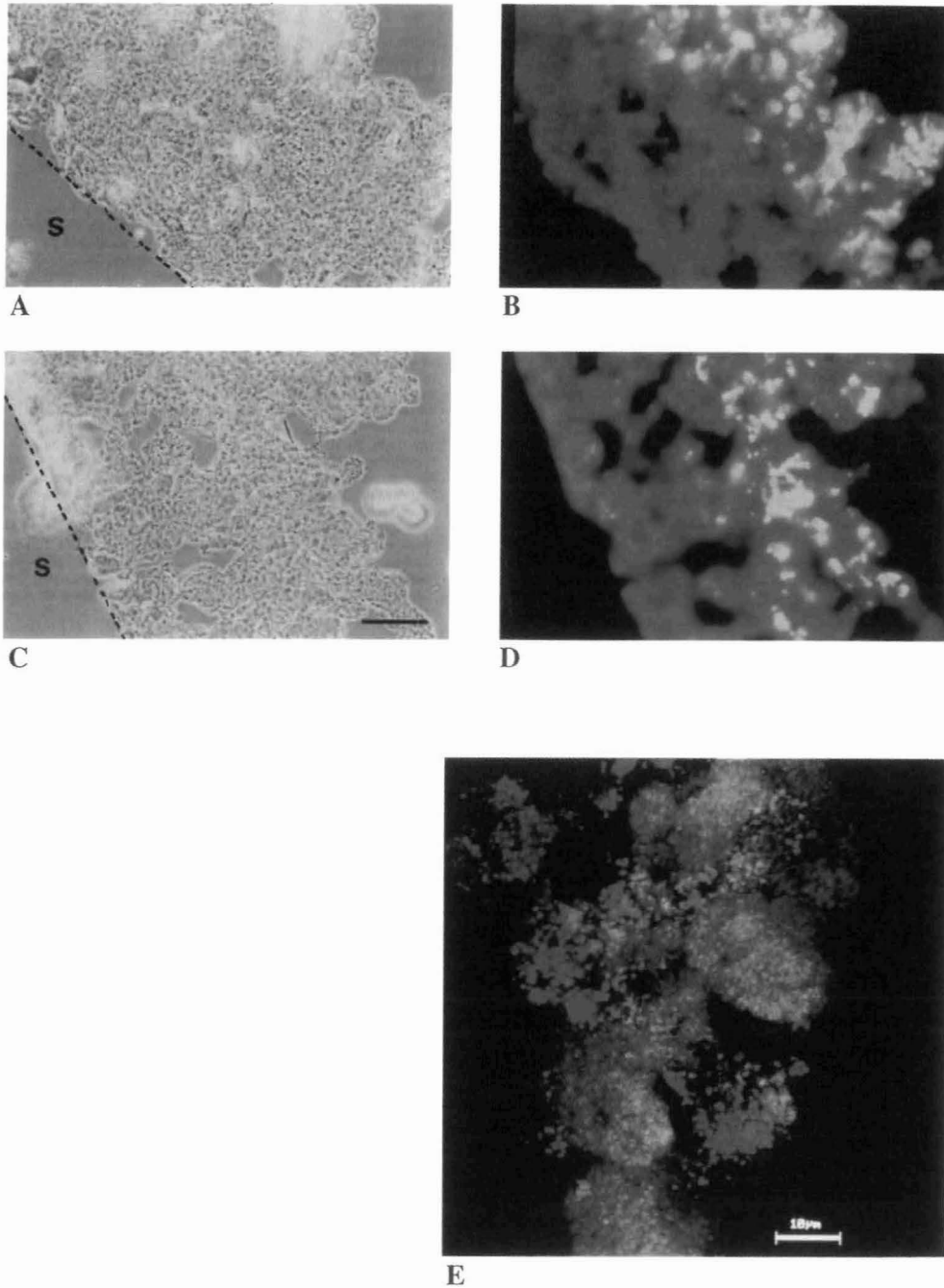
FIG. 2. In situ hybridizations of vertical biofilm sections. (A and B) Phase-contrast and epifluorescence micrographs, respectively, after hybridization with CY3-labelled probe NEU23a. (C and D) Phase-contrast and epifluorescence micrographs, respectively after, hybridization with a combination of CY3-labelled probes NIT2 and NIT3. With the CY3 HQ-filter set, probe-conferred CY3 fluorochromes are visualized in yellow, whereas autofluorescence of the biofilm appears in red (magnification, ×400; scale bar, 50 μm, S, substratum). (E) CLSM projection (all in focus) of a 20-μm-thick biofilm section after simultaneous hybridization with FLUOS-labelled probe NEU23a (green) and CT-labeled probes NIT2 and NIT3 (red). Only a detail of 78 by 78 μm from the nitrification zone is shown; the biofilm surface is on the right. Yellow signals do not yield from binding of both probes to one cell but are the result of overlaying red and green cells. Background fluorescence was reduced by the CLSM technique (magnification, ×1,000; scale bar, 10 μm).

(e.g., see reference 1), small numbers of nitrifiers were present in the deeper layers of the biofilm. There may be several explanations for the survival of nitrifiers in these layers. (i) Because of hydraulic flow within pores of the biofilm (16), oxic microniches may have existed in deeper layers. Such locally deep oxygen penetration was never detected during our microsensor work in the laboratory, but the hydraulic conditions in our setup could be very different from those in the trickling filter. (ii) Formerly oxic layers might have been overgrown during biofilm development. It has been shown that some bacteria, including *Nitrosomonas* species, are able to maintain their ribosome content during periods of nutrient starvation or inhibition (18, 51). (iii) Anaerobic metabolisms such as a combined ammonia oxidation-denitrification (9, 30) or dissimilatory reduction of NO_3^- with organic electron donors (20) may enable the survival of ammonia oxidizers and nitrite oxidizers, respectively, during periods without or at low concentrations of oxygen. For further investigation of the anaerobic *Nitrobacter* cells, a nitrite microsensor would be a useful tool to monitor specifically their metabolism in situ.

The close vicinity of ammonia and nitrite oxidizers as shown by the CLSM is a direct result of the sequential metabolism of ammonia via nitrite to nitrate. By this spatial arrangement, the diffusion path from the *Nitrosomonas* clusters to the surrounding *Nitrobacter* cells is extremely short and facilitates an efficient transfer of the intermediate NO_2^-. When considering the K_m values for oxygen of *Nitrosomonas* species and *Nitrobacter* species (see above), it is obvious that *Nitrosomonas* species could outcompete *Nitrobacter* species for oxygen under the low-oxygen concentrations obtained in the nitrification zone, and this could be one reason for the accumulation of nitrite in the bulk water. Additionally, dissimilatory reduction of nitrate to nitrite, nitric acid, or nitrous oxide, which is performed by *Nitrobacter* species in the anoxic layers (20), would be another source of nitrite in the system. The different K_m values for oxygen could also result in the different cluster size, since *Nitrosomonas* cells formed large ball-shaped clusters of as much as 50 μm, whereas the *Nitrobacter* colonies generally appear to be smaller and more irregular. Perhaps *Nitrobacter* cells are forced to disaggregate at a smaller size than *Nitrosomonas* cells because of oxygen depletion in the center of the cluster to levels less than their K_m values.

In conclusion, the combination of a microsensor technique with specific oligonucleotide probes provides reliable and direct information about nitrification as it occurs in nature. Data on community structure can be related to the metabolic functions of the respective populations. For further detailed investigations, microsensors for nitrite and additional oligonucleotide probes for nitrifiers are under development.

ACKNOWLEDGMENT

REFERENCES

1. **Abeliovich, A.** 1987. Nitrifying bacteria in wastewater reservoirs. Appl. Environ. Microbiol. **53:**754–760.
2. **Amann, R. I., J. Stromley, R. Devereux, R. Key, and D. A. Stahl.** 1992. Molecular and microscopic identification of sulfate-reducing bacteria in multispecies biofilms. Appl. Environ. Microbiol. **58:**614–623.
3. **Amann, R. I., L. Krumholz, and D. A. Stahl.** 1990. Fluorescent-oligonucleotide probing of whole cells for determinative, phylogenetic, and environmental studies in microbiology. J. Bacteriol. **172:**762–770.
4. **Amann, R. I., W. Ludwig, and K.-H. Schleifer.** 1995. Phylogenetic identification and in situ detection of individual microbial cells without cultivation. Microbiol. Rev. **59:**143–169.
5. **Belser, I. W.** 1979. Population ecology of nitrifying bacteria. Annu. Rev. Microbiol. **33:**309–333.
6. **Belser, L. W., and E. L. Schmidt.** 1978. Serological diversity within a terrestrial ammonia-oxidizing population. Appl. Environ. Microbiol. **36:**589–593.
7. **Bock, E., and H.-P. Koops.** 1992. The genus *Nitrobacter* and related genera, p. 2302–2309. *In* A. Balows, H. G. Trüper, M. Dworkin, W. Harder, and K.-H. Schleifer (ed.), The prokaryotes, 2nd ed. Springer-Verlag, New York.
8. **Bock, E., H.-P. Koops, U. C. Möller, and M. Rudert.** 1990. A new facultatively nitrite oxidizing bacterium, *Nitrobacter vulgaris* sp. nov. Arch. Microbiol. **153:**105–110.
9. **Bock, E., I. Schmidt, R. Stüven, and D. Zart.** 1995. Nitrogen loss caused by denitrifying *Nitrosomonas* cells using ammonium or hydrogen as electron donors and nitrite as electron acceptor. Arch. Microbiol. **163:**16–20.
10. **Bower, C. E., and T. Holm-Hansen.** 1980. A salicylate-hypochlorite method for determining ammonia in seawater. Can. J. Fish. Aquat. Sci. **37:**794–798.
11. **Broecker, W. S., and T.-H. Peng.** 1974. Gas exchange rates between air and sea. Tellus **26:**21–35.
12. **Dalsgaard, T., and N. P. Revsbech.** 1992. Regulating factors of denitrification in trickling filter biofilms as measured with the oxygen/nitrous oxide microsensor. FEMS Microbiol. Ecol. **101:**151–164.
13. **Damgaard, L. R., L. H. Larsen, and N. P. Revsbech.** 1995. Microscale biosensors for environmental monitoring. Trends Anal. Chem. **14:**300–303.
14. **DeBeer, D., and J.-P. R. A. Sweerts.** 1989. Measurement of nitrate gradients with an ion-selective microelectrode. Anal. Chim. Acta **219:**351–356.
15. **DeBeer, D., and J. C. van den Heuvel.** 1988. Response of ammonium-selective microelectrodes based on the neutral carrier nonactin. Talanta **35:**728–730.
16. **DeBeer, D., and P. Stoodley.** 1995. Relation between the structure of an aerobic biofilm and transport phenomena. Water Sci. Technol. **32:**11–18.
17. **DeBeer, D., J. C. van den Heuvel, and S. P. P. Ottengraf.** 1993. Microelectrode measurements of the activity distribution in nitrifying bacterial aggregates. Appl. Environ. Microbiol. **59:**573–579.
18. **Flärdh, K., P. S. Cohen, and S. Kjelleberg.** 1992. Ribosomes exist in large excess over the apparent demand for protein synthesis during carbon starvation in marine *Vibrio* sp. Strain CCUG 15956. J. Bacteriol. **174:**6780–6788.
19. **Focht, D. D., and W. Verstraete.** 1977. Biochemical ecology of nitrification and denitrification. Adv. Microbiol. Ecol. **1:**135–214.
20. **Freitag, A., M. Rudert, and E. Bock.** 1987. Growth of *Nitrobacter* by dissimilatory nitrate reduction. FEMS Microbiol. Lett. **14:**105–109.
21. **Glud, R. N., J. K. Gundersen, N. P. Revsbech, and B. B. Jørgensen.** 1994. Effects on the benthic diffusive boundary layer imposed by microelectrodes. Limnol. Oceanogr. **39:**462–467.
22. **Glud, R. N., K. Jensen, and N. P. Revsbech.** 1995. Diffusivity in surficial sediments and benthic mats determined by use of a combined N_2O-O_2 microsensor. Geochim. Cosmochim. Acta **59:**231–237.
23. **Hall, G. H.** 1984. Measurement of nitrification rates in lake sediments: comparison of the nitrification inhibitors nitrapyrin and allylthiourea. Microb. Ecol. **10:**25–36.
24. **Jensen, K., N. P. Revsbech, and L. P. Nielsen.** 1993. Microscale distribution of nitrification activity in sediment determined with a shielded microsensor for nitrate. Appl. Environ. Microbiol. **59:**3287–3296.
25. **Jensen, K., N. P. Sloth, N. Risgaard-Petersen, S. Rysgaard, and N. P. Revsbech.** 1994. Estimation of nitrification and denitrification from microprofiles of oxygen and nitrate in model sediment systems. Appl. Environ. Microbiol. **60:**2094–2100.
26. **Jørgensen, B. B., and N. P. Revsbech.** 1985. Diffusive boundary layers and the oxygen uptake of sediment and detritus. Limnol. Oceanogr. **30:**11–21.
27. **Koike, I., and A. Hattori.** 1977. Simultaneous determination of nitrification and nitrate reduction in coastal sediments by ^{15}N dilution technique. Appl. Environ. Microbiol. **35:**853–857.
28. **Koops, H.-P., B. Böttcher, U. C. Möller, A. Pommerening-Röser, and G. Stehr.** 1991. Classification of eight new species of ammonia-oxidizing bacteria: *Nitrosomonas communis* sp. nov., *Nitrosomonas urea* sp. nov., *Nitrosomonas aestuarii* sp. nov., *Nitrosomonas marina* sp. nov., *Nitrosomonas nitrosa* sp. nov., *Nitrosomonas eutropha* sp. nov., *Nitrosomonas oligotropha* sp. nov., *Nitrosomonas halophila* sp. nov. J. Gen. Microbiol. **137:**1689–1699.
29. **Koops, H.-P., and U. C. Möller.** 1992. The lithotrophic ammonia-oxidizing bacteria. p. 2625–2637. *In* A. Balows, H. G. Trüper, M. Dworkin, W. Harder, and K.-H. Schleifer (ed.), The prokaryotes, 2nd ed. Springer-Verlag, New York.
30. **Kuenen, J. G., and L. A. Robertson.** 1994. Combined nitrification-denitrification processes. FEMS Microbiol. Rev. **15:**109–117.
31. **Larsen, L. H., N. P. Revsbech, and S. J. Binnerup.** 1996. A microsensor for

nitrate based on immobilized denitrifying bacteria. Appl. Environ. Microbiol. **62:**1248–1251.

32. **Li, Y.-H., and S. Gregory.** 1974. Diffusion of ions in sea water and in deep-sea sediments. Geochim. Cosmochim. Acta **38:**703–714.

33. **Macdonald, R. M.** 1986. Nitrification in soil: an introductory history. Spec. Publ. Soc. Gen. Microbiol. **20:**1–16.

34. **Manz, W., R. Amann, W. Ludwig, M. Wagner, and K.-H. Schleifer.** 1992. Phylogenetic oligodeoxynucleotide probes for the major subclasses of proteobacteria: problems and solutions. Syst. Appl. Microbiol. **15:**593–600.

35. **Manz, W., U. Szewzyk, P. Eriksson, R. Amann, K.-H. Schleifer, and T. A. Stenström.** 1993. *In situ* identification of bacteria in drinking water and adjoining biofilms by hybridization with 16S and 23S rRNA-directed fluorescent oligonucleotide probes. Appl. Environ. Microbiol. **59:**2293–2298.

36. **Nielsen, L. P., P. B. Christensen, N. P. Revsbech, and J. Sørensen.** 1990. Denitrification and oxygen respiration in biofilms studied with a microsensor for nitrous oxide and oxygen. Microb. Ecol. **19:**63–72.

37. **Nielsen, T. H., and N. P. Revsbech.** 1994. Diffusion chamber for ^{15}N determination of coupled nitrification-denitrification associated with organic hotspots in soil. Soil Sci. Soc. Am. J. **58:**795–800.

38. **Painter, H. A.** 1986. Nitrification in the treatment of sewage and wastewaters. Spec. Publ. Soc. Gen. Microbiol. **20:**185–213.

39. **Poth, M.** 1986. Dinitrogen production from nitrite by a *Nitrosomonas* isolate. Appl. Environ. Microbiol. **52:**957–959.

40. **Prosser, J. I. (ed.)** 1986. Nitrification. Society for General Microbiology, Oxford.

41. **Ramsing, N. B., M. Kühl, and B. B. Jørgensen.** 1993. Distribution of sulfate-reducing bacteria, O_2, and H_2S in photosynthetic biofilms determined by oligonucleotide probes and microelectrodes. Appl. Environ. Microbiol. **59:**3840–3849.

42. **Revsbech, N. P.** 1989. An oxygen microelectrode with a guard cathode. Limnol. Oceanogr. **34:**474–478.

43. **Revsbech, N. P.** 1994. Analysis of microbial mats by use of electrochemical microsensors: recent advances, p. 149–163 *In* L. J. Stal and P. Caumette (ed.), Microbial mats: structure, development, and environmental significance. Springer, New York.

44. **Revsbech, N. P., P. B. Christensen, L. P. Nielsen, and J. Sørensen.** 1989. Denitrification in a trickling filter biofilm studied by a microsensor for oxygen and nitrous oxide. Water Res. **23:**867–871.

45. **Revsbech, N. P., and B. B. Jørgensen.** 1986. Microelectrodes: their use in microbial ecology. Adv. Microb. Ecol. **9:**293–352.

46. **Rysgaard, S., N. Risgaard-Petersen, L. P. Nielsen, and N. P. Revsbech.** 1993. Nitrification and denitrification in lake and estuarine sediments measured by the ^{15}N dilution technique and isotope pairing. Appl. Environ. Microbiol. **59:**2093–2098.

47. **Strickland, J. D. H., and T. R. Parson.** 1972. A practical handbook of seawater analysis. Bulletin 167. Fisheries Research Board of Canada, Ottawa.

48. **Swerinski, H., S. Gaiser, and D. Bardtke.** 1985. Immunofluorescence for the quantitative determination of nitrifying bacteria: interference of the test in biofilm reactors. Appl. Microbiol. Biotechnol. **21:**125–128.

49. **Velghe, N., and A. Claeys.** 1985. Rapid spectrophotometric determination of nitrate in mineral waters with resorcinol. Analyst **110:**313–314.

50. **Wagner, M., B. Aßmus, A. Hartmann, P. Hutzler, and R. Amann.** 1994. *In situ* analysis of microbial consortia in activated sludge using fluorescently labeled, rRNA-targeted oligonucleotide probes and confocal scanning laser microscopy. J. Microscopy **176:**181–187.

51. **Wagner, M., G. Rath, R. Amann, H.-P. Koops, and K.-H. Schleifer.** 1995. In situ identification of ammonia-oxidizing bacteria. Syst. Appl. Microbiol. **18:**251–264.

52. **Wagner, M., G. Rath, H.-P. Koops, J. Flood, and R. Amann.** 1996. *In situ* analysis of nitrifying bacteria in sewage treatment plants. Water Sci. Tech. **34:**237–244.

53. **Weiss, R. F., and B. A. Price.** 1980. Nitrous oxide solubility in water and seawater. Mar. Chem. **8:**347–359.

nitrate based on immobilized denitrifying bacteria. Appl. Environ. Microbiol. **62**:1248–1251.

32. **Li, Y.-H., and S. Gregory.** 1974. Diffusion of ions in sea water and in deep-sea sediments. Geochim. Cosmochim. Acta **38**:703–714.

33. **Macdonald, R. M.** 1986. Nitrification in soil: an introductory history. Spec. Publ. Soc. Gen. Microbiol. **20**:1–16.

34. **Manz, W., R. Amann, W. Ludwig, M. Wagner, and K.-H. Schleifer.** 1992. Phylogenetic oligodeoxynucleotide probes for the major subclasses of proteobacteria: problems and solutions. Syst. Appl. Microbiol. **15**:593–600.

35. **Manz, W., U. Szewzyk, P. Eriksson, R. Amann, K.-H. Schleifer, and T. A. Stenström.** 1993. *In situ* identification of bacteria in drinking water and adjoining biofilms by hybridization with 16S and 23S rRNA-directed fluorescent oligonucleotide probes. Appl. Environ. Microbiol. **59**:2293–2298.

36. **Nielsen, L. P., P. B. Christensen, N. P. Revsbech, and J. Sørensen.** 1990. Denitrification and oxygen respiration in biofilms studied with a microsensor for nitrous oxide and oxygen. Microb. Ecol. **19**:63–72.

37. **Nielsen, T. H., and N. P. Revsbech.** 1994. Diffusion chamber for ^{15}N determination of coupled nitrification-denitrification associated with organic hotspots in soil. Soil Sci. Soc. Am. J. **58**:795–800.

38. **Painter, H. A.** 1986. Nitrification in the treatment of sewage and wastewaters. Spec. Publ. Soc. Gen. Microbiol. **20**:185–213.

39. **Poth, M.** 1986. Dinitrogen production from nitrite by a *Nitrosomonas* isolate. Appl. Environ. Microbiol. **52**:957–959.

40. **Prosser, J. I. (ed.)** 1986. Nitrification. Society for General Microbiology, Oxford.

41. **Ramsing, N. B., M. Kühl, and B. B. Jørgensen.** 1993. Distribution of sulfate-reducing bacteria, O_2, and H_2S in photosynthetic biofilms determined by oligonucleotide probes and microelectrodes. Appl. Environ. Microbiol. **59**:3840–3849.

42. **Revsbech, N. P.** 1989. An oxygen microelectrode with a guard cathode. Limnol. Oceanogr. **34**:474–478.

43. **Revsbech, N. P.** 1994. Analysis of microbial mats by use of electrochemical

microsensors: recent advances, p. 149–163 *In* L. J. Stal and P. Caumette (ed.), Microbial mats: structure, development, and environmental significance. Springer, New York.

44. **Revsbech, N. P., P. B. Christensen, L. P. Nielsen, and J. Sørensen.** 1989. Denitrification in a trickling filter biofilm studied by a microsensor for oxygen and nitrous oxide. Water Res. **23**:867–871.

45. **Revsbech, N. P., and B. B. Jørgensen.** 1986. Microelectrodes: their use in microbial ecology. Adv. Microb. Ecol. **9**:293–352.

46. **Rysgaard, S., N. Risgaard-Petersen, L. P. Nielsen, and N. P. Revsbech.** 1993. Nitrification and denitrification in lake and estuarine sediments measured by the ^{15}N dilution technique and isotope pairing. Appl. Environ. Microbiol. **59**:2093–2098.

47. **Strickland, J. D. H., and T. R. Parson.** 1972. A practical handbook of seawater analysis. Bulletin 167. Fisheries Research Board of Canada, Ottawa.

48. **Swerinski, H., S. Gaiser, and D. Bardtke.** 1985. Immunofluorescence for the quantitative determination of nitrifying bacteria: interference of the test in biofilm reactors. Appl. Microbiol. Biotechnol. **21**:125–128.

49. **Velghe, N., and A. Claeys.** 1985. Rapid spectrophotometric determination of nitrate in mineral waters with resorcinol. Analyst **110**:313–314.

50. **Wagner, M., B. Aßmus, A. Hartmann, P. Hutzler, and R. Amann.** 1994. *In situ* analysis of microbial consortia in activated sludge using fluorescently labeled, rRNA-targeted oligonucleotide probes and confocal scanning laser microscopy. J. Microscopy **176**:181–187.

51. **Wagner, M., G. Rath, R. Amann, H.-P. Koops, and K.-H. Schleifer.** 1995. In situ identification of ammonia-oxidizing bacteria. Syst. Appl. Microbiol. **18**:251–264.

52. **Wagner, M., G. Rath, H.-P. Koops, J. Flood, and R. Amann.** 1996. *In situ* analysis of nitrifying bacteria in sewage treatment plants. Water Sci. Tech. **34**:237–244.

53. **Weiss, R. F., and B. A. Price.** 1980. Nitrous oxide solubility in water and seawater. Mar. Chem. **8**:347–359.

Chapter 3

A Nitrite Microsensor for Profiling Environmental Biofilms
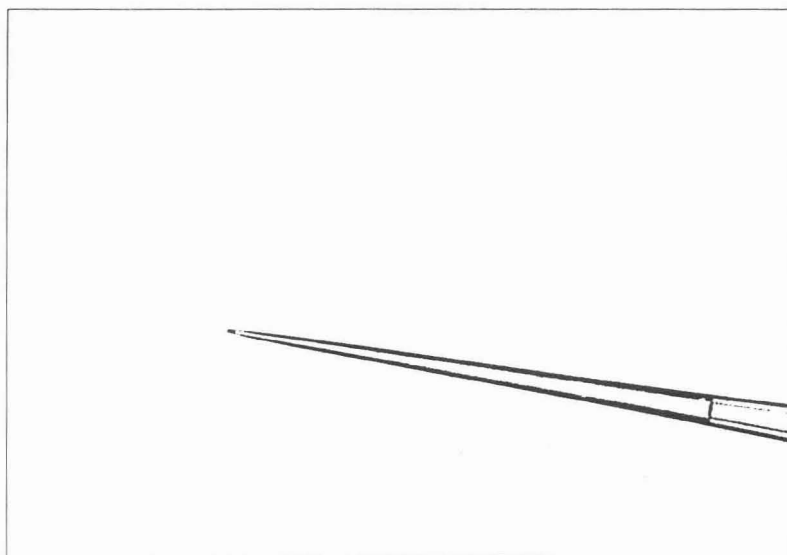
Front page:

Microscopic view of the tip of a LIX microsensor. The liquid membrane that is visible in the glass capillary has a length of about 300 µm, the tip diameter is about 5 µm.
Picture courtesy of Dirk de Beer.

A Nitrite Microsensor for Profiling Environmental Biofilms

DIRK DE BEER,[1]* ANDREAS SCHRAMM,[1,2] CECILIA M. SANTEGOEDS,[1] AND MICHAEL KÜHL[1]

*Max Planck Institute for Marine Microbiology, Bremen,[1] and Department of Microbiology,
Technical University of Munich, Munich,[2] Germany*

A highly selective liquid membrane nitrite microsensor based on the hydrophobic ion-carrier aquocyano-cobalt(III)-hepta(2-phenylethyl)-cobrynate is described. The sensor has a tip diameter of 10 to 15 μm. The response is log-linear in freshwater down to 1 μM NO_2^- and in seawater to 10 μM NO_2^-. A method is described for preparation of relatively large polyvinyl chloride (PVC)-gelled liquid membrane microsensors with a tip diameter of 5 to 15 μm, having a hydrophilic coating on the tip. The coating and increased tip diameter resulted in more sturdy sensors, with a lower detection limit and a more stable signal than uncoated nitrite sensors with a tip diameter of 1 to 3 μm. The coating protects the sensor membrane from detrimental direct contact with biomass and can be used for all PVC-gelled liquid membrane sensors meant for profiling microbial mats, biofilms, and sediments. Thanks to these improvements, liquid membrane sensors can now be used in complex environmental samples and in situ, e.g., in operating bioreactors. Examples of measurements in denitrifying, nitrifying, and nitrifying/denitrifying biofilms from wastewater treatment plants are shown. In all of these biofilms high nitrite concentrations were found in narrow zones of less than 1 mm.

Many intermediates and reactants of the nitrogen cycle can be measured with microelectrodes; however, nitrite is a notable exception. Microsensors for N_2O (28), NH_4^+ (8, 9), NO_3^- (16, 31), and O_2 (26) have been used for nitrification and denitrification studies in sediments and biofilms. Nitrite is an intermediate of both nitrification and denitrification. In sediments and biofilms with a close coupling between nitrification and denitrification, more than 50% of the nitrite formed by nitrification may be reduced by denitrification (25). Nitrite is a highly toxic compound for fish (10), benthic fauna (13), plants (35), bacterioplankton (12), nitrifiers (15), and methanogens (5). High nitrite concentrations favor accumulation of nitrous oxide (34), a greenhouse gas also involved in the destruction of the ozone layer. Nitrite is formed especially during disturbances, e.g., in nitrification bioreactors during oxygen depletion or ammonium overloading (15) or suddenly increased levels of biodegradable organics (21); by denitrification during electron donor deficits (32); or in the presence of oxygen (4). Nitrite can be present in high concentrations in sediments, as shown by pore water analysis (14) and from flux chamber measurements (2). Burrowing strongly increases efflux of nitrite from sediments (7, 19), possibly by stimulation of nitrite formation by the increased variation in oxygen conditions induced by animal activity.

Since nitrite is an intermediate, its presence can be very localized and temporary. This complicates sampling, e.g., by pore water analysis, as the nitrite concentration may change during sampling and storage. A nondisturbing measurement with microsensors would result in more reliable measurements of nitrite distributions, with high spatial resolution. Recently a microbiosensor equally sensitive for nitrate and nitrite was developed (20), but a useful microsensor selectively measuring nitrite has not been reported. A highly selective liquid ion-exchanging membrane (LIX) for nitrite was described (30). However, microsensors with a 1-μm tip based on this ion

exchanger had a 10- to 100-fold higher detection limit and 10- to 100-fold lower selectivities than macrosensors. It was concluded that this ion exchanger could not be used to construct microsensors for measurement of nitrite in physiological concentrations (29). We used the same nitrite ion exchanger and, with a modified preparation procedure, constructed nitrite microsensors with a submicromolar detection limit that are sufficiently robust for profiling biofilms and sediments. The modified preparation procedure can be used for all LIX microsensors to improve their performance.

MATERIALS AND METHODS

LIX microsensors. By using a heating coil, green soda lime glass tubes (model 8516; Schott) were drawn to microcapillaries. The tip diameter was 3 to 5 μm for ammonium, nitrate, and pH microsensors and 10 to 15 μm for nitrite microsensors. After the tips were pulled, the glass surface of the capillaries was silanized to obtain a hydrophobic surface for optimal adherence of the LIX membrane. A previously described procedure was used (1), but with longer preincubation and reaction times. The capillaries were placed in a 1.5-liter glass container and baked for at least 3 h at 150°C to remove traces of water. Then, 0.25 ml of silanizing agent (*N,N*-dimethyltrimethylsilylamine) was added and the vessel was closed and left overnight at a temperature of 200°C. Excess silane vapor was released in a fume hood, and the remaining silane was baked off at 150°C for another 2 h.

Each capillary was placed in a casing made from a Pasteur pipette, with the microcapillaries protruding ca. 2 cm. The casing was glued to the capillary with a silicon kit. After the preparation as described below, the casing was filled with 0.3 M KCl solution and connected to the reference with an Ag/AgCl wire. This is a highly effective way to protect the signal from electrical noise (16).

As LIX for nitrite sensors, we used a solution of 7% (wt/wt) aquocyanocobalt-(III)-hepta(2-phenylethyl)-cobrynate (nitrite ionophore-I) and 1% (wt/wt) sodium tetraphenyl borate in 2-nitrophenyl octyl ether. We used the Orion nitrate exchanger (model 92-07-01) for nitrate microsensors, 10% (wt/wt) of nonactin and 1% (wt/wt) sodium tetraphenyl borate in 2-nitrophenyl octyl ether for ammonium microsensors, and a solution of 6% (wt/wt) 4-nonadecylpyridine (H⁺ Ionophore II, ETH1907) and 1% (wt/wt) potassium tetrakis(4-chlorophenyl)borate in 2-nitrophenyl octyl ether for pH microsensors. To a portion of each type of LIX, 10% (wt/wt) high-molecular-weight polyvinyl chloride (PVC) was added. Then, ca. 3 volumes of tetrahydrofuran (Selectophore quality) was added to the mixture. The PVC was dissolved within 24 h, after which the solution was mixed carefully. Addition with PVC improves the stability and performance of LIX microsensors, as described previously (33). The nitrate LIX was obtained from Orion, and all other LIX components, the tetrahydrofuran, and the silanizing agent were obtained from Fluka.

The filling electrolytes used were 10 mM sodium nitrite, 300 mM KCl, and 10 mM sodium phosphate adjusted to pH 7.0 for the nitrite sensor, 50 mM KNO_3 and 50 mM KCl for the nitrate sensor, 30 mM KCl for the ammonium sensors, and 300 mM KCl and 50 mM sodium phosphate adjusted to pH 7.0 for the pH

* Corresponding author. Mailing address: Max-Planck-Institut für Marine Mikrobiologie, Celsiusstraße 1, 28359 Bremen, Germany. Phone: (0)421 2028 836. Fax: (0)421 2028 690. E-mail: dirk@postgate.mpi-mm.uni-bremen.de.

sensors. The filling solutions were degassed under vacuum and filtered through a 0.2-μm-pore-size Millipore membrane. The silanized capillaries were filled with electrolyte by using a plastic syringe drawn in a flame to a 0.1-mm tip; the air pocket that typically was left in the tip was pushed out by applying pressure from the back. Then, under microscopic inspection the tips were dipped in LIX and suction was applied until a membrane with a thickness of ca. 300 μm was introduced. Additionally, 100 to 200 μm of the PVC containing LIX was sucked in. The capillaries were left for at least 2 h, during which the tetrahydrofuran evaporated and a solid ion-selective membrane was formed in the tip.

After hardening of the membrane, the sensors were dipped in a solution of 10% cellulose acetate in acetone. This was done as briefly as possible to avoid dissolution of the membrane in the acetone. If this treatment caused recessing of the membrane from the tip, PVC containing LIX was reapplied. To 1 ml of 10% (wt/vol) bovine serum albumin (BSA) in 50 mM sodium phosphate (pH 7.0) 10 μl of 25% glutaraldehyde was added and immediately thoroughly mixed. This mixture solidifies in a few minutes. Under microscopic guidance the tip of a microsensor was dipped ca. 400 μm deep in the protein solution and moved in and out slowly. As soon as the protein solution became syrupy, a protein layer formed on the microsensor tip. After drying, a cross-linked protein layer of ca. 1-μm thickness was formed, which was water insoluble and firmly fixed. Finally, the casing surrounding the capillary for shielding of the signal was filled with 0.3 M KCl and connected with a Ag/AgCl wire to the reference.

Nitrite, nitrate, and ammonium microsensors were calibrated in dilution series of nitrite, nitrate, or ammonium in the medium used for the experiment. Calibration of the pH microsensors was performed with standard pH solutions.

The selectivity constants were determined by using the fixed interference method (22), with 0.6 M NaCl, 10 mM NaHCO$_3$ (pH 8.0), and 10 mM NaNO$_3$.

O$_2$ microsensor. Clark-type O$_2$ microsensors with internal references and guard cathodes were prepared and calibrated as described previously (26). Their tip diameter was 10 μm, and their stirring sensitivity was <2%.

H$_2$S microsensor. Stirring-insensitive amperometric H$_2$S gas sensors with a tip diameter of 15 μm were prepared and used as described previously (17).

Microsensor measurements. The electrodes were mounted on a micromanipulator and moved manually. The position relative to the biofilm surface was determined visually by using a dissection microscope. Due to irregularities, the surfaces of biofilms and aggregates are not always well defined. The surface was assumed to be reached if the tip disappeared.

Samples. A 2- to 3-cm-thick biofilm was removed from the walls of the outlet channel of the first activated sludge basin of the municipal wastewater treatment plant Seehausen (Bremen, Germany). After removal, it was transported to the laboratory and pieces of ca. 5 by 3 cm were incubated at 18°C in 0.5 liter of medium containing 25 mM K$_2$HPO$_4$, 380 μM (NH$_4$)$_2$SO$_4$, 100 μM Na-acetate, and 20 μM MgSO$_4$, adjusted to pH 7.0. The medium was mixed by sparging with air and refreshed twice per day. Nitrate and nitrite profiles were measured with 0.5 mM nitrate in the bulk medium.

Nitrifying aggregates were obtained from the inlet region of a lab-scale fluidized bed reactor as described previously (8). Aggregates with a diameter of ca. 2 mm were placed in a flow cell with insect needles and perfused with medium as described previously (8). The aggregates were left for 15 min before profile measurements started. Microelectrodes penetrated the aggregates at an angle of 120° with respect to the direction of flow. Microelectrodes could be positioned with an accuracy of 10 μm relative to the surface.

Nitrifying/denitrifying biofilms growing in a 22-liter pilot-scale membrane reactor were analyzed in situ. The reactor and its operating principle were described previously (24). Oxygen was supplied through permeable silicon tubing, with an exchange surface of 243 m^2/m^3, through which air was pumped under a pressure of 3 atm. The studied biofilms grew on the tubing. The reduced substrates ammonium and acetate were supplied from the bulk liquid. The reactor was fed continuously with synthetic wastewater (24) containing 34 mM ammonium and 17 mM acetate. The reactor liquid was recycled continuously with a rate of 2,000 liters/h, the liquid residence time was 4.2 h, the temperature was 26.5°C, and the pH was 7.7. The bulk liquid was anaerobic. The biofilms were 2 to 3 mm thick. The cylindrical reactor was placed horizontally with the sample ports on top, so that microsensors could be introduced through the sample ports.

RESULTS

The nitrite microsensor showed a log-linear response down to a nitrite concentration of 1 μM in 25 mM phosphate buffer and nitrite sensitivity to at least 0.1 μM (Fig. 1). Identical results were obtained in pure water (data not shown). The signal was stable, was not sensitive to noise, and drifted less than 1 to 2 mV/h. The signal was not influenced by stirring. The response time (t_{90}, the time needed to reach 90% of the end value upon a concentration change) was 10 to 15 s, allowing nitrite profiles with 25 measuring points to be measured within 10 min. Noncoated sensors showed the same calibration curve but had a response time of ca. 5 s (three sensors tested). The selectivity constants for Cl$^-$, NO$_3^-$, and HCO$_3^-$ were 10$^{-4.5}$,
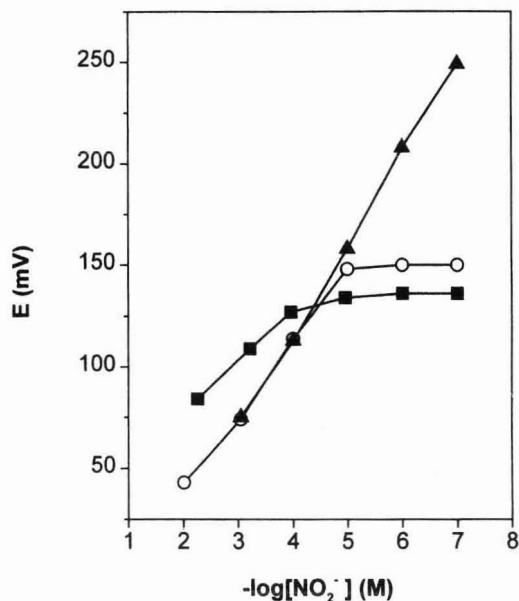
FIG. 1. Calibration curves of nitrite microsensors with a 15-μm tip in 25 mM phosphate buffer (▲), with a 15-μm tip in seawater (○), and with a 3-μm tip in 25 mM phosphate buffer (■).

10$^{-4.5}$, and 10^{-4}, respectively. Sensors with a tip diameter of 3 μm consistently (six sensors tested) had a high detection limit (Fig. 1). To obtain a useful sensor, the tip diameter had to be at least 10 μm (15 sensors tested). The response in seawater was log-linear down to 10 μM NO$_2^-$ and then bent off sharply due to chloride interference (Fig. 1). Addition of a pH buffer to the electrolyte resulted in more stable sensors. Upon exposure to more than 40 μM sulfide, the signal drifted in a negative direction and the sensitivity for nitrite was irreversibly lost. The damage could occur within a few seconds. Occasionally the sensitivity was not totally lost, but then the sensor became extremely slow, with response times measurable in minutes. Undamaged coated sensors could be used for months if stored dry and in the dark between experiments.

LIX membranes completely gelled with PVC were not stable in larger microcapillaries. Short circuits between electrolyte and sample solution occurred, due to shrinking of the membrane, or the membrane expanded by an unknown process and was pushed through the tip. Only the combination of PVC-gelled and nongelled LIX in the tip resulted in a functional microsensor. Without priming with cellulose acetate, the protein coating did not stick to the tip. After drying, the protein coating cracked and the sensor was not protected. Good results were obtained only with the combined coating of cellulose acetate and cross-linked BSA. During drying the coating shrank so that the tips sometimes became slightly curved, without affecting the sensor characteristics.

The protein coating was used for ammonium (data not shown), pH (data not shown), nitrite, and nitrate sensors with satisfying results. Uncoated nitrate sensors often drifted at nitrate concentrations below 5 μM; with protein coating, this was not observed. The response time was 5 to 10 s, similar to that for the uncoated sensor. Coated sensors could be used for

FIG. 2. Profiles of NO$_2^-$ (●), NO$_3^-$ (△), O$_2$ (▼), and H$_2$S (□) in a thick denitrifying biofilm from a wastewater treatment plant. The biofilm surface is at a depth of 0.

nitrite profiles showed a peak of 80 μM at the depth where nitrate was consumed. Nitrite profiles were measured to a depth of 0.5 mm, below which sulfide induced signal drift.

The nitrifying aggregates were rather irregularly shaped conglomerates of spheroids. The spheroids had a diameter of ca. 50 μm and were clustered into solid aggregates of ca. 2 mm in diameter. In these aggregates, ammonium was not completely converted to nitrate. The nitrite profile showed an increase to a maximu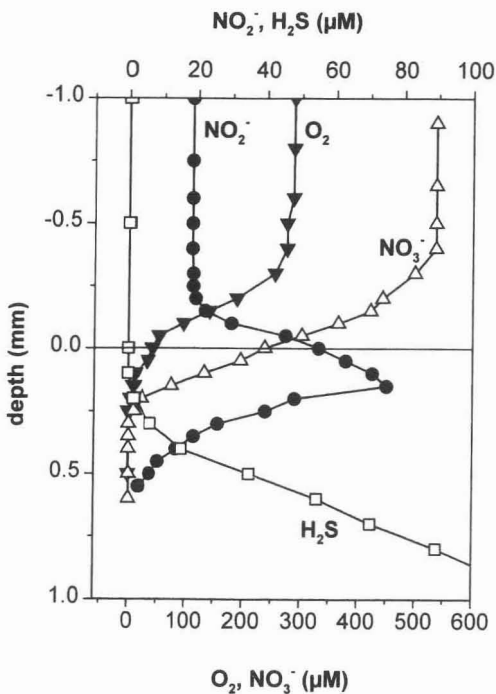m concentration of 105 μM, whereas nitrate increased only from 100 to 135 μM (Fig. 3). Oxygen penetrated 150 μm into the aggregate, and nitrate and nitrite were formed in the outer 200 μm.

Nitrite, nitrate, ammonium (not shown), and pH (not shown) profiles could be measured without noise problems in the operating pilot-scale membrane reactor placed in a hall with numerous other operating units. In the nitrifying/denitrifying biofilms the oxygen and nitrate concentration decreased in the direction from the membrane to the bulk liquid (Fig. 4). Oxygen concentration at the membrane surface was 800 μM, corresponding with the partial pressure in air under 3 atm, and decreased to zero within ca. 1.5 mm. Nitrate reached a concentration of 2 mM at the membrane and penetrated the whole biofilm, extending into the reactor liquid outside the biofilm. In the oxic zone a 300 μM nitrite peak was measured. Nitrite did not reach the anoxic zone.

DISCUSSION

Liquid membrane microsensors are relatively easy to prepare, and the great variety of ion exchangers allows measurement of many different compounds. However, their use in bioreactors and in the environment has been frustrated by three main problems: their noise sensitivity, which required working in a Faraday cage; their sensitivity to other ions; and

a few days when stored dry between experiments, while the uncoated sensors had a lifetime of ca. 5 h. For ammonium and pH sensors the coating did not influence calibration or response times (<5 s). Coated pH and ammonium sensors could also be used for a few days.

Initially well functioning microsensors (pH, ammonium, nitrate, and nitrite) without coating were immediately destroyed by touching the biofilm from the activated sludge plant. During penetration, sudden signal changes, drift, and increase or decrease of the offset potential were observed. After touching the biofilm, ammonium, nitrate, and nitrite microsensors no longer responded to substrate changes. The pH microsensor became extremely slow, with response times measurable in minutes. Microscopic inspection did not reveal any visual damage to the microsensor tip or LIX membrane. Microsensors coated with only cellulose acetate were damaged in the same way. However, the sensors coated with cellulose acetate and protein were insensitive for the destructive effect of the biofilm, even after exposure of several hours. Nitrate sensors were also sensitive to sulfide, causing a signal drift in the negative direction, but the effect was reversible. Ammonium and pH sensors were insensitive to sulfide.

The thick biofilm from the activated sludge plant showed high nitrate consumption rates. In the absence of nitrate in the bulk, no nitrate or nitrite could be detected in the oxic zone of the biofilm, indicating that nitrification was not significant. If present in the bulk, nitrate penetrated the biofilm more deeply than oxygen (Fig. 2). At a nitrate concentration of 0.5 mM,
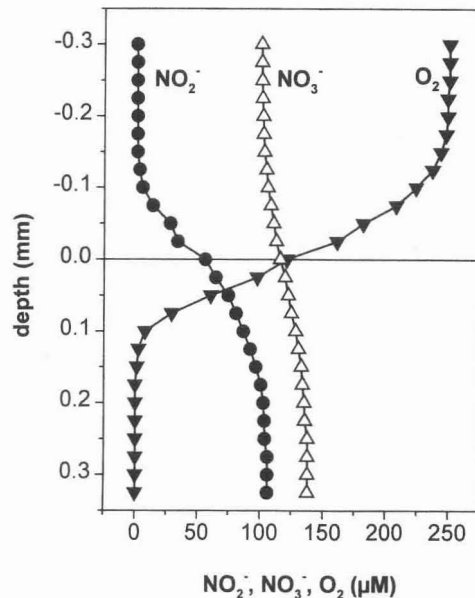

FIG. 3. Profiles of NO$_2^-$ (●), NO$_3^-$ (△), and O$_2$ (▼) in a nitrifying aggregate from a fluidized bed reactor. The aggregate surface is at a depth of 0.
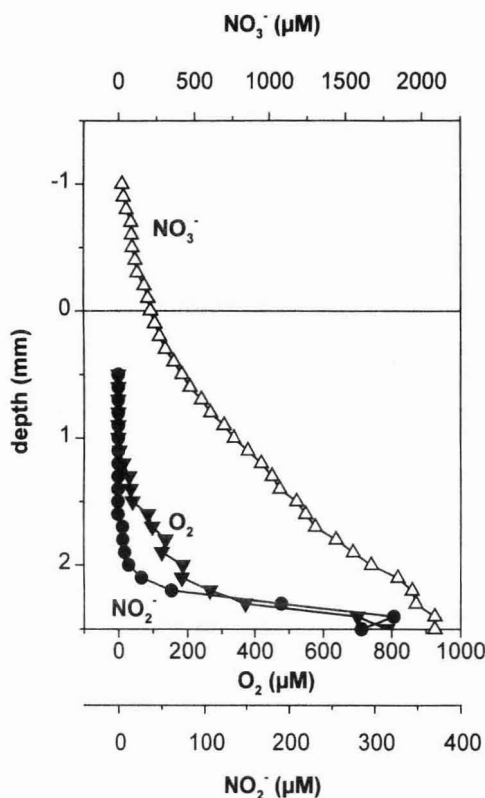
NO$_3^-$ (µM)

FIG. 4. Profiles of NO$_2^-$ (●), NO$_3^-$ (△), and O$_2$ (▼) in a nitrifying/denitrifying biofilm from a membrane reactor. The biofilm surface is at a depth of 0; the membrane surface is at a depth of 2.5 mm.

their signal instability after and during contact with biomass. The noise sensitivity was effectively cured by shielding (16), which functions much better and is more convenient than a Faraday cage. The latter two problems will be discussed below.

The interference of other ions is partly caused by the need for an extremely small sensor tip to stabilize the liquid membrane in the tip by capillary force. The contribution to the signal of ion shunts through the glass wall and at the glass-LIX interface becomes increasingly important with smaller tip diameter and can dominate over the ion exchange through the LIX membrane (6). Most likely, this phenomenon was responsible for the poor behavior of 3-µm nitrite microelectrodes. The ion shunts can to some extent be countered by good silanization (23). The problem was solved by increasing the tip diameter. However, by increasing the tip size, the capillary force was reduced and, therefore, the membrane had to be stabilized in the tip by gelation with PVC. This resulted in a nitrite microsensor with a response similar to that of a macroelectrode. Enlarging the tip also increased the mechanical strength of the microsensor. A tip diameter of ca. 10 µm excludes use for intracellular studies but is excellent for probing microbial mats and biofilms. With exception of the pH LIX, the limited selectivity of ionophores requires calibration of LIX sensors in the experimental medium.

Irregular behavior of LIX sensors, such as sudden potential shifts, loss of signal, drift, and strong increase of response time, is observed especially during measurements in environmental samples with high cell densities, such as biofilms from wastewater treatment plants and microbial mats (27). This phenomenon is unpredictable—no problems occurred in sediments (9, 16, 31) or in methanogenic and nitrifying aggregates (8)—but when it occurs it affects all types of LIX electrodes. Sensor damage occurs during contact with the biomass and not during penetration of the boundary layer, indicating that the damage on the LIX membrane is caused by direct interaction with a water-insoluble biomass component. Since no physical damage was observed, we suspect a chemical change of the LIX membrane by a hydrophobic substance. The thin protein coating shields the hydrophobic LIX membrane surface effectively from interaction with hydrophobic surfaces in the environmental sample matrix. Cross-linked BSA forms dense layers in which the diffusion coefficient is 3 orders of magnitude lower than in water (18). The unknown damaging substance cannot penetrate the protein layer, either because its pore size is too small or because the damaging substance is too hydrophobic to penetrate the hydrophilic coating. The extra diffusional resistance does not significantly increase the response time as shown by the pH and nitrate sensors. Possibly, the slower response of the nitrite sensor is caused by reversible binding of nitrite to the coating.

As a result of the improvements (increased tip diameter, gelation with PVC, protein coating, and shielding), LIX microsensors can now be used in a variety of environmental samples, outside the laboratory and even in operating reactors, as illustrated by the profiles in Fig. 4.

The irreversible damage of the nitrite sensor by sulfide is caused by reduction of the Co(III) in the porphyrin ring (11). Sulfite will have the same effect. This phenomenon is a problem for measurements in anaerobic biofilms and sediments, as nitrite and sulfide may be present simultaneously. However, from the continuous drift induced by sulfide it can easily be recognized when the nitrite signal becomes unreliable.

In both the denitrifying and nitrifying/denitrifying biofilms the nitrite and nitrate profiles were shaped differently. The straight profiles of nitrate and nitrite showed that in the aerobic zone no significant nitrogen conversions occurred. No nitrite formation was observed in the aerobic zone, which was reported to indicate aerobic denitrification (4). The nitrite accumulation was the highest where nitrate consumption occurred, just below the oxic zone. Nitrite diffused from this zone into the deeper layers of the biofilm, where it was further reduced, and it diffused out of the biofilm into the bulk liquid. The nitrite peak showed that the reduction rate of nitrate is locally higher than that of nitrite. Denitrification does not always lead to nitrite accumulation, since in the nitrifying/denitrifying biofilm a nitrite peak was observed in the nitrifying zone but not in the anaerobic denitrifying zone.

In the nitrifying aggregates the ammonium oxidation was faster than the nitrite oxidation. From the interfacial gradients it can be calculated that about six times more nitrite is produced than nitrate. No nitrite peak was observed. A previous study on aggregates from the same reactor showed complete ammonium conversion to nitrate (8). Also, the appearance of the aggregates was changed from smooth spheres into a structure resembling a bunch of grapes. This might have been caused by a population change due to a reactor breakdown 8 months prior to the measurements. The 200-µm-thick zone where nitrite and nitrate were formed did not perfectly match with the oxygen penetration of 150 µm. This may be attributed to the rather irregular surface, which made it difficult to match

the different profiles. Alternatively, the 15-min incubation time before the start of the measurements may have been too short to develop steady state.

Nitrite profiles often show a peak, as can be expected from an intermediate that is both produced and consumed. Therefore, nitrite efflux from biofilms, sediments, and aggregates can be minimal, even when considerable concentrations are present. The maximum nitrite concentrations measured in the biofilms ranged from 80 to 400 μM. Although nitrite is generally known to be toxic, consistent data are hard to find. The effect of nitrite is strongly species dependent. Nitrite is highly toxic for *Nitrobacter agilis* (K_i for HNO_2, 10 to 20 μM) but not very toxic for *Nitrosomonas europaea* (K_i HNO_2, >50 mM) (15). A concentration of 140 μM nitrite reduced methanogenesis in sewage sludge by 60%, and 700 μM totally blocked methanogenesis (5). A concentration of 700 μM nitrite killed 50% of a crayfish population in 48 h (13), 5 μM nitrite increased the susceptibility of trout to pathogens by 50% (3), and 100 μM nitrite decreased ion uptake by plant roots (35). This list is certainly not comprehensive, but it can be concluded that the measured nitrite concentrations will have a variety of physiological effects on plants, animals, and bacteria.

These preliminary studies showed that considerable nitrite concentrations are present in nitrifying and denitrifying biofilms, as well as in biofilms where both nitrification and denitrification occur simultaneously. The nitrite-containing zones were narrow, in the order of 0.5 to 1 mm in thickness. Since alternative methods such as pore water extraction or slicing do not have sufficient spatial resolution, accurate profiles could be detected only with microsensors. The nitrite microsensor is expected to be highly useful for further studies to elucidate which factors regulate the nitrite concentration in biofilms and sediments.

REFERENCES

1. **Ammann, D., T. Bührer, U. Schefer, M. Müller, and W. Simon.** 1987. Intracellular neutral carrier-based Ca^{2+} microelectrode with sub-nanomolar detection limit. Pflueg. Arch. **409**:223–228.
2. **Balls, P. W., N. Brockie, J. Dobson, and W. Johnston.** 1996. Dissolved oxygen and nitrification in the upper Forth estuary during summer (1982–1992): patterns and trends. Estuarine Coastal Shelf Sci. **42**:117–134.
3. **Carballo, M., M. J. Muñoz, M. Cuellar, and J. V. Tarazona.** 1995. Effects of waterborne copper, cyanide, ammonia, and nitrite on stress parameters and changes in susceptibility to saprolegniosis in rainbow trout (*Oncorhynchus mykiss*). Appl. Environ. Microbiol. **61**:2108–2112.
4. **Carter, J. P., Y. H. Hsiao, S. Spiro, and D. J. Richardson.** 1995. Soil and sediment bacteria capable of aerobic nitrate respiration. Appl. Environ. Microbiol. **61**:2852–2858.
5. **Chen, K. C., and Y. F. Lin.** 1993. The relationship between denitrifying bacteria and methanogenic bacteria in a mixed culture system of acclimated sludge. Water Res. **27**:1749–1759.
6. **Dagustino, M., and C. O. Lee.** 1982. Neutral carrier Na^+ and Ca^+ selective microelectrodes for intracellular application. Biophys. J. **40**:199–204.
7. **Davey, J. T., P. G. Watson, R. H. Bruce, and P. E. Frickers.** 1990. An instrument for the monitoring and collection of the vented burrow fluids of benthic infauna in sediment microcosms and its application to the polychaetes *Hediste diversicolor* and *Arenicola marina*. J. Exp. Mar. Biol. Ecol. **139**:135–149.
8. **de Beer, D., J. C. van den Heuvel, and S. P. P. Ottengraf.** 1993. Microelectrode measurements of activity distribution in nitrifying bacterial aggregates.

Appl. Environ. Microbiol. **59**:573–579.
9. **de Beer, D., J. P. Sweerts, and J. C. van den Heuvel.** 1991. Microelectrode measurement of ammonium profiles in freshwater sediments. FEMS Microbiol. Ecol. **86**:1–6.
10. **Doblander, C., and R. Lackner.** 1996. Metabolism and detoxification of nitrite by trout hepatocytes. Biochim. Biophys. Acta **1289**:270–274.
11. **Freeman, M. K., and L. G. Bachas.** 1992. Fiber optic sensor for NO_x. Anal. Chim. Acta **256**:269–275.
12. **Galvao, H. M., and A. T. Fritz.** 1991. Microbial tropodynamics in a salt marsh. Mar. Microb. Food Webs **5**:13–26.
13. **Harris, R. R., and S. Coley.** 1991. The effects of nitrite on chloride regulation in the crayfish *Pacifastus leniusculus dana* crustacea decapoda. J. Comp. Physiol. **161**:199–206.
14. **Hatton, D., and W. F. Pickering.** 1991. Determination of nitrite in lake sediments. Chem. Speciation Bioavailability **3**:1–8.
15. **Hunik, J. H.** 1993. Engineering aspects of nitrification with immobilized cells. Ph.D. thesis, Wageningen Agricultural University, Wageningen, The Netherlands.
16. **Jensen, K., N. P. Revsbech, and L. P. Nielsen.** 1993. Microscale distribution of nitrification activity in sediment determined with a shielded microsensor for nitrate. Appl. Environ. Microbiol. **59**:3287–3296.
17. **Jeroschewski, P., C. Steukart, and M. Kühl.** 1996. An amperometric microsensor for the determination of H_2S in aquatic environments. Anal. Chem., in press.
18. **Kimura, J., A. Saito, N. Ito, S. Nakamoto, and T. Kuriyama.** 1989. Evaluation of an albumin based spin-coated enzyme-immobilized membrane for an ISFET glucose sensor by computer simulation. J. Membr. Sci. **43**:291–305.
19. **Kristensen, E., M. H. Jensen, and R. C. Aller.** 1991. Direct measurement of dissolved inorganic nitrogen exchange and denitrification in individual polychaete *Nereis virens* burrows. J. Mar. Res. **49**:355–378.
20. **Larsen, L. H., N. P. Revsbech, and S. J. Binnerup.** 1996. A microsensor for nitrate based on immobilized denitrifying bacteria. Appl. Environ. Microbiol. **62**:1248–1251.
21. **Manem, J. A., and B. E. Rittmann.** 1992. The effects of fluctuations in biodegradable organic matter on nitrification filters. J. Am. Water Works Assoc. **84**:147–151.
22. **Miller, A. J.** 1995. Ion-selective microelectrodes for measurement of intracellular ion concentrations. Methods Cell Biol. **49**:275–291.
23. **Muñoz, J. L., F. Deyhimi, and J. A. Coles.** 1983. Silanization of glass in the making of ion-selective microelectrodes. J. Neurosci. Methods **8**:231–247.
24. **Özoguz, G., N. Räbiger, and H. Baumgärtl.** 1994. Membraneinsatz zur Erhöhung der Nitrifikationsleistung durch getrennte Substratversorgung. Bioforum **17**:129–135.
25. **Pedersen, F. V., and L. P. Nielsen.** Production and consumption of nitrite in biofilms measured by ^{15}N-isotope techniques. Submitted for publication.
26. **Revsbech, N. P.** 1989. An oxygen microsensor with a guard cathode. Limnol. Oceanogr. **34**:474–478.
27. **Revsbech, N. P.** 1994. Analysis of microbial mats by use of electrochemical microsensors: recent advances, p. 135. *In* L. Stal and P. Caumette (ed.), Microbial mats. Springer, Berlin, Germany.
28. **Revsbech, N. P., P. B. Cristensen, L. P. Nielsen, and J. Sorensen.** 1988. A combined oxygen and nitrous oxide microsensor for denitrification studies. Appl. Environ. Microbiol. **54**:2245–2249.
29. **Schaller, U., E. Bakker, U. E. Spichiger, and E. Pretsch.** 1994. Nitriteselective microelectrodes. Talanta **41**:1001–1005.
30. **Stepanek, R., B. Kräutler, P. Schulthess, B. Lindeman, D. Ammann, and W. Simon.** 1986. Aquocyanocobalt(III)-hepta(2-phenylethyl)-cobrynate as a cationic carrier for nitrite selective liquid membrane electrodes. Anal. Chim. Acta **182**:83–90.
31. **Sweerts, J-P. R. A., and D. de Beer.** 1989. Microelectrode measurements of nitrate gradients in the littoral and profundal sediments of a meso-eutrophic lake (Lake Vechten, The Netherlands). Appl. Environ. Microbiol. **55**:754–757.
32. **Tiedje, J. M.** 1988. Ecology of denitrification and dissimilatory nitrate reduction to ammonium, p. 179. *In* A. J. Zehnder (ed.), Biology of anaerobic microorganisms. John Wiley, New York, N.Y.
33. **Tsien, R. Y., and T. J. Rink.** (1981) Ca^{2+}-selective electrodes: a novel PVC gelled neutral carrier mixture compared with other currently available sensors. J. Neurosci. Methods **4**:73–86.
34. **von Schulthess, R., M. Kühni, and W. Gujer.** 1995. Release of nitric and nitrous oxides from denitrifying activated sludge. Water Res. **29**:215–226.
35. **Zsoldos, F., E. Haunold, A. Vashegyi, and P. Herger.** 1993. Nitrite in the root zone and its effects on ion uptake and growth of wheat seedlings. Physiol. Plant. **89**:626–631.

the different profiles. Alternatively, the 15-min incubation time before the start of the measurements may have been too short to develop steady state.

Nitrite profiles often show a peak, as can be expected from an intermediate that is both produced and consumed. Therefore, nitrite efflux from biofilms, sediments, and aggregates can be minimal, even when considerable concentrations are present. The maximum nitrite concentrations measured in the biofilms ranged from 80 to 400 μM. Although nitrite is generally known to be toxic, consistent data are hard to find. The effect of nitrite is strongly species dependent. Nitrite is highly toxic for *Nitrobacter agilis* (K_i for HNO_2, 10 to 20 μM) but not very toxic for *Nitrosomonas europaea* (K_i HNO_2, >50 mM) (15). A concentration of 140 μM nitrite reduced methanogenesis in sewage sludge by 60%, and 700 μM totally blocked methanogenesis (5). A concentration of 700 μM nitrite killed 50% of a crayfish population in 48 h (13), 5 μM nitrite increased the susceptibility of trout to pathogens by 50% (3), and 100 μM nitrite decreased ion uptake by plant roots (35). This list is certainly not comprehensive, but it can be concluded that the measured nitrite concentrations will have a variety of physiological effects on plants, animals, and bacteria.

These preliminary studies showed that considerable nitrite concentrations are present in nitrifying and denitrifying biofilms, as well as in biofilms where both nitrification and denitrification occur simultaneously. The nitrite-containing zones were narrow, in the order of 0.5 to 1 mm in thickness. Since alternative methods such as pore water extraction or slicing do not have sufficient spatial resolution, accurate profiles could be detected only with microsensors. The nitrite microsensor is expected to be highly useful for further studies to elucidate which factors regulate the nitrite concentration in biofilms and sediments.

ACKNOWLEDGMENTS

REFERENCES

1. **Ammann, D., T. Bührer, U. Schefer, M. Müller, and W. Simon.** 1987. Intracellular neutral carrier-based Ca^{2+} microelectrode with sub-nanomolar detection limit. Pflueg. Arch. **409:**223–228.
2. **Balls, P. W., N. Brockie, J. Dobson, and W. Johnston.** 1996. Dissolved oxygen and nitrification in the upper Forth estuary during summer (1982–1992): patterns and trends. Estuarine Coastal Shelf Sci. **42:**117–134.
3. **Carballo, M., M. J. Muñoz, and J. V. Tarazona.** 1995. Effects of waterborne copper, cyanide, ammonia, and nitrite on stress parameters and changes in susceptibility to saprolegniosis in rainbow trout (*Oncorhynchus mykiss*). Appl. Environ. Microbiol. **61:**2108–2112.
4. **Carter, J. P., Y. H. Hsiao, S. Spiro, and D. J. Richardson.** 1995. Soil and sediment bacteria capable of aerobic nitrate respiration. Appl. Environ. Microbiol. **61:**2852–2858.
5. **Chen, K. C., and Y. F. Lin.** 1993. The relationship between denitrifying bacteria and methanogenic bacteria in a mixed culture system of acclimated sludge. Water Res. **27:**1749–1759.
6. **Dagustino, M., and C. O. Lee.** 1982. Neutral carrier Na^+ and Ca^+ selective microelectrodes for intracellular application. Biophys. J. **40:**199–204.
7. **Davey, J. T., P. G. Watson, R. H. Bruce, and P. E. Frickers.** 1990. An instrument for the monitoring and collection of the vented burrow fluids of benthic infauna in sediment microcosms and its application to the polychaetes *Hediste diversicolor* and *Arenicola marina.* J. Exp. Mar. Biol. Ecol. **139:**135–149.
8. **de Beer, D., J. C. van den Heuvel, and S. P. P. Ottengraf.** 1993. Microelectrode measurements of activity distribution in nitrifying bacterial aggregates.

Appl. Environ. Microbiol. **59:**573–579.
9. **de Beer, D., J. P. Sweerts, and J. C. van den Heuvel.** 1991. Microelectrode measurement of ammonium profiles in freshwater sediments. FEMS Microbiol. Ecol. **86:**1–6.
10. **Doblander, C., and R. Lackner.** 1996. Metabolism and detoxification of nitrite by trout hepatocytes. Biochim. Biophys. Acta **1289:**270–274.
11. **Freeman, M. K., and L. G. Bachas.** 1992. Fiber optic sensor for NO_x. Anal. Chim. Acta **256:**269–275.
12. **Galvao, H. M., and A. T. Fritz.** 1991. Microbial tropodynamics in a salt marsh. Mar. Microb. Food Webs **5:**13–26.
13. **Harris, R. R., and S. Coley.** 1991. The effects of nitrite on chloride regulation in the crayfish *Pacifastus leniusculus dana* crustacea decapoda. J. Comp. Physiol. **161:**199–206.
14. **Hatton, D., and W. F. Pickering.** 1991. Determination of nitrite in lake sediments. Chem. Speciation Bioavailability **3:**1–8.
15. **Hunik, J. H.** 1993. Engineering aspects of nitrification with immobilized cells. Ph.D. thesis, Wageningen Agricultural University, Wageningen, The Netherlands.
16. **Jensen, K., N. P. Revsbech, and L. P. Nielsen.** 1993. Microscale distribution of nitrification activity in sediment determined with a shielded microsensor for nitrate. Appl. Environ. Microbiol. **59:**3287–3296.
17. **Jeroschewski, P., C. Steukart, and M. Kühl.** 1996. An amperometric microsensor for the determination of H_2S in aquatic environments. Anal. Chem., in press.
18. **Kimura, J., A. Saito, N. Ito, S. Nakamoto, and T. Kuriyama.** 1989. Evaluation of an albumin based spin-coated enzyme-immobilized membrane for an ISFET glucose sensor by computer simulation. J. Membr. Sci. **43:**291–305.
19. **Kristensen, E., M. H. Jensen, and R. C. Aller.** 1991. Direct measurement of dissolved inorganic nitrogen exchange and denitrification in individual polychaete *Nereis virens* burrows. J. Mar. Res. **49:**355–378.
20. **Larsen, L. H., N. P. Revsbech, and S. J. Binnerup.** 1996. A microsensor for nitrate based on immobilized denitrifying bacteria. Appl. Environ. Microbiol. **62:**1248–1251.
21. **Manem, J. A., and B. E. Rittmann.** 1992. The effects of fluctuations in biodegradable organic matter on nitrification filters. J. Am. Water Works Assoc. **84:**147–151.
22. **Miller, A. J.** 1995. Ion-selective microelectrodes for measurement of intracellular ion concentrations. Methods Cell Biol. **49:**275–291.
23. **Muñoz, J. L., F. Deyhimi, and J. A. Coles.** 1983. Silanization of glass in the making of ion-selective microelectrodes. J. Neurosci. Methods **8:**231–247.
24. **Özoguz, G., N. Räbiger, and H. Baumgärtl.** 1994. Membraneinsatz zur Erhöhung der Nitrifikationsleistung durch getrennte Substratversorgung. Bioforum **17:**129–135.
25. **Pedersen, F. V., and L. P. Nielsen.** Production and consumption of nitrite in biofilms measured by ^{15}N-isotope techniques. Submitted for publication.
26. **Revsbech, N. P.** 1989. An oxygen microsensor with a guard cathode. Limnol. Oceanogr. **34:**474–478.
27. **Revsbech, N. P.** 1994. Analysis of microbial mats by use of electrochemical microsensors: recent advances, p. 135. *In* L. Stal and P. Caumette (ed.), Microbial mats. Springer, Berlin, Germany.
28. **Revsbech, N. P., P. B. Cristensen, L. P. Nielsen, and J. Sorensen.** 1988. A combined oxygen and nitrous oxide microsensor for denitrification studies. Appl. Environ. Microbiol. **54:**2245–2249.
29. **Schaller, U., E. Bakker, U. E. Spichiger, and E. Pretsch.** 1994. Nitriteselective microelectrodes. Talanta **41:**1001–1005.
30. **Stepanek, R., B. Kräutler, P. Schulthess, B. Lindeman, D. Ammann, and W. Simon.** 1986. Aquocyanocobalt(III)-hepta(2-phenylethyl)-cobrynate as a cationic carrier for nitrite selective liquid membrane electrodes. Anal. Chim. Acta **182:**83–90.
31. **Sweerts, J-P. R. A., and D. de Beer.** 1989. Microelectrode measurements of nitrate gradients in the littoral and profundal sediments of a meso-eutrophic lake (Lake Vechten, The Netherlands). Appl. Environ. Microbiol. **55:**754–757.
32. **Tiedje, J. M.** 1988. Ecology of denitrification and dissimilatory nitrate reduction to ammonium, p. 179. *In* A. J. Zehnder (ed.), Biology of anaerobic microorganisms. John Wiley, New York, N.Y.
33. **Tsien, R. Y., and T. J. Rink.** (1981) Ca^{2+}-selective electrodes: a novel PVC gelled neutral carrier mixture compared with other currently available sensors. J. Neurosci. Methods **4:**73–86.
34. **von Schulthess, R., M. Kühni, and W. Gujer.** 1995. Release of nitric and nitrous oxides from denitrifying activated sludge. Water Res. **29:**215–226.
35. **Zsoldos, F., E. Haunold, A. Vashegyi, and P. Herger.** 1993. Nitrite in the root zone and its effects on ion uptake and growth of wheat seedlings. Physiol. Plant. **89:**626–631.

32

Chapter 4

Identification and Activities In Situ

of *Nitrosospira* and *Nitrospira* spp. as Dominant Populations

in a Nitrifying Fluidized Bed Reactor
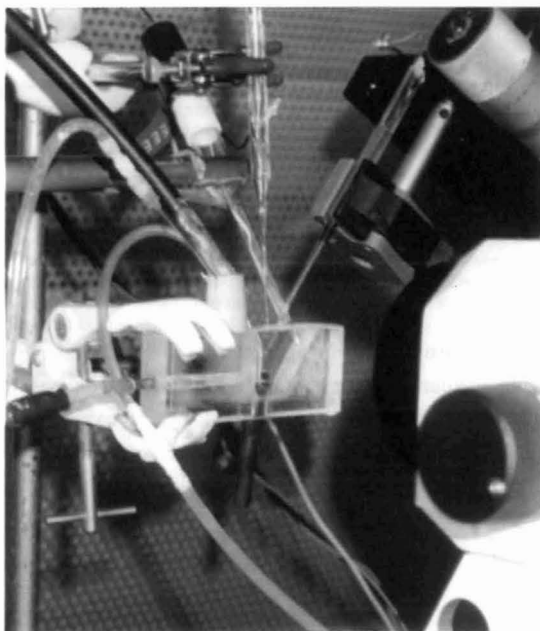
Front page:

Flow cell for microsensor measurements in aggregates. The bacterial aggregate is fixed by two needles and perfused with medium via the tubing to the left. An oxygen microsensor (middle) is inserted in the medium chamber to monitor the bulk water oxygen concentration during the measurements. The profiling microsensor is mounted on a micromanipulator to the right. Sensor tip and aggregate surface are watched by help of a dissection microscope (right, in front).

Identification and Activities In Situ of *Nitrosospira* and *Nitrospira* spp. as Dominant Populations in a Nitrifying Fluidized Bed Reactor

ANDREAS SCHRAMM,[1]* DIRK DE BEER,[1] MICHAEL WAGNER,[2] AND RUDOLF AMANN[1]

*Max-Planck-Institut für Marine Mikrobiologie, D-28359 Bremen,[1] and Lehrstuhl für Mikrobiologie,
Technische Universität München, D-80290 Munich,[2] Germany*

Bacterial aggregates from a chemolithoautotrophic, nitrifying fluidized bed reactor were investigated with microsensors and rRNA-based molecular techniques. The microprofiles of O_2, NH_4^+, NO_2^-, and NO_3^- demonstrated the occurrence of complete nitrification in the outer 125 μm of the aggregates. The ammonia oxidizers were identified as members of the *Nitrosospira* group by fluorescence in situ hybridization (FISH). No ammonia- or nitrite-oxidizing bacteria of the genus *Nitrosomonas* or *Nitrobacter*, respectively, could be detected by FISH. To identify the nitrite oxidizers, a 16S ribosomal DNA clone library was constructed and screened by denaturing gradient gel electrophoresis and selected clones were sequenced. The organisms represented by these sequences formed two phylogenetically distinct clusters affiliated with the nitrite oxidizer *Nitrospira moscoviensis*. 16S rRNA-targeted oligonucleotide probes were designed for in situ detection of these organisms. FISH analysis showed that the dominant populations of *Nitrospira* spp. and *Nitrosospira* spp. formed separate, dense clusters which were in contact with each other and occurred throughout the aggregate. A second, smaller, morphologically and genetically different population of *Nitrospira* spp. was restricted to the outer nitrifying zones.

Lithoautotrophic nitrification, the sequential transformation of NH_4^+ via NO_2^- to NO_3^-, is typically catalyzed by two phylogenetically distinct groups of bacteria, i.e., the ammonia-oxidizing bacteria and the nitrite-oxidizing bacteria. All characterized freshwater ammonia oxidizers belong to a coherent group within the β subclass of the class *Proteobacteria*, comprising the genera *Nitrosomonas* (formerly *Nitrosococcus mobilis* and *Nitrosomonas*), and *Nitrosospira* (formerly *Nitrosospira*, *Nitrosovibrio*, and *Nitrosolobus*) (14, 30). For a long time, all nitrite oxidizers isolated from freshwater habitats belonged to the genus *Nitrobacter* within the α subclass of *Proteobacteria* (7). Recently, *Nitrospira moscoviensis*, a member of an independent phylum (13), was isolated from a corroded iron pipe in Moscow.

Although nitrification is the central aerobic process of microbial nitrogen cycling, only limited knowledge about the ecological relevance of its various protagonists is available. Medium selectivity and the ability of some *Nitrosomonas* strains to outcompete other ammonia oxidizers in liquid cultures (6) made *Nitrosomonas europaea* the most commonly isolated and best investigated ammonia oxidizer. However, there is increasing evidence of dominance by other species or genera in particular environments (24). This situation might be similar for the *Nitrobacter* spp., the best-investigated nitrite oxidizers. The introduction of molecular techniques into microbial ecology has enabled the detection and reliable quantification of natural populations of nitrifiers. Based on comparative 16S rRNA sequence analysis, PCR primers (15, 20, 31, 35) and oligonucleotide probes (16, 21, 33) specific for ammonia oxidizers from the β subclass of the class *Proteobacteria* have been developed. Application of specific PCR in combination with the construction of clone libraries (28) or denaturing gradient gel electro-

phoresis (DGGE) (18) revealed a high genetic diversity within the ammonia oxidizers of the β subclass of *Proteobacteria* and a wide distribution of *Nitrosospira*-like sequences in natural samples like lake water, sediments, or soils. On the other hand, quantitative hybridizations with oligonucleotide probes showed that in ammonium-rich systems like activated sludge (33) or biofilm reactors (21, 26), the dominant ammonia oxidizers were members of the genus *Nitrosomonas*.

DNA from the genus *Nitrobacter* has been amplified from soil by using specific PCR primers (12), and oligonucleotide probes have been designed for use in quantitative hybridizations (34). However, with the exception of two biofilm reactors (21, 26), no *Nitrobacter* spp. could be detected in activated sludge, eutrophic and oligotrophic biofilms, river water (21, 34), or aquaria (16) by using molecular techniques. It was therefore suggested that other nitrite oxidizers are present and active in these systems. Consistent with this hypothesis, Hovanec et al. recently reported *Nitrospira* spp. to be associated with nitrite oxidation in freshwater aquaria (17).

In this study, the nitrifying community of a chemolithoautotrophic fluidized bed reactor was investigated. The reactor, originally operated with high ammonia concentrations (11), was for this study operated with low ammonia concentrations, so that it rather resembled a natural freshwater habitat than a wastewater treatment system (24). The construction of a 16S rRNA clone library from directly isolated DNA was combined with fluorescence in situ hybridization (4). Microsensor measurements to relate the localization of the nitrifying populations to functional zones within the biofilm were performed.

MATERIALS AND METHODS

Nitrifying aggregates. The lab-scale fluidized bed reactor used as a source for nitrifying aggregates has been described in detail before (11). However, the recirculation rate was increased from 1 to 1.8 ml/s, resulting in ammonium limitation in the reactor instead of oxygen limitation; i.e., ammonium was depleted 50 cm above the inlet but oxygen was still present. At the time of sampling, the reactor had been running for more than 8 months under constant conditions. The

* Corresponding author. Mailing address: Max-Planck-Institut für Marine Mikrobiologie, Celsiusstraße 1, D-28359 Bremen, Germany. Phone: 49 421 2028 834. Fax: 49 421 2028 690. E-mail: aschramm@mpi-bremen.de.

Structure-function analysis of a nitrifying bioreactor

TABLE 1. Oligonucleotide probes

Probe	Specificity	Probe sequence (5'-3')	Target site[a] (rRNA positions)	% FA[b]	NaCl (mM)[c]	Reference
EUB338	Bacteria	GCTGCCTCCCGTAGGAGT	16S (338–355)	20	225	3
ALF1b	α Subclass of the class *Proteobacteria*, several members of the δ subclass of *Proteobacteria*, genus *Nitrospira*, most spirochetes	CGTTCGYTCTGAGCCAG	16S (19–35)	20	225	19
BET42a	β Subclass of *Proteobacteria*	GCCTTCCCACTTCGTTT	23S (1027–1043)	35[d]	80	19
GAM42a	γ Subclass of *Proteobacteria*	GCCTTCCCACATCGTTT	23S (1027–1043)	35[e]	80	19
NSO190	Ammonia-oxidizing β-subclass *Proteobacteria*	CGATCCCCTGCTTTTCTCC	16S (190–208)	55	20	21
NSV443	*Nitrosospira* spp.	CCGTGACCGTTTCGTTCCG	16S (444–462)	30	112	21
NSM156	*Nitrosomonas* spp.	TATTAGCACATCTTTCGAT	16S (653–670)	5	636	21
NIT3	*Nitrobacter* spp.	CCTGTGCTCCATGCTCCG	16S (1035–1048)	40[f]	56	34
NSR826	Freshwater *Nitrospira* spp.	GTAACCGCCGACACTTA	16S (826–843)	20	225	This study
NSR1156	Freshwater *Nitrospira* spp.	CCCGTTCTCCTGGGCAGT	16S (1156–1173)	30	112	This study
NSR447	Clones g6, o9, and o14	GGTTTCCCGTTCCATCTT	16S (447–464)	30	112	This study

[a] *E. coli* numbering (9).
[b] Percentage formamide in the hybridization buffer.
[c] Millimolar concentration of sodium chloride in the washing buffer.
[d] Used with an equimolar amount of unlabeled competitor oligonucleotide GAM42.
[e] Used with an equimolar amount of unlabeled competitor oligonucleotide BET42a.
[f] Used with an equimolar amount of unlabeled competitor oligonucleotide CNIT3 (34).

temperature was kept at 30°C, and the pH was adjusted to 8 in the aeration tank. Chemical parameters at the sampling point, 30 cm above the inlet, were as follows: $[O_2]$, 150 μM; $[NH_4^+]$, 40 μM; $[NO_2^-]$, 6.7 μM; $[NO_3^-]$, 5.5 mM; pH 7.7. No organic carbon source was added to the reactor. The nitrifying aggregates were irregularly shaped conglomerates with diameters of 1 to 2 mm and consisted of spheroid subunits with ca. 50-μm diameters.

Microsensor measurements. Clark-type O_2 microsensors with internal references and guard cathodes were prepared and calibrated as described previously (25). Tip diameters were <10 μm, and stirring sensitivities were <2%.

Liquid ion-exchanging membrane (LIX) microsensors for NH_4^+, NO_2^-, and NO_3^- with solidified tips and protein coatings were prepared as described by de Beer et al. (10). The tip diameters were 5 μm for NH_4^+ and NO_3^- microsensors and 15 μm for NO_2^- microsensors. Calibration was done in a dilution series of NH_4^+, NO_2^-, and NO_3^- in the medium used for the measurements.

Aggregates were attached to insect needles, placed in a flow cell, and perfused with medium as described previously (11). $[O_2]$, $[NH_4^+]$, $[NO_2^-]$, pH, and temperature in the medium were adjusted to in situ conditions; $[NO_3^-]$ was 100 μM. After 15 min of incubation, sufficient time to reach steady state, microprofiles were recorded by moving the sensors with a motor-driven micromanipulator at depth steps of 25 μm from the bulk liquid into the aggregate. The position relative to the aggregate surface was determined with a dissection microscope.

Chemical analysis. $[NH_4^+]$, $[NO_2^-]$, and $[NO_3^-]$ in the reactor column were determined colorimetrically (Spectroquant; Merck, Darmstadt, Germany). $[O_2]$ and pH were measured by an O_2 microsensor and a pH electrode (Radiometer, Copenhagen, Denmark), respectively, which were positioned in the reactor at the sampling point.

DNA extraction. Aggregate samples were homogenized by vigorous vortexing and subjected to three freeze-thaw cycles. An aliquot of 200 μl was suspended in 500 μl of AE buffer (20 mM sodium acetate [pH 5.5], 1 mM EDTA), and 1 ml of hot phenol-chloroform-isoamyl alcohol (25:24:1) and 100 μl of 25% (wt/vol) sodium dodecyl sulfate (SDS) were added. The mixture was shaken at 60°C for 30 min and then chilled on ice. The subsequent hot phenol extraction was done as described in the protocol of Wawer et al. (36). Nucleic acids were resuspended in distilled, sterile water, and their quality was checked by agarose gel electrophoresis (1%, wt/vol).

Amplification and cloning of 16S rDNA. Almost-full-length bacterial 16S rRNA gene (rDNA) fragments were amplified from extracted DNA by the PCR. According to Muyzer et al. (23), primer pair GM3F (*Escherichia coli* 16S ribosomal DNA positions 8 to 24 [9])-GM4R (*E. coli* positions 1492 to 1507) was used. One microliter of the PCR product was directly ligated into the pGEM-T vector cloning system (Promega, Mannheim, Germany) and transformed into competent cells (high-efficiency *E. coli* JM109 [Promega]) as described in the manufacturer's instructions.

DGGE screening of the gene library. A 550-bp-long 16S rDNA fragment for DGGE analysis was directly amplified from each 16S rDNA clone by using 1 μl of cell suspension in the PCR. PCR and DGGE were performed as described by Muyzer et al. (22). For DGGE, a gradient of 35 to 65% denaturant at 60°C and an electrophoresis time of 17 h at 100 V were used.

16S rDNA sequencing. Plasmids were extracted and purified from clones of interest with the Wizard Plus Minipreps DNA purification system (Promega) in accordance with the manufacturer's instructions. Sequencing of the 16S rDNA inserts was done with a LICOR automated sequencer by MWG-Biotech, Ebersberg, Germany. Partial sequences (ca. 900 bases) and almost full sequences (ca. 1,500 bases) were determined on one strand.

Data analysis. Sequences were added to the 16S rRNA database of the Technical University Munich by use of the program package ARB (29). The tool ARB_EDIT was used for sequence alignment. The 16S rRNA-based phylogenetic tree was calculated by using distance matrix, maximum-parsimony, and maximum-likelihood analyses, and the topologies of the resulting trees were compared. Branchings not supported by all three methods are displayed as multifurcations. Only sequences that were at least 90% complete were used for tree reconstruction. Partial sequences were added by using maximum parsimony without changing the overall topology of the tree.

Based on the newly retrieved *Nitrospira*-like sequences, oligonucleotide probes were designed. Their specificity was evaluated by using the ARB tool PROBE_FUNCTIONS and the rRNA database of the Technical University Munich (version 3/97).

Fixation and sectioning of aggregates. For in situ hybridization, aggregates were fixed in 4% paraformaldehyde for 1 h at 4°C, washed in phosphate-buffered saline, and stored in a 1:1 mixture of phosphate-buffered saline and 96% ethanol at −20°C (2). Prior to the cryosectioning, aggregates were embedded in OCT compound (Tissue-Tek II; Miles, Elkhart, Ind.) overnight and subsequently frozen in a cryomicrotome (Mikrom, Walldorf, Germany) at −35°C. Semithick cryosections (5 to 20 μm) were cut at −17°C, and the single sections were placed on poly-L-lysine (0.01% solution; Sigma, Deisenhofen, Germany)-coated micro-
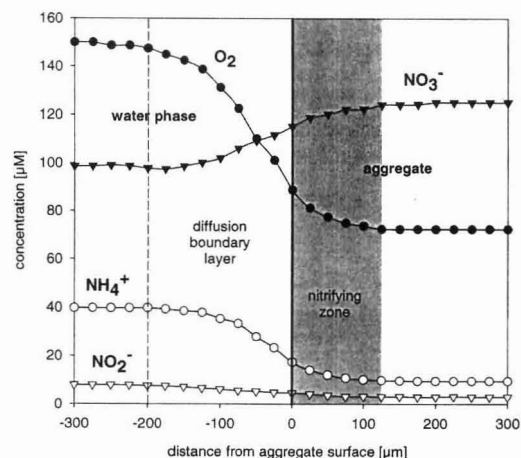

FIG. 1. Typical microprofiles of $[O_2]$, $[NH_4^+]$, $[NO_2^-]$, and $[NO_3^-]$ in nitrifying aggregates. The gray area marks the zone with nitrifying activity.

36

TABLE 2. Similarity matrix of clones affiliated with *Nitrospira* spp.

Species or clone	% Similarity to:						
	N. mosco-viensis	N. marina	b2	b18	b30	g6	o9
N. moscoviensis							
N. marina	89.3						
b2	92.8	87.8					
b18	92.1	87.5	97.1				
b30	92.8	88.2	98.9	97.5			
g6	95.8	87.6	91.7	92.6	91.6		
o9	95.8	87.6	90.1	92.3	90.1	99.5	
Clone 710-9 (17)	94.7	87.7	90.4	90.1	90.3	92.3	89.9

scopic slides. After air drying overnight to allow optimal attachment of the sections to the slides, the OCT compound was removed by dissolving it in a drop of distilled water and carefully dipping the slide in distilled water. Again the slides were allowed to air dry. Finally, the sections were dehydrated in an ethanol dilution series (50, 70, and 96%) and stored at room temperature.

Oligonucleotide probes. The following rRNA-targeted oligonucleotides were used (probe nomenclature according to Alm et al. [1] is given in parentheses): (i) EUB (S-D-Bact-0338-a-A-18); (ii) ALF1b (S-Sc-aProt-0019-a-A-17), BET42a (L-Sc-bProt-1027-a-A-17), and GAM42a (L-Sc-gProt-1027-a-A-17); (iii) NSO190 (S-*-Ntros-0190-a-A-19); (iv) NSV443 (S-*-Ntros-0443-a-A-19); (v) NSM156 (S-*-Nsom-0156-a-A-19); (vi) NIT3 (S-G-Nbac-1035-a-A-18); (vii) NSR1156 (S-*-Nspir-1156-a-A-18); (viii) NSR826 (S-*-Nspir-0826-a-A-18); and (ix) NSR447 (S-*-Nspir-0447-a-A-18). Oligonucleotides were synthesized and fluorescently labeled with a hydrophilic sulfoindocyanine dye, CY3 or CY5, or with 5(6)-carb-oxyfluorescein-*N*-hydroxysuccinimide ester (FLUOS) at the 5′ end by Interactiva

Biotechnologie GmbH (Ulm, Germany). All probe sequences, their hybridization conditions, and references are given in Table 1. The respective target organisms of probes specific for nitrifying bacteria are indicated in the phylogenetic tree (see Fig. 2).

In situ hybridization. All hybridizations were performed as described by Manz et al. (19) at 46°C for 90 min in hybridization buffer containing 0.9 M NaCl, formamide at the percentage shown in Table 1, 20 mM Tris-HCl (pH 7.4), and 0.01% SDS. The probe concentration was 5 ng/μl. Hybridization was followed by a stringent washing step at 48°C for 10 min in washing buffer containing 20 mM Tris-HCl (pH 7.4), NaCl at the concentrations listed in Table 1, and 0.01% SDS. Washing buffer was removed by rinsing the slides with distilled water. The slides were air dried, stained with 4,6-diamidino-2-phenylindole (DAPI; 1 μg/ml) for 10 min in the dark on ice, and finally rinsed again with distilled water. The slides were mounted in Vectashield (Vector Laboratories Inc., Burlingame, Calif.) to avoid bleaching and examined with a Zeiss Axioplan epifluorescence microscope equipped with filter sets CY3-HQ and CY5-HQ (Chroma Technology Corp., Brattleboro, Vt.) and 01 and 09 (Carl Zeiss, Jena, Germany). A Zeiss LSM 510 confocal laser scanning microscope, equipped with an Ar ion laser (488 nm) and two HeNe lasers (543 nm, 633 nm), was used to record optical sections as described by Wagner et al. (32).

Nucleotide sequence accession numbers. 16S rDNA sequence data obtained in this study will appear in the EMBL, GenBank, and DDBJ databases under accession no. AJ224038 to AJ224047.

RESULTS

Microsensor measurements. All investigated aggregates showed consumption of O_2, NH_4^+, and NO_2^- and production of NO_3^- (Fig. 1). The consumed NH_4^+ was completely converted to NO_3^- without an intermediate NO_2^- peak, and even NO_2^- present in the bulk water was consumed. This indicates that nitrite oxidation was at least as fast as ammonia oxidation.
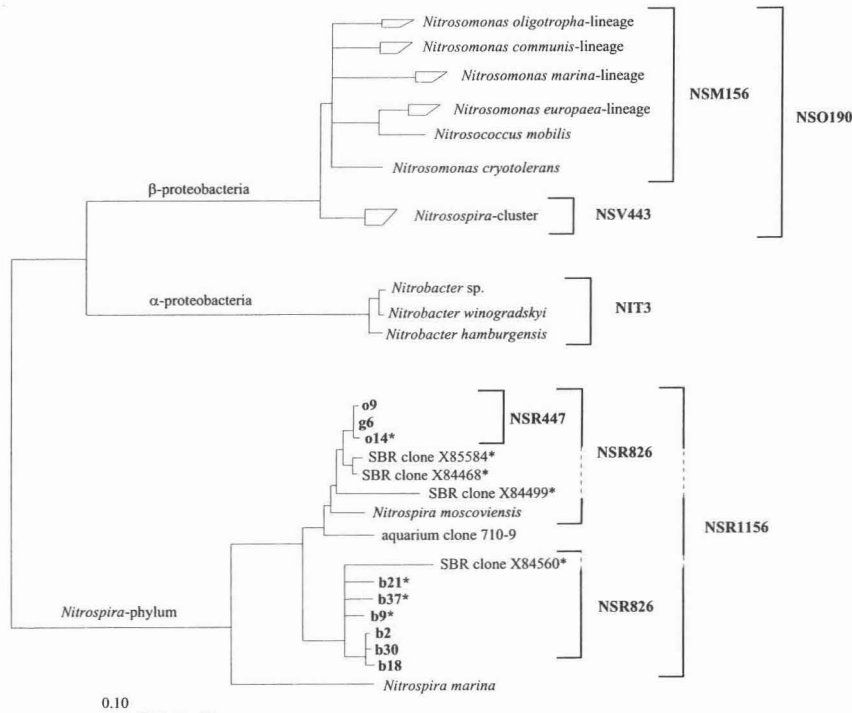
FIG. 2. Phylogenetic tree inferred from comparative analysis of 16S rRNA sequences. The tree is based on the results of maximum-likelihood analysis of sequences of >1,400 nucleotides. Partial sequences (marked by an asterisk) were added by maximum-parsimony analysis without changing the tree topology. Target organisms of probes used in this study are indicated by brackets; SBR clones are not sequenced in the probe target regions. The bar represents 0.1 estimated change per nucleotide.
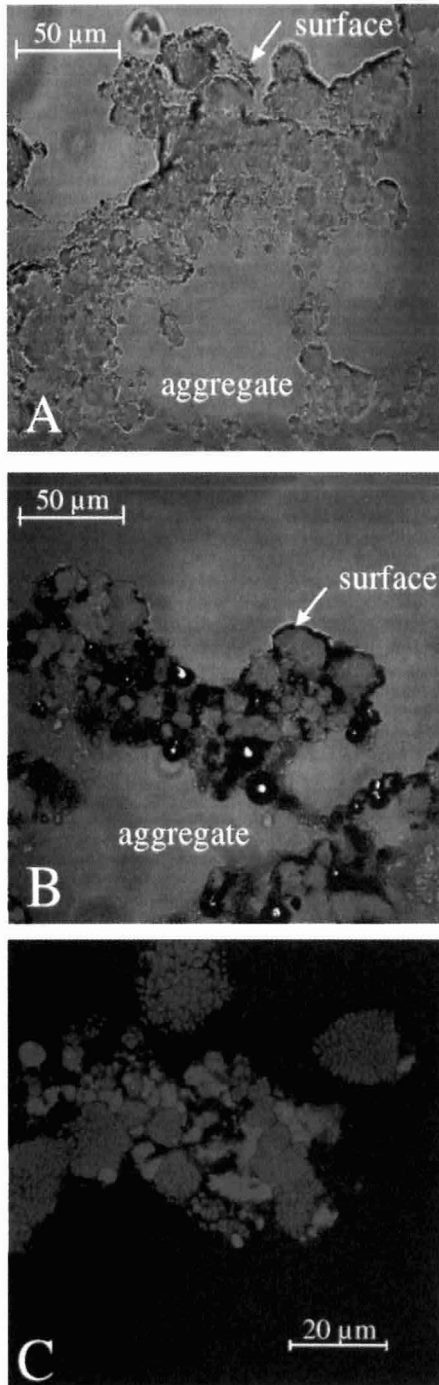
The active nitrifying zone was restricted to the outer 125 μm of the aggregates, although O_2 and NH_4^+ were both still present in the center of the aggregates at concentrations of about 75 and 10 μM, respectively.

FISH analysis. Phase-contrast light microscopy of the aggregate sections showed dense bacterial clusters, void spaces, and an irregular surface. If excited with blue light (488 nm), cells and extracellular material exhibited strong green autofluorescence, which made it difficult to reliably detect FLUOS-labeled oligonucleotide probes. Therefore, we exclusively applied CY3- or CY5-labeled probes for fluorescence in situ hybridization (FISH) analysis.

In situ hybridization with probe EUB proved that the ribosome content of most cells was sufficient for single-cell detection and that probes penetrated most, if not all, cell clusters. Only a few DAPI-stained cells in the central regions of aggregates were not detectable by FISH. Application of probes ALF1b, BET42a, and GAM42a indicated that the population consisted mainly of approximately equal fractions of ALF1b- and BET42a-positive cells. No cells hybridizing with probe GAM42a were detected. ALF1b-positive cells had diameters of below 0.6 μm and formed clusters 3 to 10 μm in size which were situated close to BET42a-positive cells that had diameters of ca. 1 μm and formed clusters 5 to 20 μm in size. Taken together, both populations made up >90% of all cells in the nitrifying zone as well as in the central region of the aggregates. Virtually all cells detected by probe BET42a also hybridized with probes NSO190 and NSV443 (Fig. 3), but no cells could be detected with probe NSM156. Thereby, the ammonia-oxidizing cells were identified as members of the genus *Nitrosospira*. In contrast, none of the cells detected by probe ALF1b hybridized with probe NIT3, which was specific for the nitrite-oxidizing bacteria of the α subclass of *Proteobacteria* of the genus *Nitrobacter*.

Clone library. A 16S rDNA clone library was constructed from aggregate samples to identify the unknown nitrite oxidizers. Fifty-five clones were selected at random. To avoid redundant sequencing, PCR-amplified rDNA fragments of all clones were analyzed by DGGE. Ten distinct categories of bands could be identified, and one representative of each category was selected for comparative sequence analysis. The 16S rRNA sequences of 9 of the 10 clones were affiliated with those of the nitrite oxidizers of the genus *Nitrospira* (13). Three clone sequences (g6, o9, and o14) were closely related to *Nitrospira moscoviensis* (96% similarity), whereas the other six (b2, b9, b18, b21, b30, and b37) formed a distinct branch within the genus *Nitrospira* but were still more closely related to *Nitrospira moscoviensis* (92% similarity) than to *Nitrospira marina* (87% similarity). Table 2 shows the 16S rRNA similarity values for the five almost-full-length sequences determined in this study, and Fig. 2 illustrates their affiliation in a phylogenetic tree. The remaining partial sequence (g14) was related to the 16S rRNA gene of a *Hyphomonas* sp. of the α subclass of *Proteobacteria*.

FIG. 3. In situ identification of nitrifying bacteria in aggregate sections demonstrating their spatial distribution. Images are composed of overlays of phase-contrast microscopic images and two confocal microscopic images. (A) Simultaneous in situ hybridization with CY5-labeled probe NSV443 and CY3-labeled probe NSR1156. Cells of *Nitrosospira* spp. are shown in blue; cells of *Nitrospira*-like bacteria are red. (B) Simultaneous in situ hybridization with CY5-labeled probe NSV443 and CY3-labeled probe NSR447. Cells of *Nitrosospira* spp. are blue; a smaller subpopulation of *Nitrospira* spp. is visualized in red. (C) Simultaneous in situ hybridization with CY5-labeled probe NSV443 and CY3-labeled probe NSR1156 displaying the morphology and close association of ammonia- and nitrite-oxidizing bacteria.

No sequences affiliated with the genus *Nitrobacter* or with any known ammonia-oxidizing bacterium were retrieved.

Probe design and in situ detection of *Nitrospira*. Based on the retrieved sequences, two probes specific for all clones that included *Nitrospira moscoviensis*, NSR1156 and NSR826 (with one mismatch to clone b18), were developed. Another probe, NSR447, was designed to be complementary to clones g6, o9, and o14 only (Fig. 2). Hybridization conditions of the probes were evaluated in situ by using increasing concentrations of formamide in the hybridization buffer. Probes NSR1156 and NSR447 showed good signal and specificity in buffer with 30% formamide; probe NSR826 did so in buffer with 20% formamide. When applied to the aggregate sections, probes NSR1156 and NSR826 hybridized to virtually all ALF1b-positive cells. A 16S rRNA sequence database check revealed that, indeed, all *Nitrospira* spp. have the target sequence for probe ALF1b. The nitrifying community active in the fluidized bed reactor was shown to consist of members of the genera *Nitrosospira* and *Nitrospira* (Fig. 3A). Only a minor fraction of all NSR1156- and NSR826-positive cells also hybridized with probe NSR447. These cells were slightly bigger, formed smaller clusters than the major part of the *Nitrospira* sp. cells, and were located exclusively in the nitrifying part of the aggregates (Fig. 3B). Single-cell resolution of the very small *Nitrospira* spp. was almost impossible even with confocal laser scanning microscopy (Fig. 3C).

DISCUSSION

Microprofiles. The in situ activity measurements clearly indicate that both ammonia and nitrite oxidizers were active within a 125-μm zone at the aggregate surface (Fig. 1). In contrast, no activity was measured in the inner part of the aggregates, although dense populations of nitrifiers could be detected (Fig. 3) and oxygen and ammonium were present. One possible explanation is that the ammonium concentration in this zone (10 μM) was substantially below the half-saturation constant (K_s) for ammonia oxidation. Indeed, the lowest K_s values reported so far for ammonia-oxidizing bacteria are 30 to 75 μM NH_4^+ plus NH_3 (at pH 7.8) for strains of the *Nitrosomonas oligotropha* group, isolated from the River Elbe (27). No such data are currently available for members of the genus *Nitrosospira*.

Ammonia oxidizers. By using FISH with a set of specific probes, it was shown that members of the genus *Nitrosospira* (in its extended definition [14] also including the former genera *Nitrosolobus* and *Nitrosovibrio*) were the only ammonia-oxidizing bacteria in the aggregates. As previously shown for members of the genus *Nitrosomonas* in biofilms (21, 26), *Nitrosospira* spp. also tended to form monospecies clusters in close association with clusters of nitrite oxidizers. Cluster formation could be disadvantageous due to the longer diffusion path of substrates. However, since the nitrifying bacteria rely on CO_2 fixation by ribulose bisphosphate carboxylase (RubisCO), it might be a mechanism for increasing the efficacy of CO_2 fixation by lowering the $[O_2]$ in the clusters. Cluster formation might also provide protection against hazardous environmental factors, or it might just be an ecologically neutral result of cell division. In our study, the clustering of *Nitrosospira* sp. was probably the reason that no 16S rDNA clone sequences of this genus were obtained. Intact clusters could still be detected after the DNA isolation procedure, indicating resistance against the DNA extraction protocol based on freeze-thawing and hot phenol and SDS extraction. This potential for formation of highly resistant clusters should be considered in all attempts to monitor ammonia-oxidizing bacteria with methods based on DNA extraction.

The in situ detection of *Nitrosospira* spp. in this ammonium-poor system is in agreement with observations that in natural systems that are low in ammonium, *Nitrosospira* spp. can be detected rather than *Nitrosomonas* spp. (15, 18, 28). However, these studies depend on DNA extraction and PCR while true quantitative in situ analyses of these habitats are missing. In contrast, *Nitrosomonas* spp., i.e., members of the *Nitrosomonas europaea* lineage, are more abundant in activated sludge, biofilms, and enrichments with millimolar concentrations of ammonium (21, 26, 28, 33). The main adaptations to the different niches are probably via the ammonia oxidation kinetics and the growth rate. In that respect, *Nitrosospira* and *Nitrosomonas* seem to be typical K and r strategists, respectively (5). However, the isolation of *Nitrosomonas oligotropha* and related strains with remarkably low K_s values (27) already indicates limits for such a generalizing statement.

Nitrite oxidizers. *Nitrospira*-like bacteria were identified in the nitrifying aggregates by a combination of comparative 16S rRNA sequence analysis and FISH. Their localization within the nitrifying zone and their association with the ammonia-oxidizing *Nitrosospira* species lend strong evidence that they are responsible for nitrite oxidation in our system. Two genetically different populations were distinguished in this study. The main population, which was more distantly related to *Nitrospira moscoviensis*, also occurred in the inactive center of the aggregates. The second, smaller population had a higher level of 16S rRNA similarity to *Nitrospira moscoviensis*. It was restricted to the active nitrifying zone. The genotypic differences obviously coincide with different physiological adaptations leading to these distinct spatial distributions. The exact description of the differing physiological properties of the new nitrite oxidizers, however, will require their isolation. A directed isolation can be monitored by the oligonucleotide probes developed in this study.

The detection of *Nitrospira* spp. also yields independent support for a recent molecular study reporting that *Nitrospira*-like bacteria were the main nitrite-oxidizing population in freshwater aquaria (17). Before, *Nitrospira*-like 16S rDNA sequences had also been isolated from activated sludge (8), but, at that time, reference sequences of cultured *Nitrospira* spp. with proven nitrite-oxidizing capability were not available. Therefore, it was impossible to link the genotype with a phenotype. This clearly shows the importance of cultivation of bacteria. Considering the rare in situ detection of *Nitrobacter* species in freshwater systems (16, 21, 34), *Nitrospira* spp. might be of more general importance for nitrite oxidation. The molecular detection of *Nitrospira*-like bacteria in habitats as diverse as activated sludge, freshwater aquaria, and an oligotrophic fluidized bed reactor and the initial isolation of *Nitrospira moscoviensis* from a corroded water pipe may indicate a wide distribution in nitrifying systems.

Conclusion. *Nitrosospira* and *Nitrospira* spp. were identified as main components of nitrifying aggregates. Their activity and spatial distribution could be shown by the combination of microsensor measurements and in situ hybridization. Whether the combination of these two genera is unique to the investigated system or is of general relevance in more oligotrophic freshwater habitats must be evaluated in the future.

REFERENCES

1. **Alm, E. W., D. B. Oerther, N. Larsen, D. A. Stahl, and L. Raskin.** 1996. The oligonucleotide probe database. Appl. Environ. Microbiol. **62:**3557–3559.
2. **Amann, R. I., B. J. Binder, R. J. Olson, S. W. Chisholm, R. Devereux, and D. A. Stahl.** 1990. Combination of 16S rRNA-targeted oligonucleotide probes with flow cytometry for analyzing mixed microbial populations. Appl. Environ. Microbiol. **56:**1919–1925.
3. **Amann, R. I., L. Krumholz, and D. A. Stahl.** 1990. Fluorescent-oligonucleotide probing of whole cells for determinative, phylogenetic, and environmental studies in microbiology. J. Bacteriol. **172:**762–770.
4. **Amann, R. I., W. Ludwig, and K. H. Schleifer.** 1995. Phylogenetic identification and in situ detection of individual microbial cells without cultivation. Microbiol. Rev. **59:**143–169.
5. **Andrews, J. H., and R. F. Harris.** 1986. *r*- and *K*-selection and microbial ecology. Adv. Microb. Ecol. **9:**99–147.
6. **Belser, L. W.** 1979. Population ecology of nitrifying bacteria. Annu. Rev. Microbiol. **33:**309–333.
7. **Bock, E., and H.-P. Koops.** 1992. The genus *Nitrobacter* and related genera, p. 2302–2309. *In* A. Balows, H. G. Trüper, M. Dworkin, W. Harder, and K.-H. Schleifer (ed.), The prokaryotes, 2nd ed. Springer-Verlag, New York, N.Y.
8. **Bond, P. L., P. Hugenholtz, J. Keller, and L. L. Blackall.** 1995. Bacterial community structure of phosphate-removing and non-phosphate-removing activated sludges from sequencing batch reactors. Appl. Environ. Microbiol. **61:**1910–1916.
9. **Brosius, J., T. J. Dull, D. D. Sleeter, and H. F. Noller.** 1981. Gene organization and primary structure of a ribosomal RNA operon from *Escherichia coli*. J. Mol. Biol. **148:**107–127.
10. **de Beer, D., A. Schramm, C. M. Santegoeds, and M. Kühl.** 1997. A nitrite microsensor for profiling environmental biofilms. Appl. Environ. Microbiol. **63:**973–977.
11. **de Beer, D., J. C. van den Heuvel, and S. P. P. Ottengraf.** 1993. Microelectrode measurements of the activity distribution in nitrifying bacterial aggregates. Appl. Environ. Microbiol. **59:**573–579.
12. **Degrange, V., and R. Bardin.** 1995. Detection and counting of *Nitrobacter* populations in soil by PCR. Appl. Environ. Microbiol. **61:**2093–2098.
13. **Ehrich, S., D. Behrens, E. Lebedeva, W. Ludwig, and E. Bock.** 1995. A new obligately chemolithoautotrophic, nitrite-oxidizing bacterium, *Nitrospira moscoviensis* sp. nov., and its phylogenetic relationship. Arch. Microbiol. **164:**16–23.
14. **Head, I. M., W. D. Hiorns, T. M. Embley, A. J. McCarthy, and J. R. Saunders.** 1993. The phylogeny of autotrophic ammonia-oxidizing bacteria as determined by analysis of 16S ribosomal gene sequences. J. Gen. Microbiol. **139:**1147–1153.
15. **Hiorns, W. D., R. C. Hastings, I. M. Head, A. J. McCarthy, J. R. Saunders, R. W. Pickup, and G. H. Hall.** 1995. Amplification of 16S ribosomal RNA genes of autotrophic ammonia-oxidizing bacteria demonstrates the ubiquity of nitrosospiras in the environment. Microbiology **141:**2793–2800.
16. **Hovanec, T. A., and E. F. DeLong.** 1996. Comparative analysis of nitrifying bacteria associated with freshwater and marine aquaria. Appl. Environ. Microbiol. **62:**2888–2896.
17. **Hovanec, T. A., L. T. Taylor, A. Blakis, and E. F. Delong.** 1998. *Nitrospira*-like bacteria associated with nitrite oxidation in freshwater aquaria. Appl. Environ. Microbiol. **64:**258–264.
18. **Kowalchuk, G. A., J. R. Stephen, W. de Boer, J. I. Prosser, T. M. Embley, and J. W. Woldendorp.** 1997. Analysis of ammonia-oxidizing bacteria of the β subdivision of the class *Proteobacteria* in coastal sand dunes by denaturing

gradient gel electrophoresis and sequencing of PCR-amplified 16S ribosomal DNA fragments. Appl. Environ. Microbiol. **63:**1489–1497.
19. **Manz, W., R. Amann, W. Ludwig, M. Wagner, and K.-H. Schleifer.** 1992. Phylogenetic oligodeoxynucleotide probes for the major subclasses of proteobacteria: problems and solutions. Syst. Appl. Microbiol. **15:**593–600.
20. **McCaig, A. E., T. M. Embley, and J. I. Prosser.** 1994. Molecular analysis of enrichment cultures of marine ammonia oxidisers. FEMS Microbiol. Lett. **120:**363–368.
21. **Mobarry, B. K., M. Wagner, V. Urbain, B. E. Rittmann, and D. A. Stahl.** 1996. Phylogenetic probes for analyzing abundance and spatial organization of nitrifying bacteria. Appl. Environ. Microbiol. **62:**2156–2162.
22. **Muyzer, G., T. Brinkhoff, U. Nübel, C. M. Santegoeds, H. Schäfer, and C. Wawer.** 1998. Denaturing gradient gel electrophoresis (DGGE) in microbial ecology, p. 1–27. *In* A. D. L. Akkermans, J. D. van Elsas, and F. J. de Bruijn (ed.), Molecular microbial ecology manual, supplement 3. Kluwer Academic Publishers, Dordrecht, The Netherlands.
23. **Muyzer, G., A. Teske, C. O. Wirsen, and H. W. Jannasch.** 1995. Phylogenetic relationships of *Thiomicrospira* species and their identification in deep-sea hydrothermal vent samples by denaturing gradient gel electrophoresis of 16S rDNA fragments. Arch. Microbiol. **164:**165–172.
24. **Prosser, J. I.** 1989. Autotrophic nitrification in bacteria. Adv. Microb. Physiol. **30:**125–181.
25. **Revsbech, N. P.** 1989. An oxygen microelectrode with a guard cathode. Limnol. Oceanogr. **34:**474–478.
26. **Schramm, A., L. H. Larsen, N. P. Revsbech, N. B. Ramsing, R. Amann, and K.-H. Schleifer.** 1996. Structure and function of a nitrifying biofilm as determined by in situ hybridization and the use of microelectrodes. Appl. Environ. Microbiol. **62:**4641–4647.
27. **Stehr, G., B. Böttcher, P. Dittberner, G. Rath, and H.-P. Koops.** 1995. The ammonia-oxidizing nitrifying population of the River Elbe estuary. FEMS Microbiol. Ecol. **17:**177–186.
28. **Stephen, J. R., A. E. McCaig, Z. Smith, J. I. Prosser, and T. M. Embley.** 1996. Molecular diversity of soil and marine 16S rRNA gene sequences related to β-subgroup ammonia-oxidizing bacteria. Appl. Environ. Microbiol. **62:**4147–4154.
29. **Strunk, O., O. Gross, B. Reichel, M. May, S. Hermann, N. Stuckmann, B. Nonhoff, M. Lenke, T. Ginhart, A. Vilbig, T. Ludwig, A. Bode, K.-H. Schleifer, and W. Ludwig.** ARB: a software environment for sequence data. http://www.mikro.biologie.tu-muenchen.de. Department of Microbiology, Technische Universität München, Munich, Germany.
30. **Teske, A., E. Alm, J. M. Regan, S. Toze, B. E. Rittmann, and D. A. Stahl.** 1994. Evolutionary relationships among ammonia- and nitrite-oxidizing bacteria. J. Bacteriol. **176:**6623–6630.
31. **Voytek, M. A., and B. B. Ward.** 1995. Detection of ammonia-oxidizing bacteria of the beta-subclass of the class *Proteobacteria* in aquatic samples with the PCR. Appl. Environ. Microbiol. **61:**1444–1450.
32. **Wagner, M., B. Assmus, A. Hartmann, P. Hutzler, and R. Amann.** 1994. *In situ* analysis of microbial consortia in activated sludge using fluorescently labelled, rRNA-targeted oligonucleotide probes and confocal scanning laser microscopy. J. Microsc. **176:**181–187.
33. **Wagner, M., G. Rath, R. Amann, H.-P. Koops, and K.-H. Schleifer.** 1995. *In situ* identification of ammonia-oxidizing bacteria. Syst. Appl. Microbiol. **18:**251–264.
34. **Wagner, M., G. Rath, H.-P. Koops, J. Flood, and R. Amann.** 1996. *In situ* analysis of nitrifying bacteria in sewage treatment plants. Water Sci. Technol. **34:**237–244.
35. **Ward, B. B., M. A. Voytek, and K.-P. Witzel.** 1997. Phylogenetic diversity of natural populations of ammonia oxidizers investigated by specific PCR amplification. Microb. Ecol. **33:**87–96.
36. **Wawer, C., M. S. M. Jetten, and G. Muyzer.** 1997. Genetic diversity and expression of the [NiFe] hydrogenase large-subunit gene of *Desulfovibrio* spp. in environmental samples. Appl. Environ. Microbiol. **63:**4360–4369.

Chapter 5

Microscale Distribution of Populations and Activities

of *Nitrosospira* and *Nitrospira* spp. along a Macroscale Gradient

in a Nitrifying Bioeactor: Quantification by

In Situ Hybridization and the Use of Microsensors
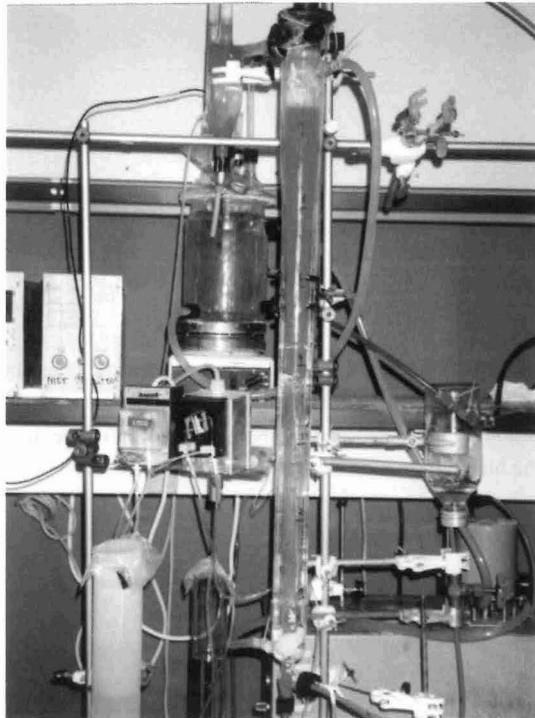
This chapter has been submitted to Applied and Environmental Microbiology

Front page:

Fluidized bed reactor with nitrifying aggregates. The vertical reactor consists of a conical reaction column (middle), a settler (left, on top), and a conditioning vessel (left). Fresh medium is introduced to the bottom of the reaction column, and part of the purified water is recirculated from settler and conditioning vessel via the blue tubing.

Microscale Distribution of Populations and Activities of *Nitrosospira* and *Nitrospira* spp. along a Macroscale Gradient in a Nitrifying Bioreactor: Quantification by In Situ Hybridization and the Use of Microsensors

ANDREAS SCHRAMM[1], DIRK DE BEER[1], JOHAN C. VAN DEN HEUVEL[2], SIMON OTTENGRAF[2], AND RUDOLF AMANN[1]

Max-Planck-Institute for Marine Microbiology, D-28359 Bremen, Germany[1] and Department of Chemical Engineering, University of Amsterdam, NL-1018WV Amsterdam, The Netherlands[2]

The change of activity and abundance of *Nitrosospira* sp. and *Nitrospira* sp. along a bulk water gradient in a nitrifying fluidized bed reactor was analyzed by the combination of microsensor measurements and fluorescence in situ hybridization. Nitrifying bacteria were immobilized in bacterial aggregates that remained in fixed positions within the reactor column due to the flow regime. Nitrification occurred in a narrow zone of 100-150 µm on the surface of these aggregates, the same layer that contained an extremely dense community of nitrifying bacteria. The central part of the aggregates was inactive, and significantly less nitrifiers were found there. Under conditions prevailing in the reactor, i.e. when ammonium was limiting, ammonium was completely oxidized to nitrate within the active layer of the aggregates, the rates decreasing with increasing reactor height. To analyze the nitrification potential, profiles were also recorded in aggregates subjected to a short-term incubation under elevated substrate concentrations. This lead to a shift in activity from ammonium to nitrite oxidation along the reactor and correlated well with the distribution of the nitrifying population: Along the whole reactor the numbers of ammonia-oxidizing bacteria decreased while the numbers of nitrite-oxidizing bacteria increased. Finally, volumetric reaction rates were calculated from microprofiles and related to cell numbers of nitrifying bacteria in the active shell. Therefore it was possible for the first time to estimate the cell-specific activity of *Nitrosospira* sp. and hitherto uncultured *Nitrospira*-like bacteria in situ.

Immobilized micro-organisms are used for the purification of a variety of wastewaters in fixed-film treatment plants like trickling filters, rotating biological contactors or fluidized beds (7). In all these systems, the organisms responsible for treatment are present in a microbial biofilm. Unlike in well-mixed activated sludge basins, sequential transformations of the sewage compounds may occur while the wastewater passes the filter, and pronounced gradients of, e.g., oxygen, dissolved organic carbon (DOC) or ammonium can be measured in the bulk water along such a reactor (7). In comparison, changes of the underlying microbial communities and activities within the biofilm are more difficult to assess. However, these data are needed for the improvement of mathematical models used to design and dimension fixed-filter reactors.

Nowadays, fluorescence in situ hybridization with rRNA-targeted oligonucleotide probes offers a reliable tool for the direct identification and quantification of bacteria in their natural environment (1, 3). For the determination of gradients and activities on a micrometer scale microsensors have been developed for various compounds (22, 30). The combination of both methods (2) has been shown to

bear great potential for direct observations of structure and function of sulfate reducing (28) and nitrifying biofilms (32, 34).

In this study, a lab-scale fluidized bed reactor (12) was used as a model system for the in situ analysis of structure and function of a whole biofilm reactor. The nitrifying community of this reactor had recently been identified as *Nitrosospira* sp. and *Nitrospira* sp. by the rRNA approach (32). Here, we present data on the changes of abundance and activity of these nitrifying populations with the bulk water gradient along the reactor. In a more ecological context, this can be regarded as an example how environmental parameters structure microbial communities.

In an additional experiment, the microsensor measurements were repeated under excess of substrate (ammonium or nitrite) to test the nitrification potential of the system and to evaluate the maximum specific activities of its components. This again is important for mathematical models but also to estimate the competitiveness of yet uncultured species like *Nitrospira* sp. in the environment.

(A preliminary account of part of this work appeared in *Proceedings of the 2nd International Conference on Microorganisms in Activated Sludge and Biofilms, IAWQ, Berkeley, CA, 1997*)

METHODS

Reactor operation. The conical 360-ml continuous-upflow reactor used as a model system has been described in detail by de Beer et al. (12). For this study, it was fed with mineral medium containing 72 μM NH_4^+ (influent concentration), and the liquid phase was recirculated at a rate of 1.8 ml s^{-1} (32). Temperature was kept at 30°C. The chemical gradients that developed along the reactor are displayed in Table 1. The conical shape of the vertical reactor column creates also a flow velocity gradient that stabilizes aggregates of different diameter and density at different heights in the column according to their settling velocity. Aggregate samples were taken from three different points of the reactor, labeled A1 through A3.

TABLE 1. Axial gradient along the nitrifying fluidized bed reactor

sample	distance from inlet [cm]	O_2 [μM]	pH	NH_4^+ [μM]	NO_2^- [μM]	aggregate diameter [mm]
inlet	0	236	8.0	72	0	-
A1	10	212	7.9	50	3	2.0-2.5
A2	30	142	7.7	40	7	1.5-2.0
A3	50	87	7.5	0	4	0.8-1.3
outlet	80	59	7.3	0	0	-

Microsensor measurements. Clark-type O_2 microsensors (29) and liquid ion-exchanging membrane (LIX) microsensors for NH_4^+, NO_2^-, and NO_3^- (11) were prepared and calibrated as described previously. Tip diameters were <10 μm for O_2, 5 μm for NH_4^+ and NO_3^-, and 15 μm for NO_2^- microsensors.

Aggregates were placed in a flow cell, perfused with medium, and microprofiles were recorded at depth steps of 25 μm from the bulk liquid into the aggregate as described by de Beer et al. (12) and Schramm et al. (32). Measurements were performed under in situ conditions, i.e. when [O_2], [NH_4^+], [NO_2^-], and pH in the medium were adjusted to the values at the respective sampling points (referred to as "in situ conditions", see Table 1), and in air-saturated mineral medium containing 300 μM NH_4^+ (referred to as "incubation conditions"). Profiles of aggregate samples from point A3 were also recorded in air-saturated mineral medium containing 300 μM NO_2^- (labeled "A3$_{nitrite}$"). [NO_3^-] was always 100 μM.

Chemical analysis. [NH$_4^+$], [NO$_2^-$], and [NO$_3^-$] in the reactor column were determined colorimetrically (Spectroquant, Merck). [O$_2$] and pH were measured by an O$_2$ microsensor and a pH electrode (Radiometer, Denmark) which were lowered into the reactor to the sampling points.

Calculations. Oxygen uptake and the rates of ammonium and nitrite oxidation were determined from the O$_2$, NH$_4^+$ and NO$_3^-$ profiles as the fluxes, J, through the diffusive boundary layer (DBL). Net fluxes for O$_2$, NH$_4^+$, NO$_2^-$ and NO$_3^-$ were calculated using Fick's first law:

$$J = -D_W \cdot \frac{C_\infty - C_0}{\delta_{eff}} \qquad (1)$$

where D_W is the molecular diffusion coefficient in water, C_∞ is the bulk water concentration, C_0 is the concentration at the aggregate surface, and δ_{eff} is the effective DBL thickness. The δ_{eff} is defined by extrapolating the concentration gradient at the aggregate-water interface to the bulk water phase concentration (26). Diffusion coefficients of O$_2$, NH$_4^+$, NO$_2^-$ and NO$_3^-$ at 30°C were taken as $2.75 \cdot 10^{-5}$, $2.25 \cdot 10^{-5}$, $2.17 \cdot 10^{-5}$ and $2.16 \cdot 10^{-5}$ cm^2 s^{-1}, respectively (8, 23).

Volumetric reaction rates were calculated from the volume of the active shell and the net fluxes into whole aggregates:

$$V = \frac{J \cdot 4\pi r^2}{\frac{4}{3}\pi r^3 - \frac{4}{3}\pi (r - r_a)^3} \qquad (2)$$

where $4\pi r^2$ and $4/3\ \pi r^3$ are the surface and the volume of a the aggregate, respectively, r_a is the thickness of the active shell as determined by microsensor measurements, and $4/3\ \pi (r - r_a)^3$ is the volume of the inactive central part of the aggregate.

Oligonucleotide probes. Previously described oligonucleotide probes specific for certain ammonia- (25) and nitrite- (32) oxidizing bacteria were used. Their sequences and target sites are presented in Table 2. Probes were synthesized and fluorescently labeled with the hydrophilic sulfoindocyanine dyes CY3 or CY5 at the 5´ end by Interactiva Biotechnologie GmbH (Ulm, Germany).

TABLE 2. Oligonucleotide probes applied

Probe	Specificity	Sequence (5´-3´) of probe	rRNA target site[a]	[%] FA[b]	[mM] NaCl[c]
NSO1225	ammonia-oxidizing β-proteobacteria	CGCCATTGTATTACGTGTGA	16S, 1225-1244	35	80
NSV443	*Nitrosospira* spp.	CCGTGACCGTTTCGTTCCG	16S, 444-462	30	112
NSR826	*Nitrospira* spp.	GTAACCCGCCGACACTTA	16S, 826-843	20	225
NSR1156	*Nitrospira* spp.	CCCGTTCTCCTGGGCAGT	16S, 1156-1173	30	112
NSR447	*Nitrospira* spp.	GGTTTCCCGTTCCATCTT	16S, 447-464	30	112

[a] *E. coli* numbering (9)

[b] percentage formamide in the hybridization buffer

[c] mM sodium chloride in the washing buffer

Sample preparation and in situ hybridization. Aggregates were fixed in paraformaldehyde, cut on a cryomicrotome, and the single cryosections (thickness 14 µm) were immobilized on microscopic slides. This whole procedure was described in detail by Schramm et al.(32). In situ hybridization of fixed and dehydrated aggregate sections was carried out at 46°C in an isotonically equilibrated

humidity chamber according to the protocol of Amann et al. (4). Stringent hybridization conditions for the different oligonucleotide probes were adjusted using the formamide and sodium chloride concentrations listed in Table 2 in the hybridization and washing buffers, respectively (24). Double-hybridizations with two probes that require different stringencies (e.g. NSR826+NSR1156) were done as subsequent hybridizations starting with the probe of higher thermal stability.

Confocal microscopy and image analysis. Digital images of aggregates after hybridization were taken by confocal laser scanning microscopy (CLSM) on a Zeiss LSM510 (Carl Zeiss, Jena, Germany), equipped with two HeNe lasers (543 nm, 633 nm). We applied optical sections of 1.5 and 0.7 μm thickness for *Nitrosospira* sp. and *Nitrospira* sp., respectively. As these represent about the mean cell diameters of the two populations the optical sections were assumed to contain single-cell layers. For each probe, cell numbers per volume were derived from randomly chosen optical sections using the "area" function of the standard software delivered with the instrument. A threshold was set manually to exclude empty spaces and background fluorescence from the record, and the remaining cell area was quantified relative to the total aggregate area. Threshold levels were calibrated separately for each probe and sample by determining mean values for the area of at least 300 single cells, counting cells within a defined area, and adjusting the threshold to match the calculated total cell area. The same calibrations were used to calculate cell numbers from the cell area values. Assuming only one layer of cells in an optical section, this numbers were regarded as cell numbers per volume, where the volume was the total measured area multiplied with the thickness of the optical section. Nitrifying bacteria in the active shell and in the central part of the aggregates were enumerated separately.

RESULTS

Microgradients. For all three sampling sites 3-7 profiles (Table 3) of O_2, NH_4^+, NO_2^- and NO_3^- were measured each in a separate aggregate under in situ and under incubation conditions. Examples of these profiles are shown in Fig. 1. The effective diffusive boundary layers (DBL) ranged from 70 to 225 μm, depending on aggregate size, surface structure, and solute type (data not shown). Oxygen consumption, ammonium and nitrite oxidation were always restricted to a shell of 75-200 μm at the aggregate surface while the central part of the aggregates appeared to be inactive. The mean thickness of the nitrifying zone as defined by ammonium, nitrite and nitrate profiles decreased with increasing distance of the aggregate sampling site from the inlet from about 150 μm (sample A1) to 125 μm (A2) to 100 μm (A3).

Under in situ conditions, oxygen was only partially consumed within the nitrifying zone. In contrast, ammonium and nitrite present in the bulk water phase were almost completely converted to nitrate within the aggregate, only less then 10 μM ammonium being left in the central part of A1 and A2 aggregates (Fig. 1a, c, e).

Because nitrification obviously was substrate limited under reactor conditions, we also measured microprofiles while aggregates were incubated in 300 μM ammonium under air saturation to extract some information about the nitrification potential (Fig. 1b, d, f). In A1 and A2 aggregates, oxygen was now depleted within the nitrifying zone while ammonium was consumed to concentrations down to 100-150 μM within the aggregate. Nitrite accumulated to significant concentrations (~100 μM) in A1 aggregates but only to negligible amounts in A2. Almost no change in the concentrations of oxygen, ammonium and nitrate were detected in A3 aggregates, showing very low ammonium oxidation potential. Therefore, a third set of microprofiles was measured in these aggregates, supplying 300 μM nitrite under air saturation (Fig. 1g). Oxygen and nitrite were consumed but not depleted within the active shell, resulting in an enhanced production of nitrate.

46
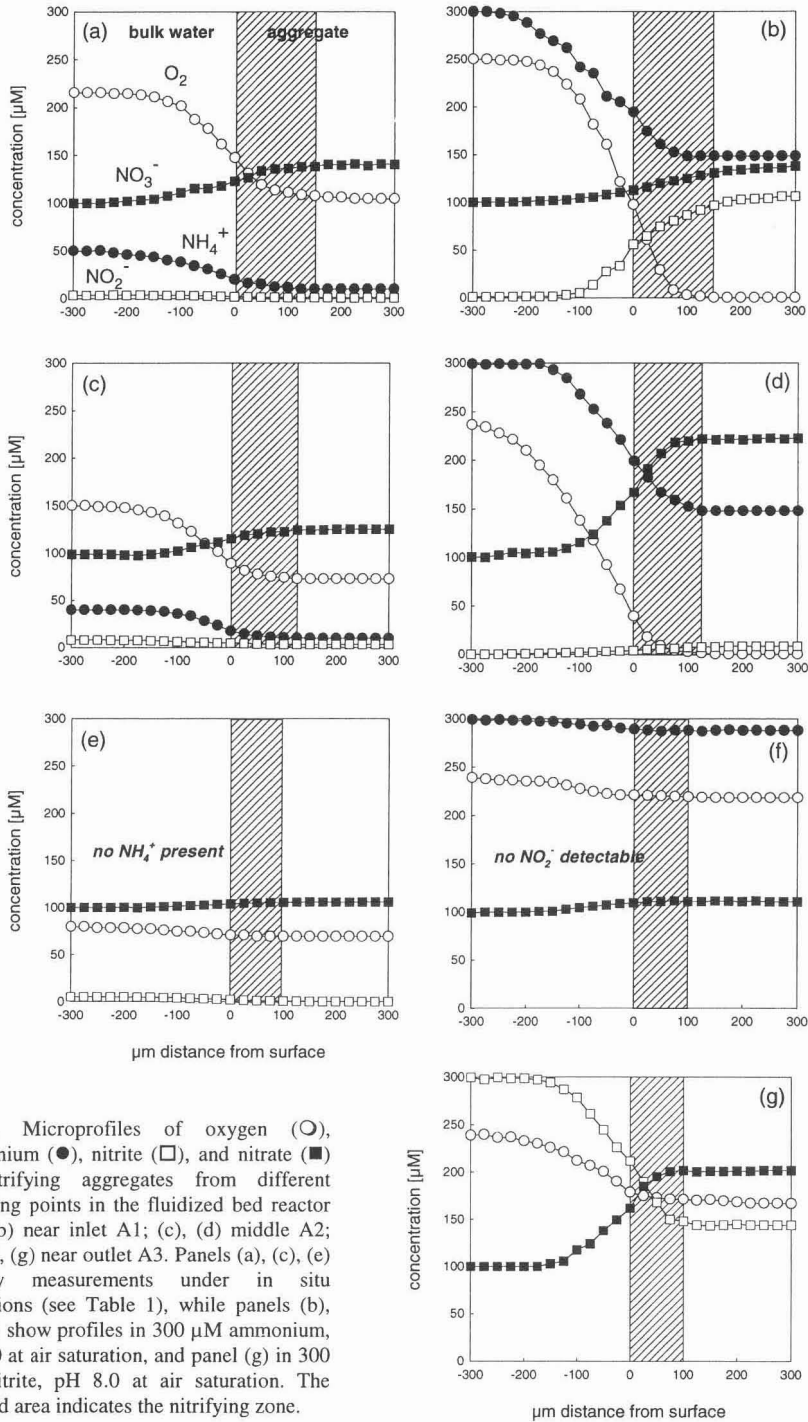
FIG.1. Microprofiles of oxygen (○), ammonium (●), nitrite (□), and nitrate (■) in nitrifying aggregates from different sampling points in the fluidized bed reactor ((a), (b) near inlet A1; (c), (d) middle A2; (e), (f), (g) near outlet A3. Panels (a), (c), (e) display measurements under in situ conditions (see Table 1), while panels (b), (d), (f) show profiles in 300 μM ammonium, pH 8.0 at air saturation, and panel (g) in 300 μM nitrite, pH 8.0 at air saturation. The hatched area indicates the nitrifying zone.

47

TABLE 3. Fluxes through the aggregate-bulk liquid interface calculated from microprofiles

	flux [nmol·mm^{-2}·h^{-1}][a]			
in situ conditions[b]				
sample	oxygen	ammonium	nitrite	nitrate
A1	-4.67 ± 1.02 (5)	-1.83 ± 0.86 (3)	-0.16 ± 0.02 (3)	2.06 ± 0.11 (4)
A2	-3.62 ± 0.96 (4)	-1.30 ± 0.43 (4)	-0.16 ± 0.05 (3)	1.46 ± 0.14 (3)
A3	-0.44 ± 0.02 (3)	not detectable	-0.23 ± 0.07 (3)	0.62 ± 0.01 (3)
incubation conditions[c]				
sample	oxygen	ammonium	nitrite	nitrate
A1	-13.70 ± 5.50 (7)	-6.69 ± 3.84 (3)	3.18 ± 0.92 (3)	4.03 ± 0.52 (3)
A2	-9.78 ± 2.49 (4)	-4.60 ± 3.29 (4)	0.34 ± 0.04 (3)	3.85 ± 3.15 (5)
A3$_{ammonium}$	-1.51 ± 0.01 (3)	-0.62 (1)	0.00 (2)	0.62 (2)
A3$_{nitrite}$	-4.13 ± 2.51 (3)	no NH$_4^+$ present	-6.09 ± 1.02 (3)	5.60 ± 2.47 (3)

[a] mean values ± SD (95% confidence limit); the number of profiles is given in parentheses.

[b] in situ conditions refer to the conditions as measured in the reactor (Table 1)

[c] incubation conditions were 300 µM ammonium, pH 8.0, air saturation for samples A1, A2, and A3$_{ammonium}$, ; for sample A3$_{nitrite}$ it was 300 µM nitrite, pH 8.0, and air saturation.

Rate calculations. Net fluxes of oxygen, ammonium, nitrite and nitrate through the aggregate-bulk liquid interface were calculated from the microprofiles and are summarized in Table 3. In general, the fluxes measured under incubation conditions exceeded the in situ fluxes. Rates were highest at the bottom (A1) of the reactor and lowest at the top (A3) with one exception: the highest nitrite oxidation rate was found in A3$_{nitrite}$ aggregates.

The ratio of the fluxes for NH$_4^+$-O$_2$-NO$_3^-$ was close to 1:2:1 for all samples where all species were present. When ammonium was absent (i.e. in samples A3$_{in\ situ}$ and A3$_{nitrite}$) the ratio of the fluxes of NO$_2^-$-O$_2$-NO$_3^-$ was 1:1.9:2.7 and 1:0.7:0.92, respectively.

Volumetric reaction rates of respiration, ammonium and nitrite oxidation were calculated from the net fluxes into the active layer of the aggregates (Table 4). Again, the rates were higher for the incubation conditions than in situ, and for the in situ incubations highest on the bottom of the reactor. The same was true for the volumetric respiration and ammonium oxidation rates under incubation conditions.

TABLE 4. Volumetric conversion rates calculated from microprofiles

	volumetric rates [nmol·mm^{-3}·h^{-1}]		
in situ conditions			
sample	respiration	ammonium oxidation	nitrite oxidation
A1	35.82 ± 7.82	14.01 ± 6.65	15.77 ± 0.87
A2	33.40 ± 8.86	11.98 ± 3.99	13.44 ± 1.27
A3	5.44 ± 0.22	no NH$_4^+$ present	7.65 ± 0.15
incubation conditions			
sample	respiration	ammonium oxidation	nitrite oxidation
A1	105.03 ± 42.16	51.29 ± 29.43	30.90 ± 3.97
A2	90.15 ± 22.95	42.45 ± 30.38	35.46 ± 29.07
A3$_{ammonium}$	18.51 ± 0.23	7.61	7.65
A3$_{nitrite}$	50.75 ± 30.84	no NH$_4^+$ present	68.86 ± 30.32

In contrast, the nitrite oxidation potential increased from bottom to top (taken the values for A3$_{nitrite}$ as potential activity; the nitrite oxidation rates for A3$_{ammonium}$ just equaled the ammonium oxidation rates).

In situ detection, quantification and specific reaction rates of nitrifying bacteria

The principal composition of the nitrifying community of the reactor had been resolved previously as *Nitrosospira* spp. and *Nitrospira* spp. by the rRNA approach (32). Here, the stratification of these populations within the aggregates as well as along the reactor column is reported (Table 5 and Fig. 2). The relative close match of cell numbers for probes NSO1225 and NSV443, targeting all ammonia-oxidizing β-*Proteobacteria* and all known members of the genus *Nitrosospira*, respectively, confirmed our observation that *Nitrosospira* spp. represent the vast majority if not all ammonia-oxidizing bacteria in the system. The numbers of ammonia-oxidizers decreased from the bottom (A1, Fig. 2a) to the top (A3, Fig. 2c) of the reactor, and much fewer cells were detected in the central aggregate than in the outer shell. Moreover, ammonia-oxidizers in the nitrifying zone formed substantially larger cell clusters than in the inner part of the aggregate (Fig. 2). Concerning the stratification within a single aggregate, the same observation is also true for nitrite-oxidizing bacteria of the genus *Nitrospira* as detected by a combination of probes NSR826 and NSR1156. Taken together, these probes target all known *Nitrospira*-like sequences from freshwater habitats.
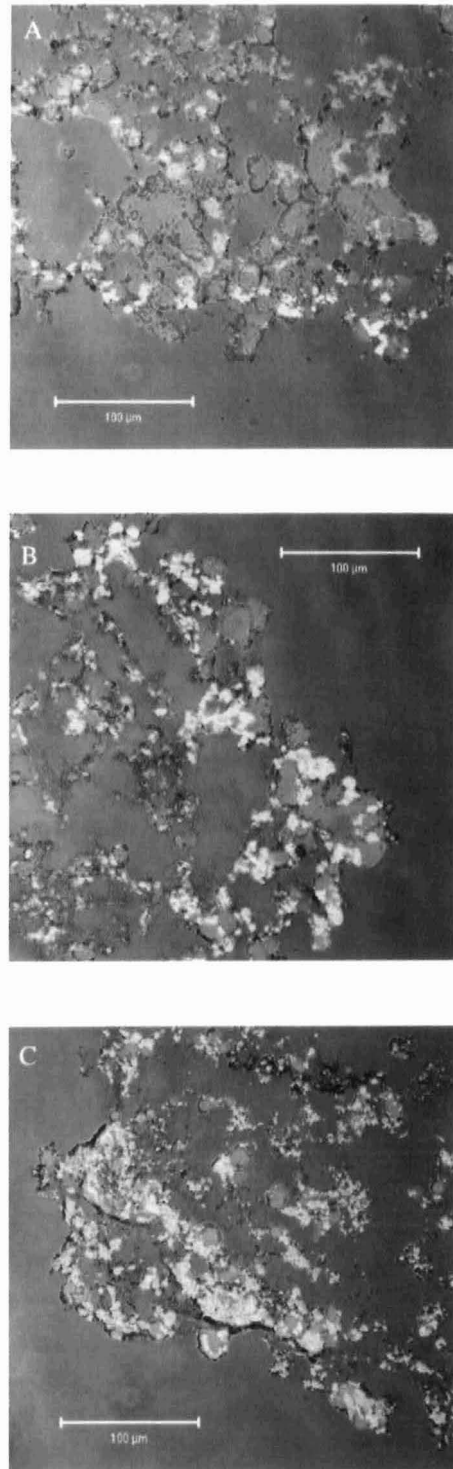
FIG.2. CLSM-images of part of aggregate cross-sections after FISH with CY5-labelled probe NSV443, specific for *Nitrosospira* sp. (displayed in red), and with CY3-labelled probes NSR826 + NSR1156, specific for *Nitrospira* sp. (displayed in yellow). For each picture, two confocal images and the respective phase contrast image were combined. Aggregates are shown from A1 (a), A2 (b), and A3 (c). The aggregate surface is indicated by arrows. bar = 100 µm.

TABLE 5. Quantification of nitrifying bacteria by FISH

sample	cells $[10^7 \cdot mm^{-3}]$ detected by probe			
	NSO1225	NSV443	NSR826/NSR1156	NSR447
A1 shell[a]	5.55 ± 2.75	4.30 ± 0.70	62.1 ± 17.9	1.71 ± 0.90
center[b]	1.80 ± 0.62	1.35 ± 0.13	12.3 ± 11.6	0.06 ± 0.02
A2 shell	4.39 ± 2.22	4.80 ± 2.56	78.5 ± 25.4	1.75 ± 0.90
center	1.92 ± 0.59	1.87 ± 0.54	31.3 ± 19.0	0.07 ± 0.02
A3 shell	2.74 ± 0.38	2.24 ± 1.17	93.4 ± 55.0	3.9 ± 0.71
center	0.97 ± 0.57	1.14 ± 0.21	42.1 ± 27.3	0.14 ± 0.12

[a] cell numbers within the active, nitrifying shell of the aggregates

[b] cell numbers within the inactive central part of the aggregates

In contrast, the cell volume of *Nitrospira* sp. increased from the bottom to the top of the reactor, and equaled in aggregate A2 the cell volume of *Nitrosospira* sp. (cf. Fig. 2). However, due to their much smaller cell size, numbers of nitrite-oxidizing bacteria exceeded that of ammonia-oxidizing bacteria for more than an order of magnitude. Interestingly, a distinct, minor part of *Nitrospira* sp., as detected by probe NSR447, was almost exclusively restricted to the active shell of the aggregates.

Cell numbers were used to calculate specific oxidation rates of ammonium and nitrite per cell from the volumetric ammonium and nitrite oxidation rates (Table 6). Generally, the specific reaction rates of *Nitrosospira* sp. were one order of magnitude higher than the rates of *Nitrospira*, and rates were higher under incubation conditions than in situ. However, no significant change in the specific rates per cell was observed along the reactor column. An exception was the ammonium oxidation rate of *Nitrosospira* sp. in aggregate A3 that was considerably lower than the rates from aggregates A1 and A2 when incubated with 300 µM ammonium.

TABLE 6. Specific reaction rates of nitrifying bacteria in the active shell

	in situ conditions		*incubation conditions*		
sample	specific reaction rates $[10^{-4} \, pmol \cdot cell^{-1} \cdot h^{-1}]$		sample	specific reaction rates $[10^{-4} \, pmol \cdot cell^{-1} \cdot h^{-1}]$	
	AOR[a]	NOR[b]		AOR	NOR
A1	2.5 ± 2.4	0.2 ± 0.1	A1	9.2 ± 9.9	0.5 ± 0.2
A2	2.7 ± 2.3	0.2 ± 0.1	A2	9.7 ± 11.8	0.5 ± 0.5
A3	0	0.1 ± 0.05	A3$_{ammonium}$	2.8 ± 0.4	0.1 ± 0.05
			A3$_{nitrite}$	0	0.7 ± 0.8

[a] ammonium oxidation rate per NSO1225-positive cell

[b] nitrite oxidation rate per NSR826/NSR1156-positive cell

DISCUSSION

Accuracy of the calculations. The nitrifying aggregates investigated in this study were rather heterogeneous regarding their irregular surface structures and the patchy distribution of nitrifying bacteria within the active shell (Fig. 2). Consequently, also the measured profiles showed some variability, and the standard deviations on both rate calculation and FISH quantification, were rather high. The ratio of the fluxes for NH_4^+-O_2-NO_3^-, however, was close to the expected stoichiometric

ratio of 1:2:1, thus lending support to our mean values. In contrast, in sample A3 (in situ conditions) the flux ratio clearly indicates that not enough profiles have been measured to reliable calculate average fluxes of nitrite and/or nitrate. A small source of uncertainty, again due to the irregular shape of the aggregates, was the determination of the radius used to calculate volumetric reaction rates. However, the error made by a deviation of ±100 µm was only about 2% and can therefore be neglected.

For the FISH-based quantification of nitrifying populations the threshold set point for the area measurement was critical. Thus, special effort was taken in its calibration, and occasionally the results from image analysis were compared with conventional counts of hybridized cells in defined areas of an optical slice. The results from both procedures never differed more than 10%, and we concluded that the enumeration of nitrifying bacteria per area by our image analysis procedure was accurate enough for our study. However, this was only possible because of the morphological homogeneity of the respective nitrifying populations. Another source of uncertainty was the extrapolation of these values to cell numbers per volume. Biofilm samples have been reported to shrink during immobilization to microscopic slides and dehydration, especially in z-direction (33). This would lead to an underestimation of the total aggregate volume and hence to an overestimation of the cell numbers per volume. A comparison of the thickness of sections after hybridization with the cryosection thickness revealed a shrinkage of about 15% for all samples. Therefore, the numbers of nitrifiers per volume might have been overestimated by 15%, while the specific rates per cell might have been underestimated by 15%, but both to the same amount in all samples. For all the reasons discussed above, we are aware that the absolute numbers reported in this study, especially for the specific reaction rates per cell, might be best estimates only. Still we are convinced that they reliably describe the trends in the investigated system and are within the right order of magnitude.

Analysis under in situ conditions. The decrease of ammonium in the bulk water along the reactor column (Table 1) most likely leads to the decreasing numbers of ammonia-oxidizing bacteria in the active shell with increasing reactor height (Table 5, Fig.2) and to a decreasing thickness of this shell (Fig. 1 a, c, e). However, as also the volumetric ammonium oxidation rate decreases from A1 to A2 (Table 4) the specific rates per cell *Nitrosospira* sp. remain about the same at these points (Table 6). Their value of approximately 0.25 fmol·cell^{-1}·h^{-1} is comparable to specific rates reported by Wagner *et al.* (20, 35) for *Nitrosococcus mobilis* in activated sludge but is one to two orders of magnitude below the rates reported for *Nitrosospira* sp. and other ammonia oxidizers from pure culture studies (6, 27). This might be due to the apparent ammonium limitation under in situ conditions but might as well be a strain-specific feature. In aggregates from the top of the reactor (A3) and in the central parts of all aggregates no or very low concentrations of ammonium (probably below K_m as has been discussed previously (32)) and no ammonium oxidation activity were detected (Fig. 1). Nevertheless, ammonia-oxidizing bacteria were detectable by FISH although in significantly lower numbers than in the active zones (Fig. 2, Table 5). This again demonstrates the capacity of ammonia-oxidizing bacteria to maintain their ribosomes even under conditions not conducive to activity and growth (34, 35).

Nitrite oxidation was almost completely coupled to nitrite production by ammonia-oxidizers. Consequently, despite an increase in number of *Nitrospira* sp. found in the active shell from A1 to A3 (Fig. 2, Table 5) nitrite oxidation rates decreased with reactor height (Table 4). Specific nitrite oxidation rates per cell also slightly decreased but were always extremely low (max. 0.02 fmol·cell^{-1}·h^{-1}). No pure culture data are currently available for *Nitrospira* sp. but the values reported for *Nitrobacter* sp. are about 200-2000 times higher (27). Again, this difference might result from unfavorable in situ conditions and/or from the differing physiological properties of these only distantly related (13) nitrite-oxidizers.

Nitrification activity under elevated substrate concentrations. To test the nitrifying capacity of the system additional measurements were performed under air saturation in medium containing 300 μM ammonium (A1, A2, A3) or 300 μM nitrite (A3). The volumetric respiration rates in A1 and A2 are high (~100 nmol·mm^{-3}·h^{-1}) compared to values of 2 - 40 nmol·mm^{-3}·h^{-1} reported from sediments (31), activated sludge flocs (Schramm *et al.* unpublished), and heterotrophic aggregates (26) or biofilms (21). But they are similar to rates determined earlier under the same conditions in the same system (12), in a nitrifying trickling filter biofilm (34), or in a hypersaline microbial mat (19). Such high rates are only possible if bacteria and hence activities are extremely concentrated like shown for the nitrifying shell in this study (Fig. 2).

The specific ammonium oxidation rates per cell under incubation conditions (Table 6) are approximately the same in A1 and A2, and both are higher than the rates under in situ conditions. Although oxygen limited, we assume this values to be close to the maximum specific activity as higher levels of oxygen had been previously shown to inhibit nitrification in the same system (12). Still the specific activity is well below the rates reported for pure cultures (see above). Interestingly, ammonia-oxidizers in A3, i.e. the population subjected to starvation in situ, developed significantly less activity even when supplied with enough substrate (Tables 4 and 6, A3$_{ammonium}$). This leads to the hypothesis that *Nitrosospira* sp. adapts to starvation by entering a dormant or inactive state that is not coupled to the reduction of the sellular ribosome level as proven by FISH. Whether this is due to a decreased activity or concentration of ammonia monooxygenase, or by some other unknown mechanisms, might be addressed by the application of mRNA-targeted probes or ammonia monooxygenase-targeted antibodies in the future.

Cell-specific nitrite oxidation rates increased for all sampling points when aggregates were released from nitrite limitation (Table 6). However, it is questionable if maximum nitrite oxidation activity was reached during the incubation. Ammonia-oxidizers are thought to possess lower K_m values for oxygen than nitrite-oxidizers (14, 27). Therefore, the nitrite accumulation detected in A1 and A2 (Fig 1 b, d) might indicate that ammonia-oxidizers have out-competed nitrite-oxidizers for oxygen. On the other hand, K_m values are only available for *Nitrosomonas* spp. and *Nitrobacter* spp., and nitrite accumulation was less pronounced in A2 although the oxygen concentration within the active layer was even less than in A1. Furthermore in A3, when neither oxygen nor nitrite were limiting, the specific nitrite oxidation rates were not significantly higher. For these reasons, we assume that the specific rates at least closely approached the maximum activity. Like mentioned for the ammonia-oxidizers, still these activities are much lower (100-900 times) than those described for *Nitrobacter*. The recent detection of *Nitrospira*-like sequences and cells in various environments (10, 13, 16, 20) and the absence of *Nitrobacter* sp. in similar habitats (15, 33, 36) might therefore indicate other competitive advantages of *Nitrospira* sp. like, e.g., higher substrate affinities for oxygen and/or nitrite, better adaptations to starvation, or better resistance against toxic shocks.

In principle, substrate affinities (expressed as K_M values) can be estimated from ammonium and nitrite microprofiles and cell numbers assuming Michaelis-Menten kinetics. For this approach, cell-specific reaction rates were calculated for each data point using the second derivative of the profiles. Relating these values to the respective substrate concentration in a Lineweaver-Burk-plot, K_M values as low as 40 μM ammonium (pH 7.8) and 10 μM nitrite were retrieved for *Nitrosospira* sp. and *Nitrospira* sp., respectively. This was one to two orders of magnitude lower than the K_M values for *Nitrosomonas europaea* and most other *Nitrosomonas* strains (18, 27) and most *Nitrobacter* spp. (17, 27) found in literature. In an ecological context, *Nitrosospira* sp. and *Nitrospira* sp. thus could indeed be regarded as typical *K*-strategists with high substrate affinities and low maximum activity (or growth rate) compared to the *r*-strategists *Nitrosomonas europaea* and *Nitrobacter* sp. (5, 32). However, it has to

be stressed again that a lot of uncertainties affect these numbers: firstly, the sample is highly heterogeneous as has been discussed above; secondly, it is not absolutely sure whether maximum reaction rates could be reached at all under the conditions applied; thirdly, the oligonucleotide probes used in this study are not specific on the species level, leaving a possibility for phylogenetic and physiological diversity as discussed for *Nitrospira* sp. below. Therefore, these numbers again should be regarded as the best possible estimates, correct within the order of magnitude.

It may be tempting to speculate about the small fraction of *Nitrospira* sp. that was detected exclusively in the active shell of the aggregates by probe NSR447. What makes them different compared to the main population? This can certainly not be decided on the basis of this study, and is more intended to read as a caution: There are currently two dozens of *Nitrospira*-like sequences available, representing probably at least five distinct species, that must not be presumed to have identical physiologies. Clearly, pure culture studies are needed to address this question.

In conclusion, the combination of microsensor measurements and FISH allowed a detailed analysis of the in situ structure and function of the nitrifying bioreactor on a microscale. Measurements under elevated substrate concentrations were used to extract valuable information about the in situ activity of hitherto uncultured nitrifying bacteria.

ACKNOWLEDGEMENTS

REFERENCES

1. **Amann, R., F. O. Glöckner, and A. Neef.** 1997. Modern methods in subsurface microbiology: in situ identification of microorganisms with nucleic acid probes.
    FEMS Microbiol. Rev. **20**:191-200.

2. **Amann, R., and M. Kühl.** 1998. *In situ* methods for assessment of microorganisms and their activities. Cur.Opin.Microbiol. **1**:352-358.

3. **Amann, R. I., W. Ludwig, and K.-H. Schleifer.** 1995. Phylogenetic identification and in situ detection of individual microbial cells without cultivation. Microbiol. Rev. **59**: 143-169

4. **Amann, R. I., L. Krumholz, and D. A. Stahl.** 1990. Fluorescent-oligonucleotide probing of whole cells for determinative, phylogenetic, and environmental studies in microbiology. J.Bacteriol. **172**:762-770.

5. **Andrews, J. H., and R. F. Harris.** 1986. *r*- and *K*-selection and microbial ecology. Adv.Microb.Ecol. **9**:99-147.

6. **Belser, L. W.** 1979. Population ecology of nitrifying bacteria. Annu.Rev.Microbiol. **33**:309-333.

7. **Bishop, P. L., and N. E. Kinner.** 1986. Aerobic fixed-film processes, p. 113-176. *In* W. Schönborn (ed.), Microbial Degradations, 1st ed, vol. 8. VCH, Weinheim, Germany.

8. **Broecker, W. S., and T.-H. Peng.** 1974. Gas exchange rates between air and sea. Tellus. **26**:21-35.

9. **Brosius, J., T. J. Dull, D. D. Sleeter, and H. F. Noller.** 1981. Gene organization and primary structure of a ribosomal RNA operon from *Escherichia coli.* J.Mol.Biol. **148:**107-127.

10. **Burrel, P. C., J. Keller, and L. L. Blackall.** 1998. Microbiology of a nitrite-oxidizing bioreactor. Appl.Environ.Microbiol. **64:**1878-1883.

11. **de Beer, D., A. Schramm, C. M. Santegoeds, and M. Kühl.** 1997. A nitrite microsensor for profiling environmental biofilms. Appl.Environ.Microbiol. **63:**973-977.

12. **de Beer, D., J. C. van den Heuvel, and S. P. P. Ottengraf.** 1993. Microelectrode measurements of the activity distribution in nitrifying bacterial aggregates. Appl.Environ.Microbiol. **59:**573-579.

13. **Ehrich, S., D. Behrens, E. Lebedeva, W. Ludwig, and E. Bock.** 1995. A new obligately chemolithoautotrophic, nitrite-oxidizing bacterium, *Nitrospira moscoviensis* sp. nov. and its phylogenetic relationship. Arch.Microbiol. **164:**16-23.

14. **Focht, D. D., and W. Verstraete.** 1977. Biochemical ecology of nitrification and denitrification. Adv.Microb.Ecol. **1:**135-214.

15. **Hovanec, T. A., and E. F. DeLong.** 1996. Comparative analysis of nitrifying bacteria associated with freshwater and marine aquaria. Appl.Environ.Microbiol. **62:**2888-2896.

16. **Hovanec, T. A., L. T. Taylor, A. Blakis, and E. F. DeLong.** 1998. *Nitrospira*-like bacteria associated with nitrite oxidation in freshwater aquaria. Appl.Environ.Microbiol. **64:**258-264.

17. **Hunik, J. H., H. J. G. Meijer, and J. Tramper.** 1993. Kinetics of *Nitrobacter agilis* at extreme substrate, product and salt concentrations. Appl.Microbiol.Biotech. **40:**442-448.

18. **Hunik, J. H., H. J. G. Meijer, and J. Tramper.** 1992. Kinetics of *Nitrosomonas europaea* at extreme substrate, product and salt concentrations. Appl.Microbiol.Biotech. **37:**802-807.

19. **Jørgensen, B. B., and D. J. Des Marais.** 1990. The diffusive boundary layer of sediments: oxygen microgradients over a microbial mat. Limnol.Oceanogr. **35:**1343-1355.

20. **Juretschko, S., G. Timmermann, M. Schmidt, K.-H. Schleifer, A. Pommerening-Röser, H.-P. Koops, and M. Wagner.** 1998. Combined molecular and conventional analysis of nitrifying bacterial diversity in activated sludge: *Nitrosococcus mobilis* and *Nitrospira*-like bacteria as dominant populations. Appl.Environ.Microbiol. **64:**3042-3051.

21. **Kühl, M., and B. B. Jørgensen.** 1992. Microsensor measurement of sulfate reduction and sulfide oxidation in compact microbial communities of aerobic biofilms. Appl.Environ.Microbiol. **58:**1164-1174.

22. **Kühl, M., and N. P. Revsbech.** 1998. Microsensors for the study of interfacial biogeochemical processes, p. Chapter 8. *In* B. P. Boudreau and B. B. Jørgensen (ed.), The benthic boundary layer. Oxford University Press, Oxford.

23. **Li, Y. H., and S. Gregory.** 1974. Diffusion of ions in sea water and in deep-sea sediments. Geochim.Cosm.Acta. **38:**703-714.

24. **Manz, W., R. Amann, W. Ludwig, M. Wagner, and K.-H. Schleifer.** 1992. Phylogenetic oligodeoxynucleotide probes for the major subclasses of proteobacteria: problems and solutions. Syst.Appl.Microbiol. **15:**593-600.

25. **Mobarry, B. K., M. Wagner, V. Urbain, B. E. Rittmann, and D. A. Stahl.** 1996. Phylogenetic probes for analyzing abundance and spatial organization of nitrifying bacteria. Appl.Environ.Microbiol. **62:**2156-2162.

26. **Ploug, H., M. Kühl, B. Buchholz-Cleven, and B. B. Jørgensen.** 1997. Anoxic aggregates - an ephemeral phenomenon in the pelagic environment? Aquat.Microb.Ecol. **13:**285-294.

27. **Prosser, J. I.** 1989. Autotrophic nitrification in bacteria. Adv.Microb.Physiol. **30:**125-181.

28. **Ramsing, N. B., M. Kühl, and B. B. Jørgensen.** 1993. Distribution of sulfate-reducing bacteria, O_2, and H_2S in photosynthetic biofilms determined by oligonucleotide probes and microelectrodes. Appl.Environ.Microbiol. **59:**3840-3849.

29. **Revsbech, N. P.** 1989. An oxygen microelectrode with a guard cathode. Limnol.Oceanogr. **34:**474-478.

30. **Revsbech, N. P., and B. B. Jørgensen.** 1986. Microelectrodes: their use in microbial ecology, p. 293-352. *In* K. C. Marshall (ed.), Advances in Microbial Ecology, vol. 9. Plenum, New York.

31. **Revsbech, N. P., B. Madsen, and B. B. Jørgensen.** 1986. Oxygen production and consumption in sediments determined at high spatial resolution by computer simulation of oxygen microelectrode data. Limnol.Oceanogr. **31:**293-304.

32. **Schramm, A., D. De Beer, M. Wagner, and R. Amann.** 1998. Identification and activity in situ of *Nitrosospira* and *Nitrospira* spp. as dominant populations in a nitrifying fluidized bed reactor. Appl.Environ.Microbiol. **64:**3480-3485.

33. **Schramm, A., L. H. Larsen, N. P. Revsbech, and R. I. Amann.** 1997. Structure and function of a nitrifying biofilm as determined by microelectrodes and fluorescent oligonucleotide probes. Wat.Sci.Tech. **36:**263-270.

34. **Schramm, A., L. H. Larsen, N. P. Revsbech, N. B. Ramsing, R. Amann, and K.-H. Schleifer.** 1996. Structure and function of a nitrifying biofilm as determined by in situ hybridization and the use of microelectrodes. Appl.Environ.Microbiol. **62:**4641-4647.

35. **Wagner, M., G. Rath, R. Amann, H.-P. Koops, and K.-H. Schleifer.** 1995. *In situ* identification of ammonia-oxidizing bacteria. Syst.Appl.Microbiol. **18:**251-264.

36. **Wagner, M., G. Rath, H.-P. Koops, J. Flood, and R. Amann.** 1996. *In situ* analysis of nitrifying bacteria in sewage treatment plants. Wat.Sci.Tech. **34:**237-244.

Chapter 6

Microenvironments and Distribution of Nitrifying Bacteria

in a Membrane-Bound Biofilm

Front page:

Nitrifying/denitrifying biofilm grown on silicone tubing in the reactor pipe.

Microenvironments and Distribution of Nitrifying Bacteria
in a Membrane-Bound Biofilm

ANDREAS SCHRAMM, DIRK DE BEER, ARMIN GIESEKE, AND RUDOLF AMANN
Max Planck Institute for Marine Microbiology, D-28359 Bremen, Germany

The distribution of nitrifying bacteria of the genera *Nitrosomonas, Nitrosospira, Nitrobacter,* and *Nitrospira* was investigated in a membrane-bound biofilm system with opposed supply of oxygen and substrate. Gradients of oxygen, pH, nitrite and nitrate were determined by means of microsensors while the nitrifying populations along these gradients were identified and quantified using fluorescence *in situ* hybridisation in combination with confocal laser scanning microscopy. Due to high ammonium and nitrite concentrations the oxic part of the biofilm was dominated by close relatives of *Nitrosomonas europaea* and by members of the genus *Nitrobacter.* In contrast, *Nitrospira* sp. was most abundant in zones in which oxygen concentrations were very low or zero. In the totally anoxic part of the biofilm cell numbers of all nitrifiers were relatively low. Interestingly, *Nitrobacter* sp. frequently co-aggregated with ammonia-oxidising bacteria, whereas this was only seldom observed for *Nitrospira* sp.. Based on these observations the ecophysiology of yet uncultured *Nitrospira* sp. is discussed in the context of environmental competitiveness.

Nitrifying bacteria which participate in the nitrogen cycle by the successive oxidation of ammonium via nitrite to nitrate have been intensively studied for years using *Nitrosomonas europaea* (Koops & Möller, 1992) and *Nitrobacter* sp. (Bock & Koops, 1992) as model organisms (Laanbroek & Woldendorp, 1995; Prosser, 1989). However, recent data obtained by molecular techniques show that yet uncultured ammonia- and nitrite-oxidisers of the genera *Nitrosospira* (Hiorns *et al.*, 1995; Kowalchuk *et al.*, 1997; Stephen *et al.*, 1996) and *Nitrospira* (Burrel *et al.*, 1998; Hovanec *et al.*, 1998; Juretschko *et al.*, 1998; Schramm *et al.*, 1998) are equally or even more important in the environment. It now remains to be investigated whether ecophysiological knowledge on *Nitrosomonas* or *Nitrobacter* species can be extrapolated to *Nitrosospira* or *Nitrospira* (Laanbroek and Woldendorp, 1995). A challenging task for microbial ecologists is therefore the elucidation of characteristic properties of these uncultured strains, with the ultimate goal of understanding the environmental factors that select for certain nitrifying populations in nature.

The classical way to tackle this problem was the isolation and characterisation of ecologically relevant nitrifiers. With these fastidious and slowly growing bacteria, unfortunately, the cultivation approach appears to be difficult.

Alternatively, one might detect nitrifying bacteria in a cultivation-independent way in various habitats based on their 16S rDNA sequences and relate this to data of some important environmental factors like pH, nitrogen or oxygen concentrations (Hastings *et al.*, 1998; Kowalchuk, et al., 1997; Princic *et al.*, 1998). However, due to the occurrence of chemical microgradients and microniches in soil, sediment or biofilms, the information derived from such correlations is rather indirect and therefore

limited. More direct information about microenvironments and distribution of nitrifying bacteria can be obtained by the combined use of microsensors and fluorescence *in situ* hybridisation (FISH), as already previously demonstrated for biofilms (Schramm *et al.,* 1998; Schramm *et al.*, 1996). Recently, even the *in situ* kinetics of uncultured nitrifying bacteria have been estimated by this approach (Schramm *et al.*, this thesis, Chapter 5). Based upon these results, it was hypothesised that members of the *Nitrosomonas europaea*-lineage (Pommerening-Röser *et al.*, 1996) and *Nitrobacter* sp. could out-compete *Nitrosospira* sp. and *Nitrospira* sp. in habitats with high substrate concentrations due to their higher maximum growth rates, whereas *Nitrosospira* sp. and *Nitrospira* sp. were better competitors in low-substrate environments due to their lower K_M values (Schramm, et al., 1998), (Schramm *et al.*, this thesis, Chapter 5).

In this study, a membrane-bound nitrifying biofilm was investigated that was supplied with oxygen via a gas-permeable membrane while ammonium was provided from the bulk water. The concept of separating oxygen supply from substrate supply in order to enhance nitrification and to enable simultaneous nitrification-denitrification in biofilms, has been reported previously (Timberlake *et al.*, 1988). A similar pilot reactor (Özoguz, 1997) was shown to exhibit microgradients of oxygen, nitrite, and nitrate within the biofilm (de Beer *et al.*, 1997) and to contain a diverse nitrifying community, i.e. *Nitrosomonas* sp., *Nitrosospira* sp., *Nitrobacter* sp. and *Nitrospira* sp. (de Beer & Schramm, in press). Therefore, this reactor was chosen as a model system to study the distribution of these different nitrifiers along the microgradients.

EXPERIMENTAL PROCEDURES

Biofilm reactor operation. Design and performance of the pilot membrane reactor have been described previously (Özoguz, 1997). To facilitate biofilm sampling and true *in situ* microsensor measurements a slightly modified lab-scale reactor was established (Fig.1) and inoculated with material from the pilot plant. Pieces of silicon tubing were mounted as substratum perpendicular to the flow in the lumen of a Plexiglas pipe. Above each tubing an opening in the pipe that was sealed with a rubber stopper during normal reactor operation enabled the insertion of microsensors. The model system had a volume of 20.8 l, a recirculation rate of 900 l·h^{-1}, and artificial wastewater (K$_2$HPO$_4$ 0.14 g·l^{-1}, MgSO$_4$ 0.17 g·l^{-1}, (NH$_4$)$_2$SO$_4$ 1.32 g·l^{-1}, H$_3$BO$_3$ 2 mg·l^{-1}, MnCl 1.25 mg·l^{-1}, Na$_8$MoO$_4$ 0.27 mg·l^{-1}, ZnSO$_4$ 0.15 mg·l^{-1}, CuSO$_4$ 0.06 mg·l^{-1}, Co(NO$_3$)$_2$ 0.035 mg·l^{-1}) was added at a rate of 5 l·h^{-1}. Temperature was kept at 28°C, pH was adjusted to 7.8, and the conditioning vessel was flushed with dinitrogen gas during start-up to prevent biofilm growth apart from the O$_2$-supplying membrane. Occasionally, NH$_4^+$, NO$_2^-$, and NO$_3^-$ in the bulk water were determined by routine chemical analysis (LCK 303, 341, and 339, Dr. Lange, Germany). Oxygen and pH were monitored continuously in the conditioning vessel by macroelectrodes (WTW, Germany).
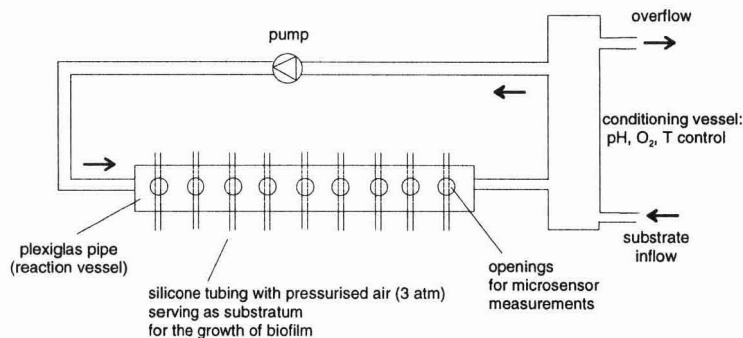
Fig. 1.
Scheme of model system set-up for growth of a membrane-bound biofilm

Microsensor measurements. Clark-type microsensors for O_2 (Revsbech, 1989) and H_2S (Kühl *et al.*, 1998), and liquid ion-exchanging membrane (LIX) microsensors for pH, NH_4^+, NO_2^-, and NO_3^- (de Beer, et al., 1997) were prepared and calibrated as described previously. Tip diameters were <10 µm for O_2 and H_2S, 5 µm for pH, NH_4^+ and NO_3^-, and 15 µm for NO_2^- microsensors. LIX microsensors were connected to a millivoltmeter, and the potential was recorded relative to a calomel reference electrode (Radiometer, Denmark), while O_2 and H_2S sensors were connected to a picoamperemeter with internal polarisation unit. Microprofiles in the biofilm were measured directly in the running reactor by inserting the microsensors through openings in the reactor pipe (de Beer, et al., 1997). The spatial resolution of the measurements was 50 µm as controlled by a micromanipulator, and the profiles were read on a strip chart recorder. For each parameter at least ten profiles were measured at different sites in the biofilm.

Biofilm preparation. After the microsensor measurements, part of the tubing with the attached biofilm was sampled and immediately fixed in paraformaldehyde solution (4% w/v) for 60 min at 4°C (Amann *et al.*, 1990). The sample was washed in phosphate buffered saline, embedded over night in OCT compound (Tissue-Tek II, Miles, Elkhart, Ind.) and frozen in a cryomicrotom at -35°C as described previously (Schramm, et al., 1998). When frozen, it was possible to cut the tubing with the biofilm into two longitudinal sections by use of a scalpel and to remove the embedded biofilm material from the tubing without losses (Yu *et al.*, 1994; Schramm, et al., 1996). The biofilm was then mounted with OCT compound to the object holder of the cryomicrotom. Sections of 14 µm thickness were made at a temperature of -17°C perpendicular to the biofilm surface, and immobilised on gelatine-coated (Amann, et al., 1990) microscopic slides as previously described (Schramm, et al., 1998).

Fluorescence *in situ* hybridisation. The sequences of all oligonucleotide probes used in this study, their target organisms, hybridisation conditions, and references are given in Table 1. Probes were synthesised and fluorescently labelled with the hydrophilic sulfoindocyanine dyes CY3 or CY5 at the 5´ end by Interactiva Biotechnologie GmbH (Ulm, Germany). *In situ* hybridisation of dehydrated biofilm sections was carried out at 46°C in an isotonically equilibrated humidity chamber according to the protocol of Amann *et al.* (Amann, et al., 1990). Stringent hybridisation conditions for the different oligonucleotide probes were adjusted using the formamide and sodium chloride concentrations listed in Table 1 in the hybridisation and washing buffers, respectively (Manz *et al.*, 1992). Double-hybridisations with two probes that require different stringencies (e.g. NSR826+NSR1156) were done as subsequent hybridisations starting with the probe of higher thermal stability.

The nitrifying populations were quantified using confocal laser scanning microscopy (LSM 510, Carl Zeiss, Jena, Germany) and image analysis as described in detail by Schramm *et al.* (this thesis, Chapter 5). Shortly, threshold values were defined to exclude background fluorescence and the probe-positive cell area was quantified. This procedure was calibrated by comparative cell counts, and the results were expressed as cells per volume. Each 50 µm-layer of the biofilm, starting at the membrane, was quantified separately.

RESULTS

Biofilm succession. Within two weeks after inoculation a thin, homogeneous biofilm became visible on the surface of the silicone tubing and traces of nitrite were measured in the bulk water. After five weeks the biofilm was about 300 µm thick, and grew up to 600 µm after 10 weeks. During the whole period, $[NH_4^+]$ in the bulk water decreased while $[NO_2^-]$ and $[NO_3^-]$ fluctuated but constantly increased, with $[NO_2^-]$ always exceeding $[NO_3^-]$. No oxygen was detectable with a macroelectrode at any time in the bulk water. From week 10 to week 14 the biofilm had reached a relatively stable state.

Table 1. Oligonucleotide probes

Probe	Specificity	Sequence (5´-3´) of probe	Target site[a] (rRNA positions)	[%] FA[b]	[mM] NaCl[c]	Ref.
EUB338	*Bacteria*	GCTGCCTCCCGTAGGAGT	16S, 338-355	20	225	Amann *et al.*, 1990
NON	non-binding control	CGACGGAGGGCATCCTCA	-	20	225	Manz *et al.*, 1992
NSO1225	ammonia-oxidising β-proteobacteria	CGCCATTGTATTACGTGTGA	16S, 1225-1244	35	80	Mobarry *et al.*, 1996
NSO190	ammonia-oxidising β-proteobacteria	CGATCCCCTGCTTTTCTCC	16S, 190-208	55	20	Mobarry *et al.*, 1996
NSV443	*Nitrosospira* spp.	CCGTGACCGTTTCGTTCCG	16S, 444-462	30	112	Mobarry *et al.*, 1996
NSM156	*Nitrosomonas* spp.	TATTAGCACATCTTTCGAT	16S, 156-174	5	636	Mobarry *et al.*, 1996
NEU23a	*Nitrosomonas europaea*-lineage	CCCCTCTGCTGCACTCTA	16S, 653-670	40	56	Wagner *et al.*,1995
CTE	unlabelled competitor for NEU23a	TTCCATCCCCCTCTGCCG	16S, 659-676	40	56	Wagner *et al.*,1995
Nse1472[d]	*N. europaea, N. eutropha, N. halophila*	ACCCCAGTCATGACCCCC	16S, 1472-1489	50	28	Juretschko *et al.*, 1998
NmV	*Nitrosococcus mobilis*	TCCTCAGAGACTACGCGG	16S, 174-191	35	80	Juretschko *et al.*, 1998
NIT3	*Nitrobacter* spp.	CCTGTGCTCCATGCTCCG	16S, 1035-1048	40	56	Wagner *et al.*, 1996
cNIT3	unlabelled competitor for NIT3	CCTGTGCTCCAGGCTCCG	16S, 1035-1048	40	56	Wagner *et al.*, 1996
NSR826	freshwater *Nitrospira* spp.	GTAACCCGCCGACACTTA	16S, 826-843	20	225	Schramm *et al.*, 1998
NSR1156	freshwater *Nitrospira* spp.	CCCGTTCTCCTGGGCAGT	16S, 1156-1173	30	112	Schramm *et al.*, 1998

[a] *E. coli* numbering (Brosius *et al.*, 1981)

[b] percentage formamide in the hybridization buffer

[c] mM sodium chloride in the washing buffer

[d] published as S-*-Nse-1472-a-A-18

However, it was obvious from the nitrite accumulation that nitrification was incomplete during the whole succession.

In week 15, acetate was added to study the effect of organic carbon amendment on the nitrifying community. The system reacted promptly by onset of denitrification and sulfate reduction, both proven by microsensor measurements, and by massive growth of fungi. This resulted in destruction of the biofilm structure by hyphae and poisoning of the biofilm community by H_2S, essentially terminating the experiment. Despite similar substrate and operational conditions, sulfate reduction was never observed in the pilot reactor. Therefore, we presume that the biomass-volume ratio in our model system was not high enough to produce sufficient amounts of nitrite/nitrate to control sulfate reducing bacteria either by direct inhibition (Reinsel *et al.*, 1996) or by competition of denitrifying bacteria for organic carbon.

Microsensor measurements. *In situ* microprofiles of oxygen, pH, nitrite and nitrate were measured in the biofilm after five, ten and 14 weeks, and again after the addition of acetate. Ammonium was shown to always penetrate the whole biofilm at concentrations of 15-20 mM but the resolution of the LIX microsensor in this concentration range was not high enough to record more accurate profiles. Detection of the biofilm surface in the reactor was difficult. However, when the sensor tip reached the silicone membrane a signal peak was observed due to the mechanic touch. When introduced further, the signal of the LIX sensors disappeared, probably because they lost electric contact to the reference electrode, while oxygen sensors showed a perfectly linear profile within the silicone membrane. Thereby it was possible to align the different profiles with respect to the biofilm base.

The profiles measured after five weeks showed depletion of oxygen usually within a distance of 150-250 µm from the membrane, and a decrease of pH from ~7.6 (biofilm surface) to 6.8 - 7.0 at the biofilm base. $[NO_2^-]$ was with 200-300 µM highest within 100 µm from the membrane and decreased towards the biofilm surface to values of 50-150 µM. The same was true for $[NO_3^-]$ although the profiles showed more heterogeneity and the concentrations were slightly lower, i.e. 50-250 µM at the biofilm base and 30-100 µM towards the surface. This indicates a nitrifying zone directly at the biofilm base with ammonium-oxidation rates exceeding nitrite-oxidation rates. As ammonia-oxidising bacteria catalyse the first reaction of a two-step process and are faster growing than nitrite-oxidising bacteria (Bock *et al.*, 1986; Prosser, 1989) this is to be expected for the start-up phase of a succession experiment.

The profiles measured in week 10 and 14 were virtually the same, and similar to the measurements in week 5. However, the concentrations of nitrate (towards the membrane: 100-400 µM; towards the biofilm surface: 80-150) and especially nitrite (towards the membrane: 400-1200 µM; towards the surface: 150-300) were now higher (Fig. 2A). Although ammonia and nitrite oxidation were obviously still not in balance we concluded that the biofilm had reached a relatively mature state, as neither bulk water measurements, microprofiles, nor the community structure of nitrifying bacteria (see below) showed any significant change from week 10 to 14. Figure 2A displays the microgradients found after 10 weeks in the biofilm.

Distribution of nitrifying bacteria. Probes EUB338 and NON were used as positive and negative controls, respectively. Probe penetration was sufficient to enable FISH in all parts of the biofilm, whereas unspecific binding of probes and autofluorescence, except for some easily distinguishable, crystalline particles, were negligible. A hierarchical set of oligonucleotide probes (Table 1) was applied to reliably identify ammonia-oxidising bacteria of the β-subclass of *Proteobacteria* as outlined before (Amann *et al.*, 1995). Populations identified by the different probes were quantified and compared on the basis of their cell area, and in all samples a close match (within the standard deviations) was found for the areas detected by probes NSO190, NSO1225 and NSM156 + NSV443.
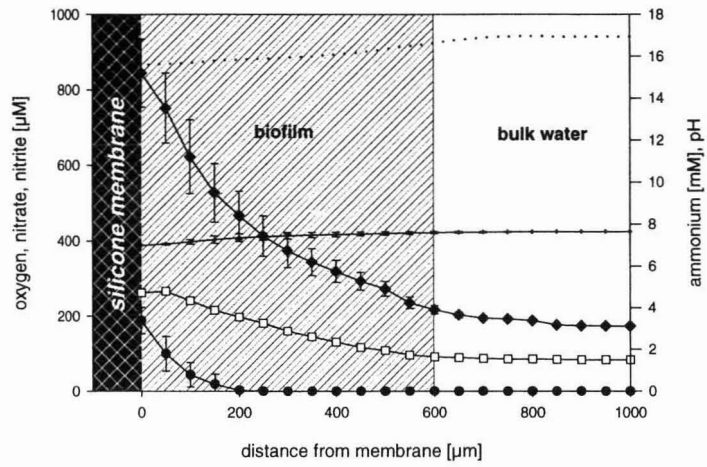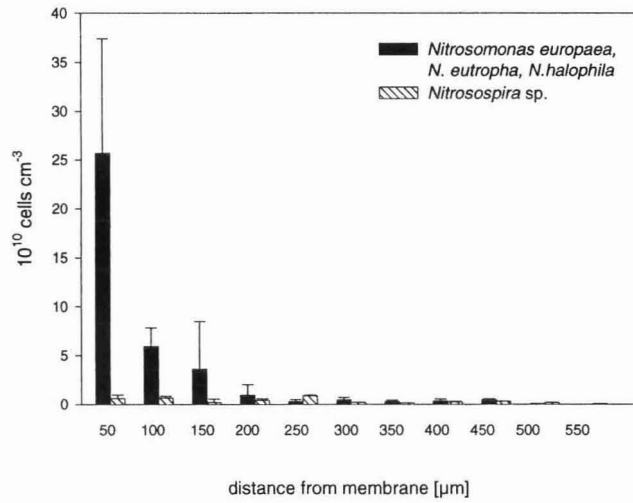
However, only about 5% of all ammonia-oxidisers hybridised also with probe NSV443, specific for the genus *Nitrosospira*. Furthermore, hybridisations with probes NSM156, NEU23a and Nse1472 yielded very similar area values. Thereby, the vast majority of the ammonia-oxidisers is demonstrated to belong to the *Nitrosomonas europaea-eutropha-halophila* group while *Nitrosospira* sp. accounted only for about 5% of all ammonia-oxidisers in all samples. Additionally, few cells of *Nitrosococcus mobilis* have been detected by probe NmV. These constituted in no case more tha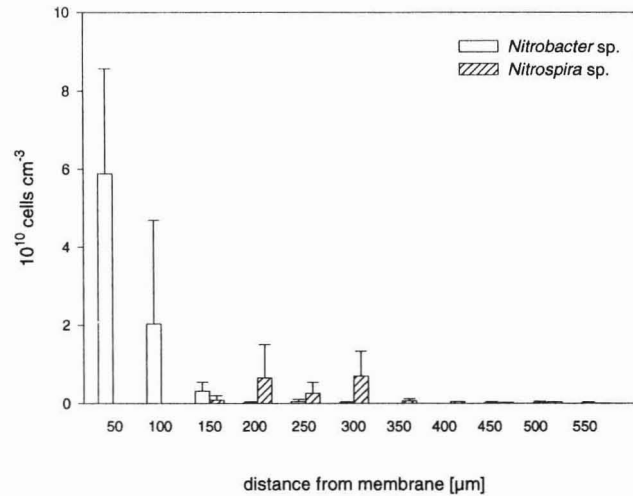n 0.1% of all ammonia-oxidisers. This low number is not surprising as *N. mobilis* is a halophilic strain which is easily overgrown by *N. europaea* in low-salt environments (Juretschko, et al., 1998). Nitrite-oxidising bacteria were identified using probe NIT3, specific for all sequenced strains of *Nitrobacter* (Wagner *et al.*, 1996) and a combination of probes NSR826 + NSR1156 which together target all known *Nitrospira*-like sequences from freshwater habitats (Schramm, et al., 1998).

After five weeks, all nitrifying populations initially detected in the pilot plant (de Beer and Schramm, in press) were also found in the model reactor. However, *N. europaea*-like ammonia-oxidisers already dominated the first 100 µm of the biofilm directly on the membrane, with cell numbers 1-2 orders of magnitude higher than those of all other nitrifiers in that zone, i.e. $1.8 \cdot 10^{11}$ cm^{-3}.

In samples from week 10 and 14, a clear stratification of nitrifying bacteria (Fig. 2B, C) was established along the gradients (Fig. 2A) within the biofilm. *N. europaea*-like ammonia-oxidisers still formed an extremely dense layer of cells directly on the membrane surface ($2.5 \cdot 10^{11}$ cells cm^{-3}), and their numbers decreased gradually with decreasing oxygen concentrations. From 250 µm, the distance from the membrane where oxygen disappeared, till almost to the biofilm surface cell numbers were in the range of $3 \cdot 10^{9}$ cm^{-3}. In contrast, *Nitrosospira* sp. occurred throughout the biofilm in lower numbers of $1 \cdot 10^{9}$ to $6 \cdot 10^{9}$ cells cm^{-3}.

Among the nitrite-oxidisers, *Nitrobacter* sp. showed a preference for the high oxygen and nitrite concentrations within the first 100 µm at the membrane. When oxygen became very low or zero, cell numbers of *Nitrobacter* sp. decreased while *Nitrospira* sp., which was absent from the first 100 µm at the membrane, reached maximum abundance in the zone where the oxygen concentration became very low. Generally, the numbers of nitrite-oxidisers were much lower than the numbers of *N. europaea* in the nitrifying zone. Maximum cell numbers of *Nitrospira* sp. were $9.7 \cdot 10^{9}$ cells cm^{-3} and thus lower than the maximum cell numbers of *Nitrobacter* sp., $7.4 \cdot 10^{10}$ cells cm^{-3}. Like reported previously (Mobarry *et al.*, 1996; Schramm, et al., 1996), *Nitrobacter* sp. was almost always situated in close proximity to ammonia-oxidisers while this was only seldomly found for *Nitrospira* sp..

Fig. 2

A) Gradients of oxygen (●), pH (+), nitrite (◆), and nitrate (□) in the 10 weeks-old membrane-biofilm as measured with microsensors. For each data point, mean values and standard deviations (95% confidence limit) out of 10 profiles are shown, except for the nitrate profile, where standard deviations were in the same range as mean values. Therefore they had to be omitted in order to keep the figure readable. The ammonium concentration (dotted line) was extrapolated from three measuring points, i.e. at the membrane, at the biofilm surface, and in the bulk water.

B) Distribution of ammonia-oxidising bacteria and

C) nitrite-oxidising bacteria in the membrane-biofilm as detected by FISH. Abundance of the different populations was quantified in steps of 50 µm starting at the membrane (to the left). Note different scale.

DISCUSSION

Questions of competition, coexistence or syntrophy of micro-organisms in the environment are often addressed by competition experiments with isolates either in chemostat (Visscher *et al.*, 1992) or gradient systems (Thomas & Wimpenny, 1993). However, this is not well suited for nitrifying bacteria because environmentally relevant strains are difficult to obtain in pure culture in high density and activity (Laanbroek and Woldendorp, 1995; Prosser, 1989). This seems to be especially true for the recently recognised *Nitrospira*-like nitrite-oxidisers (Juretschko, et al., 1998, Schramm et al., this thesis, Chapter 5). In contrast, extremely dense and active nitrifying communities have been reported from various biofilms (Mobarry, et al., 1996; Schramm, et al., 1998; Schramm, et al., 1996) and activated sludges (Juretschko, et al., 1998; Wagner *et al.*, 1995). In this study, we used therefore a biofilm reactor as natural gradient system to study competition and mutualism among nitrifying bacteria. Although the results might be somewhat restricted and more difficult to interpret than those from pure culture experiments it is currently the most direct possibility to gain information on the ecology of nitrification in the absence of relevant pure cultures. The resulting community was dominated by ammonia-oxidisers closely related to *N. europaea* and *N. eutropha*. Considering the high ammonium concentrations (15-20 mM) in the reactor, this confirms earlier reports on their adaptation to high substrate and product concentrations (Pommerening-Röser, et al., 1996). Oxygen seems to be the main factor controlling this population in the biofilm as its distribution correlates well with the oxygen concentration. A similar situation was reported previously for *Nitrosomonas* sp. in a trickling filter biofilm (Schramm, et al., 1996). *Nitrosospira* sp. was not competitive under the conditions prevailing in the biofilm. Whether this was due to a lower specific growth rate as suggested by pure culture (Belser, 1979) and *in situ* studies (Schramm *et al.*, 1998, Schramm *et al*, this thesis, Chapter 5), or due to substrate and/or product inhibition (Prosser, 1989), can not be resolved on the basis of our data.

Interestingly, the two nitrite-oxidiser populations found in our system, *Nitrobacter* sp. and *Nitrospira* sp., appear to be spatially almost fully separated. *Nitrobacter* sp. was only detected close to the membrane where oxygen and nitrite concentrations were highest. This supports the idea that *Nitrobacter* sp. outgrows *Nitrospira* sp. at high substrate concentrations (Schramm *et al*, this thesis, Chapter 5). Low growth rates have been reported for pure cultures of *Nitrospira* sp. (Ehrich *et al.*, 1995; Watson *et al.*, 1986), and low nitrite-oxidation rates were proposed for uncultered *Nitrospira* sp. *in situ* (Schramm *et al.*, this thesis, Chapter 5). Why then did *Nitrospira* sp. establish in the micro-aerobic zone of the biofilm, i.e. between 150 and 300 μm away from the membrane, even out-competing *Nitrobacter* sp.? Affinity for nitrite is unlikely to play a selective role because the nitrite concentrations in this part of the biofilm are still about 400 μM and thus above or about the $K_M(NO_2^-)$ values reported for almost all *Nitrobacter* spp. (60-600 μM, Hunik *et al.*, 1993; Prosser, 1989). Oxygen concentrations, however, are with 0-15 μM well below the $K_M(O_2)$ of *Nitrobacter* sp. (62-256 μM, Prosser, 1989). A competitive advantage for *Nitrospira* sp. on the basis of oxygen affinity would therefore imply that its $K_M(O_2)$ is significantly lower than that of *Nitrobacter* sp..

Furthermore, the differing positioning of the two nitrite-oxidisers relative to the ammonia-oxidising bacteria should be noted. This might indicate differing saturation concentrations for nitrite-oxidation of the two populations. The observed close vicinity of *Nitrobacter* sp. to any ammonia-oxidiser despite high nitrite concentrations of 500-1000 μM might be explained if nitrite-oxidation was not saturated at this level and therefore could be accelerated by the direct uptake of nitrite at the source of its production. Alternatively, the relatively high oxygen concentrations (100-230 μM) within a distance of 50 μm from the membrane might play an important role. *Nitrobacter* sp. have been

reported to be sensitive to high oxygen partial pressures (Bock and Koops, 1992) and therefore might take advantage from a local oxygen decrease due to ammonia-oxidiser neighbourhood. In contrast, *Nitrospira* sp. is subjected to high nitrite and low oxygen concentrations in the zone of its occurrence, resulting in oxygen limitation of nitrite-oxidation rates. Therefore, co-aggregation with ammonia-oxidisers might be a disadvantage because of the competition for oxygen rather than a strategy to enhance nitrite-oxidation activity, and might therefore not have been realised.

We believe that the data presented here support the idea that *Nitrospira* sp. might be a typical *K*-strategist compared to the *r*-strategist *Nitrobacter* sp. (Schramm *et al*, this thesis, Chapter 5), based on its putative higher affinities for nitrite and oxygen and its lower growth rate. In natural environments, where nitrite concentrations are often negligible and nitrifiers have to compete for oxygen with heterotrophic bacteria, *K*-strategy might provide a selective advantage. However, physiological diversity might occur within the genus *Nitrospira*, and one should be cautious to generalize our findings as long as no information as available from in situ studies on the species level or from pure culture experiments.

In conclusion, the analysis of the distribution of nitrifying bacteria along gradients of oxygen and nitrite yielded insights into the factors that might govern the establishment of populations of different nitrite-oxidising bacteria in the environment. Nevertheless, efforts should be made to isolate the respective strains to determine K_m values and growth rates for pure cultures and to evaluate their growth and competitiveness in defined co-cultures.

ACKNOWLEDGEMENTS

REFERENCES

Amann, R. I., Krumholz, L. & Stahl, D. A. (1990). Fluorescent-oligonucleotide probing of whole cells for determinative, phylogenetic, and environmental studies in microbiology. *J.Bacteriol.* **172**, 762-770.

Amann, R. I., Ludwig, W. & Schleifer, K. H. (1995). Phylogenetic identification and in situ detection of individual microbial cells without cultivation. *Microb.Rev.* **59**, 143-169.

Belser, L. W. (1979). Population ecology of nitrifying bacteria. *Annu.Rev.Microbiol.* **33**, 309-333.

Bock, E. & Koops, H.-P. (1992). The genus *Nitrobacter* and related genera. In *The Prokaryotes*, pp. 2302-2309. Edited by A. Balows, H. G. Trüper, M. Dworkin, W. Harder & K.-H. Schleifer. New York: Springer Verlag.

Bock, E., Koops, H.-P. & Harms, H. (1986). Cell biology of nitrifying bacteria. In *Nitrification*, pp. 17-38. Edited by J. I. Prosser. Oxford: IRL Press.

Brosius, J., Dull, T. J., Sleeter, D. D. , & Noller, H. F. (1981). Gene organization and primary structure of a ribosomal RNA operon from *Escherichia coli*. J.Mol.Biol. **148**, 107-127.

Burrel, P. C., Keller, J. & Blackall, L. L. (1998). Microbiology of a nitrite-oxidizing bioreactor. *Appl.Environ.Microbiol.* **64**, 1878-1883.

de Beer, D. & Schramm, A. (1999). Microenvironments and mass transfer phenomena in biofilms studied with microsensors. *Wat.Sci.Tech.* **39** (7), 173-178.

de Beer, D., Schramm, A., Santegoeds, C. M. & Kühl, M. (1997). A nitrite microsensor for profiling environmental biofilms. *Appl.Environ.Microbiol.* **63**, 973-977.

Ehrich, S., Behrens, D., Lebedeva, E., Ludwig, W. & Bock, E. (1995). A new obligately chemolithoautotrophic, nitrite-oxidizing bacterium, *Nitrospira moscoviensis* sp. nov. and its phylogenetic relationship. *Arch.Microbiol.* **164**, 16-23.

Hastings, R. C., Saunders, J. R., Hall, G. H., Pickup, R. W. & McCarthy, A. J. (1998). Application of molecular biological techniques to a seasonal study of ammonia oxidation in a eutrophic freshwater lake. *Appl.Environ.Microbiol.* **64**, 3674-3682.

Hiorns, W. D., Hastings, R. C., Head, I. M., McCarthy, A. J., Saunders, J. R., Pickup, R. W. & Hall, G. H. (1995). Amplification of 16S ribosomal RNA genes of autotrophic ammonia-oxidizing bacteria demonstrates the ubiquity of nitrosospiras in the environment. *Microbiology* **141**, 2793-2800.

Hovanec, T. A., Taylor, L. T., Blakis, A. & DeLong, E. F. (1998). *Nitrospira*-like bacteria associated with nitrite oxidation in freshwater aquaria. *Appl.Environ.Microbiol.* **64**, 258-264.

Hunik, J. H., Meijer, H. J. G. & Tramper, J. (1993). Kinetics of *Nitrobacter agilis* at extreme substrate, product and salt concentrations. *Appl.Microbiol.Biotech.* **40**, 442-448.

Juretschko, S., Timmermann, G., Schmidt, M., Schleifer, K.-H., Pommerening-Röser, A., Koops, H.-P. & Wagner, M. (1998). Combined molecular and conventional analysis of nitrifying bacterial diversity in activated sludge: *Nitrosococcus mobilis* and *Nitrospira*-like bacteria as dominant populations. *Appl.Environ.Microbiol.* **64**, 3042-3051.

Koops, H.-P. & Möller, U. C. (1992). The lithotrophic ammonia-oxidizing bacteria. In *The Prokaryotes*, pp. 2625-2637. Edited by A. Balows, H. G. Trüper, M. Dworkin, W. Harder & K.-H. Schleifer. New York: Springer Verlag.

Kowalchuk, G. A., Stephen, J. R., de Boer, W., Prosser, J. I., Embley, T. M. & Woldendorp, J. W. (1997). Analysis of ammonia-oxidizing bacteria of the β subdivision of the class *Proteobacteria* in coastal sand dunes by denaturing gradient gel electrophoresis and sequencing of PCR-amplified 16S ribosomal DNA fragments. *Appl.Environ.Microbiol.* **63**, 1489-1497.

Kühl, M., Steuckart, C., Eickert, G. & Jeroschewski, P. (1998). A H$_2$S microsensor for profiling biofilms and sediments: application in an acidic lake sediment. *Aquat.Microb.Ecol.* **15**, 201-209.

Laanbroek, H. J. & Woldendorp, J. W. (1995). Activity of chemolithotrophic nitrifying bacteria under stress in natural soils. *Adv.Microb.Ecol* **14**, 275-304.

Manz, W., Amann, R., Ludwig, W., Wagner. M. & Schleifer, K.-H. (1992). Phylogenetic oligodeoxynucleotide probes for the major subclasses of proteobacteria: problems and solutions. *Syst.Appl.Microbiol.* **15**, 593-600.

Mobarry, B. K., Wagner, M., Urbain, V., Rittmann, B. E. & Stahl, D. A. (1996). Phylogenetic probes for analyzing abundance and spatial organization of nitrifying bacteria. *Appl.Environ.Microbiol.* **62**, 2156-2162.

Özoguz, G. (1997). Stickstoffelimination durch immobilisierte Biomasse und entkoppelte Substratversorgung bei hochbelasteten Abwässern. VDI-Verlag, Düsseldorf, Germany.

Pommerening-Röser, A., Rath, G. & Koops, H.-P. (1996). Phylogenetic diversity within the genus *Nitrosomonas*. *Syst.Appl.Microbiol.* **19**, 344-351.

Princic, A., Mahne, I., Megusar, F., Paul, E. A. & Tiedje, J. M. (1998). Effects of pH and oxygen and ammonium concentrations on the community structure of nitrifying bacteria from wastewater. *Appl.Environ.Microbiol.* **64**, 3584-3590.

Prosser, J. I. (1989). Autotrophic nitrification in bacteria. *Adv.Microb.Physiol.* **30**, 125-181.

Reinsel, M. A., Sears, J. T., Stewart, P. S. & McInerney, M. J. (1996). Control of microbial souring by nitrate, nitrite or glutaraldehyde injection in a sandstone column. *J.Indust.Microbiol.* **17**, 128-136.

Revsbech, N. P. (1989). An oxygen microelectrode with a guard cathode. *Limnol.Oceanogr.* **34**, 474-478.

Schramm, A., De Beer, D., Wagner, M. & Amann, R. (1998). Identification and activity in situ of *Nitrosospira* and *Nitrospira* spp. as dominant populations in a nitrifying fluidized bed reactor. *Appl.Environ.Microbiol.* **64**, 3480-3485.

Schramm, A., Larsen, L. H., Revsbech, N. P., Ramsing, N. B., Amann, R. & Schleifer, K.-H. (1996). Structure and function of a nitrifying biofilm as determined by in situ hybridization and the use of microelectrodes. *Appl.Environ.Microbiol.* **62**, 4641-4647.

Stephen, J. R., McCaig, A. E., Smith, Z., Prosser, J. I. & Embley, T. M. (1996). Molecular diversity of soil and marine 16S rRNA gene sequences related to β-subgroup ammonia-oxidizing bacteria. *Appl.Environ.Microbiol.* **62**, 4147-4154.

Thomas, L. V. & Wimpenny, J. W. T. (1993). Method for investigation of competition between bacteria as a function of three environmental factors varied simultaneously. *Appl.Environ.Microbiol.* **59**, 1991-1997.

Timberlake, D. L., Strand, S. E. & Williamson, K. J. (1988). Combined aerobic heterotrophic oxidation, nitrification and denitrification in a permeable-support biofilm. *Wat.Res.* **22**, 1513-1517.

Visscher, P. T., Van Den Ende, F. P., Schaub, B. E. M. & Van Gemerden, H. (1992). Competition between anoxygenic phototrophic bacteria and colorless sulfur bacteria in a microbial mat. *FEMS Microbiol.Ecol.* **101**, 51-58.

Wagner, M., Rath, G., Amann, R., Koops, H.-P. & Schleifer, K.-H. (1995). *In situ* identification of ammonia-oxidizing bacteria. *Syst.Appl.Microbiol.* **18**, 251-264.

Wagner, M., Rath, G., Koops, H.-P., Flood, J. & Amann, R. (1996). *In situ* analysis of nitrifying bacteria in sewage treatment plants. *Wat.Sci.Tech.* **34**, 237-244.

Watson, S. W., Bock, E., Valois, F. W., Waterbury, J. B. & Schlosser, U. (1986). *Nitrospira marina* gen.nov.sp.nov.: a chemolithotrophic nitrite-oxidizing bacterium. *Arch.Microbiol.* **144**, 1-7.

Yu, F. P., Callis, G. M., Stewart, P. S., Griebe, T. & Mcfeters, G. A. (1994). Cryosectioning of biofilms for microscopic examination. *Biofouling* **8**, 85-91.

Chapter 7

An Interdisciplinary Approach to the Occurrence of Anoxic Microniches, Denitrification, and Sulfate Reduction in Aerated Activated Sludge
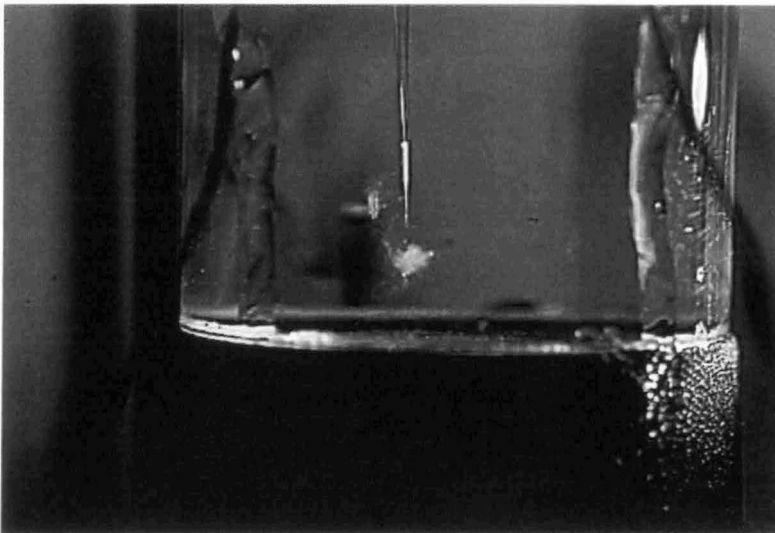
Front page:

Microsensor measurements in a single activated sludge floc by use of "Helle's net-jet". The floc is kept on a fixed position above a nylon net by an upward flow that equals the sinking velocity of the floc. Picture courtesy of Dirk de Beer.

An Interdisciplinary Approach to the Occurrence of Anoxic Microniches, Denitrification, and Sulfate Reduction in Aerated Activated Sludge

ANDREAS SCHRAMM[1*], CECILIA M. SANTEGOEDS[1],
HELLE K. NIELSEN[2], HELLE PLOUG[1], MICHAEL WAGNER[3], MILAN PRIBYL[4],
JIRI WANNER[4], RUDOLF AMANN[1], and DIRK DE BEER[1]

Max Planck Institute for Marine Microbiology, D-28359 Bremen,Germany[1], University of Aarhus, Dept. of Microbial Ecology, DK-8000 Aarhus C, Denmark[2], Technische Universität München, Lehrstuhl für Mikrobiologie,D-80290 Munich, Germany[3], Prague Institute of Chemical Technology, Dept. of Water Technology and Environmental Engineering, CZ-166 28 Prague 6, Czech Republic

A combination of different methods was applied to investigate the occurrence of anoxic processes in aerated activated sludge. Microsensor measurements (O_2, NO_2^-, NO_3^-, H_2S) were performed on single sludge flocs to detect anoxic niches, denitrification, or sulfate reduction on a microscale. Incubations of activated sludge with $^{15}NO_3^-$ and $^{35}SO_4^{2-}$ were used to determine denitrification and sulfate reduction on a batch scale.

In five out of seven investigated sludges, no anoxic zones developed during aeration, and consequently denitrification rates were very low. However, in two sludges anoxia in flocs coincided with significant denitrification rates. No sulfate reduction was found in any sludge by neither microsensor nor batch investigations, not even under totally anoxic conditions. In contrast, the presence of sulfate reducing bacteria could be shown by fluorescence in situ hybridization with 16S rRNA-targeted oligonucleotide probes and by PCR-based detection of genes encoding for the dissimilatory sulfite reductase.

A possible explanation for the absence of anoxia even in most of the larger flocs is that oxygen transport is not only diffusional but enhanced by advection, facilitated by flow through pores and channels. This is indicated by the irregularity of some oxygen profiles and further supported by confocal laser scanning microscopy of the three-dimensional floc structure which showed that flocs from the two sludges in which anoxic zones were found were apparently denser than flocs from the other sludges.

Activated sludge is currently the most widely used process for the treatment of both domestic and industrial wastewaters and, at least by scale, one of the most important microbiological technologies (18). It primarily relies on the degradation and uptake of organic matter by a microbial community under aerobic conditions. Modern plants are often supplemented with anoxic/anaerobic reactor stages to enhance nitrogen and phosphorous removal. The biomass is finally separated from the purified water by gravitational settling prior to recirculating part of it back into the aeration basin. The process, therefore, selects for microorganisms that remain in the system due to their growth in flocs.

This immobilized growth leads to conditions that markedly differ from conditions of suspended growth in the bulk water phase. Closer interactions of different physiological types of microorganisms are possible (i.e. ammonia and nitrite oxidizers (22)), and bacteria are better protected from protozoan grazing (13) or harmful substances. On the other hand, the transport of solutes (e.g. oxygen and nutrients) in flocs is expected to be mainly diffusional (50, 51). Although the vast majority of

activated sludge flocs has been reported to be smaller than 20 µm, i.e. of a size where diffusion limitation is unlikely, flocs larger than 50 µm contribute most to surface area, volume and mass (28). In those larger flocs, the development of anoxic zones has been postulated due to diffusion limitation (50, 51). This would allow for combined nitrification-denitrification in quasi-stratified flocs, hence saving reaction space and time (e.g. 16, 51, and references therein). Less beneficial, anoxic microniches could also support the survival and activity of sulfate reducing bacteria (SRB) in aerated activated sludge, resulting in the production of H_2S and subsequent problems with sludge bulking (58) or floc disintegration (38).

These hypotheses have been supported indirectly by several reports of nitrogen losses from aeration basins (16, 20, 51), and by the detection of SRB in activated sludge by cultivation (26, 58) and fluorescence in situ hybridization (FISH) (34). In contrast, no anoxic zones could be detected by microsensor measurements in large activated sludge flocs (diameter 1.6 mm) at air saturation (26).

Recently, a flow system was developed for microelectrode measurements in freely sinking aggregates ('marine snow') that also enables the analysis of smaller and more fragile flocs in a natural flow field (40, 41). We used this setup for microsensor measurements of oxygen, nitrate, nitrite and hydrogen sulfide in individual activated sludge flocs. These single floc measurements were complemented with $^{15}NO_3^-$ and $^{35}SO_4^{2-}$ incubation experiments (15, 37) to determine overall rates of denitrification and sulfate reduction in the different sludges tested. Finally, the 3D structure, that is critical for the transport mechanism in a floc (diffusion or advection), was recorded by confocal laser scanning microscopy (CLSM), and the samples were screened for SRB by FISH with rRNA-targeted oligonucleotide probes (4, 34) and by PCR specific for the dissimilatory sulfite reductase gene (53). By this interdisciplinary approach we hoped to achieve a more comprehensive picture of the occurrence and preconditions of anoxic processes in activated sludge flocs.

MATERIAL AND METHODS

Samples. Activated sludge samples were obtained from the aeration basins of municipal wastewater treatment plants (WWTP) in Bremen/Seehausen (Germany), Aarhus/Marselisborg, Odder (both Denmark), and Prague (Czech Republic), from a pilot plant in Aarhus (Denmark), and from two lab-scale sequencing batch reactors (SBR) receiving artificial wastewater (peptone 1000 mg COD l^{-1}, acetic acid 300 mg COD l^{-1}, glucose 400 mg COD l^{-1}, ethanol 300 mg COD l^{-1}, N_{total} 82 mg l^{-1}, N-NH_4^+ 0.2 mg l^{-1}, P_{total} 14 mg l^{-1}). The sulfate concentration was 102 mg SO_4^{-2} l^{-1}. Both SBR were operated with rapid filling periods (5-10 min) to simulate the conditions in a plug-flow reactor with high substrate concentration gradients. SBR1 was operated with a complete oxic cycle (23 h aeration, 1 h settling), whereas SBR2 was subjected to an alternating cycle (3 h anoxic, 8 h aeration, 1 h settling). Some operational data of the investigated sludges are summarized in Table 1.

TABLE 1. Operational data of the investigated activated sludge plants

	WWTP Aarhus	WWTP Bremen	WWTP Odder	WWTP Prague	Pilotplant Aarhus	SBR1	SBR2
*COD (mg l^{-1})	419	476	450	242	n.d.	2000	2000
*N-NH_4 (mg l^{-1})	33.1	37.5	34	20	n.d.	0.2	0.2
*P_{total} (mg l^{-1})	3.2	7.0	12	3.65	n.d.	14	14
MLSS (g l^{-1})	4.3	3.04	3.14	2.7	n.d.	7.4	3.2
reaction time (h)	5.7	6.5	n.d.	3.3	n.d.	46	33
sludge age (d)	25	10	n.d.	3.3	n.d.	25	8

*influent values; n.d. not determined

74

For microsensor measurements a small portion of sludge was diluted to avoid massive agglomeration of flocs after sampling, and single flocs were carefully transferred to the measuring setup by means of a pipette with the tip cut open. For the batch experiments freshly collected sludge was allowed to settle, the supernatant was discarded, and the concentrated sludge was used for the incubations.

Microsensor measurements. Clark-type microsensors for O_2 (42), LIX-type microsensors for NO_2^- and NO_3^- (8), and amperometric H_2S microsensors (25) were constructed, calibrated, and used for measurements as previously described. The lower detection limits of NO_2^- and H_2S were 0,1 µM and 1 µM, respectively. Microprofiles of single activated sludge flocs were recorded by keeping the flocs freely suspended in a vertical flow system, where the flow velocity opposed and balanced the sinking velocity of the individual floc. To create a parallel, non-turbulent, uniform flow a nylon stocking was mounted in the flow chamber horizontally to the flow, and the flocs were positioned just above this net (40, 41). By this net-jet system the flocs could be stabilized in the upward flowing water column allowing microsensor measurements with a spatial resolution of 25 - 50 µm inside the flocs. For practical reasons microprofiles of different chemical species were usually recorded in different flocs.

The artificial wastewater used in the flow chamber contained 200 µM sodium acetate, 760 µM $(NH_4)_2SO_4$, 220 µM KH_2PO_4, 400 µM K_2HPO_4, and 41 µM $MgSO_4$, representing an F:M (food to microorganism) ratio of approximately 0.1, which is a value typical for most nutrient removal plants (47). For measurements of NO_2^- and NO_3^- this medium was supplemented with 100 µM KNO_3. Microsensor measurements were performed at 20°C at three different oxygen concentrations: air saturation (~ 280 µM), 2 mg l^{-1} (~ 60 µM), the oxygen set-point of most aeration basins, and anoxic conditions.

Additionally, 10 ml of activated sludge were amended with a mixture of acetate, propionate and butyrate (final concentration 1 mM each) in a test-tube and incubated for approximately 1 h without aeration. After oxygen was depleted (proven by microsensor measurements) an H_2S microsensor was repeatedly introduced into the sludge.

Calculations. The volumetric oxygen respiration rate R of a sphere with zero order kinetics at steady state is described by (41):

$$R = \frac{4\pi r_0^2}{\frac{4}{3}\pi(r_0^3 - r_c^3)} \cdot \frac{D_{W(ox)}(C_\infty - C_0)}{\delta_{eff}} \tag{1}$$

where r_0 is the radius of the sphere, $4\pi r_0^2$ and $\frac{4}{3}\pi r_0^3$ are the surface area and volume, respectively, r_c is the radial distance from the center at which the oxygen concentration becomes zero (if there is no anoxic zone $r_c = 0$), $D_{W(ox)}$ is the molecular diffusion coefficient of oxygen in water, C_∞ and C_0 are the concentrations of oxygen in the bulk water phase and at the floc surface, respectively, and δ_{eff} is the effective diffusive boundary layer (DBL) thickness. The same formula was used to calculate denitrification rates of single flocs from nitrate microprofiles. D_W for oxygen at 20°C is $2.12 \cdot 10^{-5}$ cm^2 s^{-1} (5), for nitrate $1.66 \cdot 10^{-5}$ cm^2 s^{-1} (29). Determination of δ_{eff} and data processing was done by a simple diffusion-reaction model assuming zero order kinetics as described in detail by Ploug et al. (41).

Acetate concentration at the floc center was estimated from the volumetric oxygen respiration rates R using (41)

$$C_c = -\frac{R}{3} \cdot \left(\frac{r_0^2}{2D_{agg(ac)}} + \frac{r_0 \cdot \delta_{eff}}{D_{W(ac)}} \right) + C_\infty \tag{2}$$

where C_c is the acetate concentration at the floc center, δ_{eff} is the effective DBL thickness determined from the oxygen profiles, and $D_{agg(ac)}$ and $D_{W(ac)}$ are the molecular diffusion coefficients of acetate in

the floc and in water which were assumed to be the same. $D_{W(ac)}$ was calculated using standard tables and formulas (30) and corrected for co-diffusion of NH_4^+ (the cation with the highest concentration in the medium) to a value of $1.00 \cdot 10^{-5}$ cm^2 s^{-1} (29). The same formula was also applied with respect to oxygen, where C and D are concentrations and diffusion coefficients of oxygen, respectively (41). Thereby, the respiration rates required to create anoxic conditions at the floc center (i.e. $C_c = 0$) were calculated as a function of floc size at different bulk water concentrations of oxygen (Fig. 5).

$^{15}NO_3^-$**-incubations.** Denitrification rates were determined using a batch reactor with a liquid volume of 1.2 l and a gas volume of 0.5 l (including tubing). The reactor was cylindrical with a diameter of 10 cm and a height of 17 cm. The bottom section was funnel shaped with a porous glass grid in the center, through which gas was supplied. This arrangement prevented the development of stagnant zones. The gas flow rate was just sufficient to keep the flocs in suspension. Oxygen concentration measurements at different positions within the reactor showed that it was well mixed under test conditions. Prior to the incubations, N_2 in the reactor was exchanged by argon to lower the background, thereby improving the detection of ^{15}N-enriched N_2. Rate measurements were performed at air saturation, at an oxygen concentration of 40-60 µM, and in the absence of oxygen by adjusting the oxygen/argon ratio in the gas supply. An oxygen microelectrode was inserted in the reactor for continuous monitoring during the experiments. 300 ml of concentrated activated sludge was added to the reactor, which was then filled up with 1 l of artificial wastewater (as described for the microsensor measurements) and amended with sodium acetate to a concentration of 7.8 mM. The reactor contained 2 - 4 g TSS l^{-1} (TSS = total suspended solids). After the oxygen concentration was adjusted, 8.3 ml of $Na^{15}NO_3$ was added from a 12 mM stock solution of 99.2 atom% $^{15}NO_3^-$, corresponding to a final concentration of 100 µM $^{15}NO_3^-$. During the 30 min incubation experiment, gas samples of 1 ml were taken from the reactor headspace every 3 minutes through a septum with a gas-tight syringe (Hamilton, 1001RN) and transferred to gas-tight exetainers (Labco), that had been filled with N_2-free distilled water.

Subsamples of gas (250 µl) were analyzed on an isotope ratio mass spectrometer with collectors for $^{28}N_2$, $^{29}N_2$, and $^{30}N_2$ (Sira Series II, VG Isotech, Middlewich, Chesire, UK) as described previously (37, 44). Total denitrification rates were calculated as the sum of denitrification of $^{15}NO_3^-$ and $^{14}NO_3^-$, that were derived from the measured production of $^{14}N^{15}N$ and $^{15}N^{15}N$ as described in detail by Nielsen (37).

$^{35}SO_4^{2-}$**-incubations.** Sulfate reduction rates were determined by the ^{35}S-radiotracer method (15) in samples from SBR1, SBR2, and from the WWTP Prague. Reactor design, incubation conditions, and filling of the reactor were as described for the ^{15}N-experiments. After the oxygen concentration was adjusted, 20 ml of tracer was added ($Na_2^{35}SO4$, 2 Mbeq). Through a septum samples of 5 ml were taken from the reactor during the first 10 minutes once per minute, then for another 10 minutes once every two minutes. Subsequently, samples were taken every 10 minutes until one hour after the start of the test. To each sample, 5 ml of fixation solution (20% ZnAc, 1% formaline, pH 5) were added and shaken well. Samples to which 0.1 ml of tracer was added after fixation were used as blanks for each incubation. Fixed samples were stored at 4°C until further analysis within two months. The samples were then centrifuged at 10,000 g and the reduced sulfur species in the pellet were determined with the single-step chromate distillation according to Fossing and Jørgensen (15). The detection limit of the method was a sulfate reduction rate of 5 µmol S g^{-1} TSS h^{-1}.

SRB screening. Activated sludge samples were fixed with paraformaldehyde, immobilized on microscopic slides and dehydrated as described previously (3). For fluorescence in situ hybridization (FISH), a set of oligonucleotide probes specific for SRB was used, i.e. SRB385, targeting a broad range of SRB but also numerous non-sulfate-reducing bacteria (2), probes DSV698, DSV407,

DSV1292, and DSV214, specific for the family *Desulfovibrionaceae* (34), probes 221 and 660, specific for the genus *Desulfobacterium* and *Desulfobulbus*, respectively (10), and probes DSB985 and DSS658, specific for the genus *Desulfobacter* and the taxon *Desulfosarcina-Desulfococcus* (34), respectively. All probes were purchased labeled with the fluorescent dye CY3 (Interactiva Biotechnologie Ulm, Germany) and applied for FISH using the protocol and the conditions recently described by Manz et al. (34). After the hybridization procedure the samples were stained with 4',6-diamidino-2-phenylindole (DAPI) according to Wagner et al. (52), mounted with antifading reagent (Vectashield, Vector Laboratories Inc., Burlingame, CA) and examined under an epifluorescence microscope (Zeiss, Jena, Germany).

Independent testing for the presence of SRB was done by amplification of a 1.9 kb DNA fragment encoding most of the α and β subunits of the dissimilatory sulfite reductase (DSR). DNA was extracted from four activated sludge samples (WWTP Bremen and Prague, SBR1, SBR2) by a combined freeze-thaw (3 times freezing in liquid nitrogen and heating at 37°C) and hot phenol-chloroform-isoamyl alcohol treatment (49). The DSR gene fragments were then amplified using the primer pair DSR1F (5'- ACSCACTGGAAGCACG-3') and DSR4R (5'-GTGTAGCAGTTACCGCA-3') described by Wagner et al.(53). The PCR reaction mixture (100 µl) contained 100 pmol of each primer, 25 nmol of all four deoxynucleoside triphosphates, 200 µg of bovine serum albumin, 10 µl 10× PCR buffer (HT Biotechnology Ltd) and 10 - 100 ng of template DNA. A hot-start PCR program was used, in which 1 U of SuperTaq DNA polymerase (HT Biotechnology Ltd) was added at 80°C after 5 min heating at 94°C, followed by 35 cycles, each cycle consisting of 1 min at 94°C, 1 min at 60°C, and 3 min at 72°C. The PCR products were loaded and evaluated on a 1% agarose gel. As a positive control for proper PCR performance with DNA from activated sludge samples, a 550-bp-long 16S rDNA fragment was amplified with universal primers as described by Muyzer et al. (36).

3D analysis of flocs. For the staining with fluorescein-isothiocyanate (FITC) which covalently binds to proteins (19), 0.2 ml of settled flocs were added to 15 ml staining solution (0.1 M sodium phosphate, pH 7.0 and 4 mg l^{-1} FITC). After 5 minutes of gentle mixing the aggregates were allowed to settle, the solution was decanted and the flocs were washed twice with 0.1 M sodium phosphate, pH 7.0. The aggregates were stored at 4°C in 0.1 M sodium phosphate, pH 7.0, with 4% paraformaldehyde. For CLSM analysis the pH was raised to 9 by the addition of 1 M carbonate buffer. Staining with calcofluor to visualize polysaccharides was performed similarly in the same buffer with 300 mg l^{-1} calcofluor (7). The staining time was 2 hours. Washing and storage was as described above. The aggregates were microscopically examined at pH 7.0. DNA within the flocs was stained with ethidiumbromide (1 µg ml^{-1}) for 15 min in the same buffer. The flocs were washed as described above, and immediately observed under the CLSM.

CLSM-analysis. FITC-, calcofluor- and ethidiumbromide-stained flocs were transferred into 1 ml buffer to a chamber sealed on the bottom with a cover glass and analyzed with an inverse confocal laser scanning microscope (LSM510, Carl Zeiss, Jena, Germany). A 40x Plan-Neofluar 1.3 lens was used, and three different lasers (Argon-ion: UV [351-364 nm]; 458 nm and 488 nm; HeNe: 543 nm) were applied for excitation. Image processing, including three-dimensional reconstruction, was performed with the standard software package delivered with the instrument (version 2.01, service pack 2). Images were printed on a Kodak printer 8650 by use of the software package Microsoft Power Point (version 7.0, Microsoft, Redmont, USA).

RESULTS
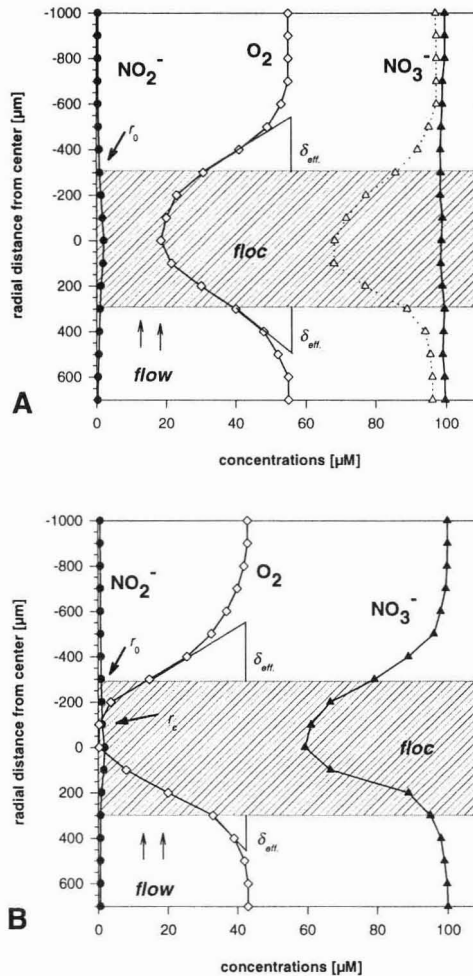
FIG. 1. Typical microprofiles of oxygen, nitrite, and nitrate in activated sludge flocs from WWTP Prague (A) and SBR1 (B), measured in the net-jet flow chamber at 2 mg $O_2 l^{-1}$.

Hatched area = floc, r_0 = floc surface, r_c = distance from floc center where oxygen disappears, $\delta_{eff.}$ = effective diffusion boundary layer (DBL). The dotted nitrate profile in Fig 1A was recorded under anoxic conditions and displays the denitrification potential of the floc.

Microprofiles. Microsensor measurements for the different parameters were performed in different activated sludge flocs, all in all in 250 individual flocs with a size range of 400 - 2300 μm (maximum length as observed by dissection microscopy). Larger flocs often consisted of a loose agglomeration of compact subunits of 50 - 100 μm, suggesting a dynamic aggregation and disintegration. Flocs smaller than 400 μm could not be sufficiently stabilized in the flow chamber for profiling.

When incubated under air saturation (~280 μM) oxygen was never depleted but showed values of 90-200 μM in the floc center. In several flocs (indicated by arrows in Fig. 3) oxygen gradients were somewhat irregular or weak, and oxygen increased locally inside the floc. This might result from advective transport of oxygen-rich bulk medium through pores into the floc. Nitrite concentrations

78

slightly increased towards the center reaching 0.5-2 µM, probably due to nitrification. Nitrate concentrations increased to above bulk water concentrations in some flocs indicating nitrifying activity, appeared unchanged in other flocs, and in only three large flocs (SBR2) a decrease of 5-10 µM was observed.

Incubation under 40-60 µM oxygen, resembling the conditions in aeration basins, lead to oxygen concentrations of typically less than 20 µM in the floc center. Complete depletion of oxygen was observed within 12 out of 14 flocs from the two SBR and within 2 out of 8 flocs from the WWTP Bremen but not within flocs from any other sample. Accordingly, a significant decrease of nitrate towards the floc center was only detected within the SBR flocs, and denitrification rates of individual flocs were calculated in the range of 2-14 $nmol \cdot mm^{-3} \cdot h^{-1}$ (average SBR1 5.9 $nmol \ mm^{-3} \ h^{-1}$, SBR2 10.2 $nmol \cdot mm^{-3} \cdot h^{-1}$). All other samples showed no or very little nitrate consumption (maximum denitrification rate 1.7 $nmol \cdot mm^{-3} \cdot h^{-1}$, averages 0-0.7 $nmol \cdot mm^{-3} \cdot h^{-1}$). Most nitrite gradients were insignificant. In some flocs nitrite accumulated to concentrations of 5-20 µM, possibly because nitrite oxidation was inhibited by low oxygen concentrations. Typical profiles of oxygen, nitrate and nitrite in activated sludge flocs from the WWTP samples and from SBR samples are displayed in Fig. 1 A and B, respectively.

To test the samples for their denitrification capacity we also recorded nitrate and nitrite profiles while oxygen was absent. A decrease of nitrate was measured in virtually all tested flocs from all sludges. The derived denitrification rates were quite heterogeneous, spanning a range of 0.5-27 $nmol \cdot mm^{-3} \cdot h^{-1}$. Nitrite profiles were similar to the ones measured under 40-60 µM oxygen, although nitrite production in this case must be attributed to nitrate reduction.

No H_2S was detectable by microsensor measurements in any floc from any sample, not even after prolonged anoxic incubations (1 h) at stagnant conditions in a test-tube.
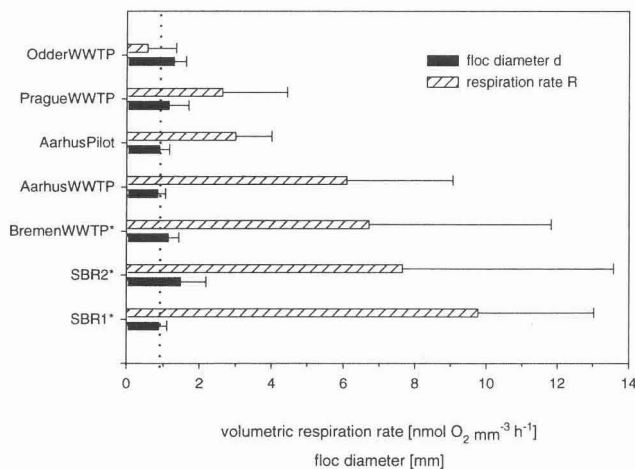
FIG. 2. Mean volumetric respiration rates R and mean floc sizes d with standard deviations of all flocs from all samples in which oxygen gradients have been measured. Sludges in which anoxic microniches were detected are marked with a star. The dotted line indicates a floc diameter of 1 mm.

Respiration rate. Volumetric respiration rates R of individual flocs were calculated from the oxygen profiles assuming diffusion to be the only transport process. They were between 0 and 18 nmol O_2 $mm^{-3}h^{-1}$, with the highest R values found in those sludges in which anoxic microniches had been detected, i.e. in SBR1, SBR2, and WWTP Bremen (Fig. 2).

Under 40-60 µM oxygen the respiration rates obviously decreased with floc size (Fig. 3B)., while this trend was not as pronounced under air saturation (Fig. 3A).
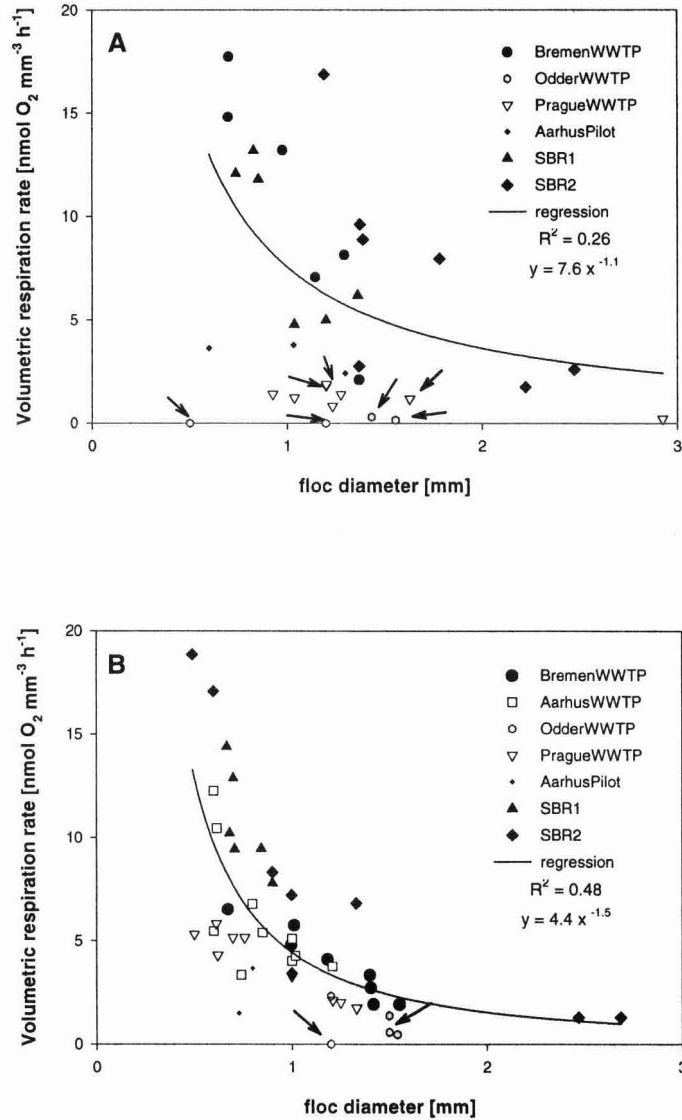
FIG. 3. Volumetric oxygen respiration rates versus floc diameter as measured under air saturation (A) and under 2 mg O_2 l^{-1} (B). Arrows indicate flocs where the oxygen profile was most likely influenced by advective transport (liquid flow). These data points were excluded from the regression curve, as the respiration rates are most probably underestimates (see discussion)

TABLE 2. Denitrification rates as determined by $^{15}NO_3$ incubations

	air saturation	20% air saturation	anoxic conditions
WWTP Aarhus	0.003±0.001	0.114±0.058	1.496±0.151
WWTP Bremen	n.d.	0.046±0.013	3.212±1.690
WWTP Odder	0.007±0.004	0.040±0.003	1.592±0.401
WWTP Prague	0.005±0.003	0.038±0.005	1.198±0.358
Pilotplant Aarhus	n.d.	n.d.	n.d.
SBR1	0.191±0.12	0.470±0.234	1.257±0.128
SBR2	0.101±0.022	0.940±0.282	1.826±0.246

all values ±SD in μmol N g^{-1} TSS min^{-1}

Incubation experiments. Batch experiments to determine denitrification and sulfate reduction rates using stable and radio-isotope techniques were performed under the same conditions, and with similar results, as the microsensor measurements (Table 2). Under air saturation virtually no denitrification occurred, and the rates under reactor conditions were extremely low except for the SBR samples. All sludges were, however, capable of denitrification under anoxic conditions, at rather diverse rates. Sulfate reduction could not be detected neither in sludge from Prague WWTP nor in sludges from the SBR, regardless of the aeration conditions applied (air saturation, reactor conditions, or anoxia).

SRB screening. FISH with probe SRB385 suggested the presence of SRB in all tested sludges. The abundance of specifically hybridized cells was roughly estimated to be 1-2% in the SBR and in the Aarhus pilot plant, and 3-5% of total cells stained by DAPI in all other samples. Of the more specific probes only DSV698 and DSV1292, complementary to the majority of *Desulfovibrio* species, detected significant numbers of target cells, i.e. 0.5-1% in the SBR and in the Aarhus pilot plant, and 2-4% of total cells in the other samples. In comparison, members of the genera *Desulfobacterium, Desulfobacter, Desulfobulbus, Desulfomicrobium,* and *Desulfosarcina* detected by FISH together made up less than 0.2% in all samples. Additionally, DNA was extracted from activated sludge samples of the SBR as well as from samples of the WWTP Prague and Bremen. Using the same amount of DNA (ca. 20 ng) for the PCR reaction we obtained no PCR product of the DSR gene fragments from the SBR samples, but distinct PCR products of the expected size were retrieved from the WWTP samples (data not shown). As dissimilatory sulfite reductase is a key-enzyme for sulfate reduction, the detection of its genes indicates the presence of sulfate reducing bacteria (or of at least their DNA) in the WWTP activated sludges but not in the SBR.

3D analysis of activated sludge flocs. For a qualitative analysis of the three-dimensional floc structure of different sludges (WWTP Prague, Bremen, SBR1, SBR2), flocs were stained either with FITC, calcofluor or ethidium bromide. These fluorescent dyes bind to proteins, polysaccharides and DNA, respectively, which represent the main compounds of extracellular polymeric substance (EPS) of activated sludge flocs (50). Staining of these substances should therefore give a good impression of its structure. A comparison of the different stains revealed that, at the low resolution needed to visualize complete flocs, all three yielded approximately the same picture, i.e. the same ratio of stained floc material to unstained pore volume. However, as FITC-conferred fluorescence of the flocs was brightest and gave best CLSM images, all further 3D analyses were performed on FITC-stained flocs. CLSM analysis revealed clear differences of the floc structure between the different sludge types. WWTP flocs appeared to have a more fluffy structure with more and larger pores (i.e. the

unstained part), which were estimated to comprise 50-80% of the entire floc volume. In contrast, SBR flocs seemed to be denser and more compact (pore volume 30-65%). An example of each kind of floc is shown in Fig. 4. It should be mentioned, however, that the numbers must be treated as estimates after examination of 52 flocs rather than as quantitative description of pore volumes and floc populations. Nevertheless, the qualitative difference in porosity and structure was evident.
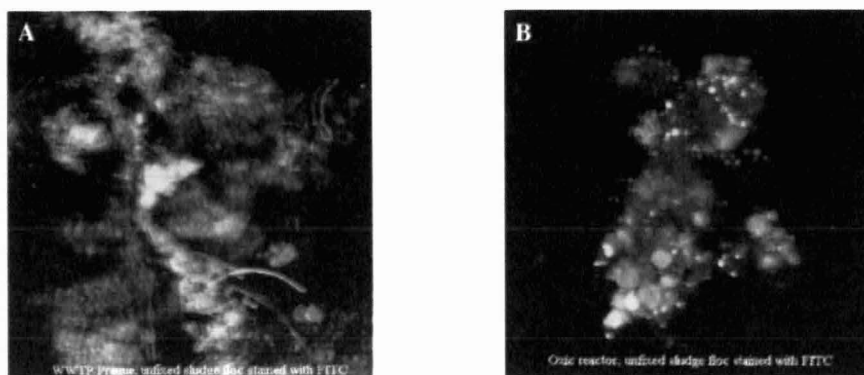

FIG. 4. CLSM image (red-green overlay, use red-green glasses) of the 3D structure of activated sludge flocs from WWTP Prague (A) and SBR1 (B) after FITC staining. 300 x 300 µm.

DISCUSSION

Anoxic microniches and denitrification. When incubated under air saturation anoxia was never detected inside activated sludge flocs which is in agreement with the measurements of Lens et al. (26). Calculation of acetate concentrations in the center of the flocs, based on the measured oxygen respiration rates (equation 2), showed that only in 2 out of 35 flocs acetate could be completely depleted. Therefore, assuming that acetate (this study) or glucose and starch (26) were suitable substrates for the microbial community in activated sludge, respiration was most likely not limited by the availability of organic carbon. This indicates that the respiration capacity of activated sludge is simply not sufficient to consume such high amounts of oxygen. However, even when incubated under more realistic conditions (2 mg O_2 l^{-1}) no anoxic zones and no denitrification were detected in activated sludge flocs except of the SBR and few flocs from Bremen WWTP. The question has to be raised how representative the microsensor measurements in single flocs have been, i.e. if the measuring approach was suited to detect anoxic microniches, and if the results are meaningful for a complete activated sludge basin. In our study we only analyzed flocs larger than 400 µm. From literature data, this seems to be not an important fraction in terms of number but might be most relevant in terms of volume or mass (12, 28), and hence the fraction that contributes most to the activity of a plant. Furthermore, anoxic zones due to diffusion limitation are primarily to be expected in larger flocs since the volumetric respiration rates required to create anoxia exactly at the center of a floc increase with the square of the floc radius (equation 2, Fig. 5; (41)). Therefore, under reactor conditions volumetric respiration rates of more than 70 nmol·mm^{-3}·h^{-1} are necessary for anoxia in flocs with a diameter of 400 µm or less. Such high rates have only been found in microbial mats (21) and nitrifying aggregates (9) while the rates reported from various other systems such as detritus

pellets (41), trickling filter biofilms (23, 24), or sediments (14, 43) are all in the same range (1.2 - 39.6 $nmol \cdot mm^{-3} \cdot h^{-1}$) as the values measured in this study (0 - 19 $nmol \cdot mm^{-3} \cdot h^{-1}$). It is thus questionable if the respiration rates required for anoxia in flocs smaller than 400 μm can be ever reached in activated sludge. Furthermore, microprofiles were investigated simulating sinking flocs, i.e. in a flow chamber with laminar flow, where no turbulent mixing or collisions of flocs occur. The latter processes, however, are typical for aerated activated sludge basins and obviously lead to a steady aggregation and disintegration of flocs. Gradients and flocs are consequently dynamic features, e.g. the center of a floc might become exposed to oxygen again after an anoxic period by the disruption of the floc. For these two reasons, the size of the studied flocs and the measuring conditions, it is more likely that we overestimated anoxic processes in the activated sludges by microsensor analysis rather than to overlook them.

The isotope incubation experiments yield independent control for the microsensor data as they averaged over all flocs present in a large sample and better simulated the mixing regime in an activated sludge basin. Consistent with the microprofiles, significant denitrification under 2 mg O_2 l^{-1} was only measured in the SBR, while under anoxic conditions all sludges showed rates of 1.2 - 3.2 μmol N g^{-1} TSS min^{-1}, comparable to conventional anoxic activated sludge basins designed for denitrification (6, 50). This shows that denitrifiers were present in all sludges, and the virtual absence of denitrification in most sludges during aeration can be indeed explained by the absence of anoxic niches inside the activated sludge flocs. Furthermore, denitrification under 2 mg O_2 l^{-1} represented a similar percentage of maximum denitrification activity in both, ^{15}N-incubations and microsensor measurements (data not shown). This indicates that microprofiles actually were recorded under realistic conditions and show data relevant for the whole aeration basin. Some nitrate microprofiles showed denitrification under air saturation, and also denitrification rates determined by ^{15}N-incubations are slightly above the detection limit in samples where no anoxic zones were found. Thus, one may speculate about the occurrence of aerobic denitrifiers (31, 39, 45). However, their contribution to overall denitrification seems to be almost negligible in the analyzed systems.
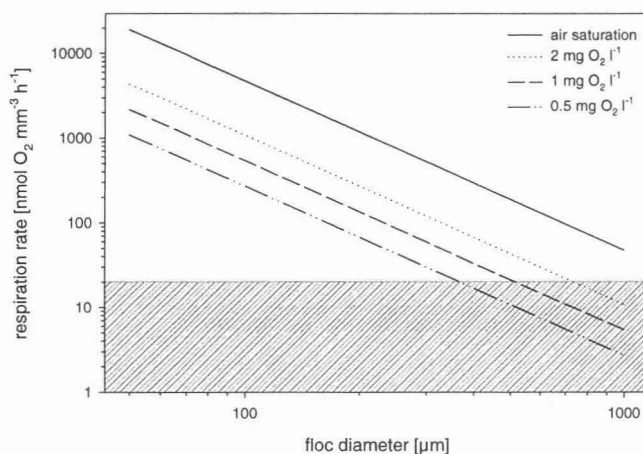
FIG. 5. Volumetric oxygen respiration rates R required to create anoxic conditions exactly at the center of a floc with a maximum DBL under different bulk oxygen concentrations (calculated from equation 2). Under such diffusion limited conditions R decreases with the square of the floc radius. The hatched area represents respiration rates that have been measured during this study.

Another considerable factor is the bulk water concentration of oxygen. Obviously, reducing the aeration of activated sludge will immediately increase the probability of anoxic microniches and

processes inside a diffusion controlled floc (Fig. 5). Indeed there have been reports on enhanced denitrification rates in aerated activated sludges when the bulk oxygen concentration was set to 0.5 - 1.5 mg l^{-1} (17, 20, 57). However, nitrification might be less effective or become incomplete; therefore attempts to achieve nitrogen removal by simultaneous nitrification-denitrification by simply lowering the bulk oxygen concentration would require continuous monitoring and careful balance of both processes.

Respiration rates. Valuable information can be derived from the measured volumetric respiration rates R of individual flocs in relation to their size. As displayed in Fig. 5, smaller flocs require higher respiration rates to become anoxic because of their higher surface to volume ratio. This also applies to the investigated samples (Fig. 2). For example, the mean floc sizes of analyzed flocs from SBR1, Aarhus WWTP and Aarhus Pilot are almost the same, however only the respiration rates of SBR1 are sufficient to create anoxic zones. Furthermore, the volumetric respiration rate R was negatively correlated with floc size d (Fig. 3). This was more pronounced for flocs under reactor conditions than for flocs under air saturation. A decrease of R with d^2 usually would indicate diffusion limitation within the floc (Fig. 5). The observed decrease of R with $d^{1.5}$ at 40-60 µM oxygen (Fig. 3B) might be explained by the different extent of oxygen limitation in the different flocs that contributed to the regression analysis: (i) flocs with anoxic centers, which are truly diffusion limited, (ii) flocs with rather low oxygen concentrations (1-10 µM), that might already slow down respiration rates, and (iii) flocs with higher oxygen levels that should allow for maximum respiration rates since the K_m for oxygen consumption by heterotrophic bacteria is about 1 µM (56). In contrast, diffusion limitation can be excluded to account for this trend under air saturation (Fig. 3A). Oxygen as well as organic carbon are present in concentrations high enough to prevent any limitations as has been discussed before. An alternative explanation lies in the structure and the geometry of the floc. Larger flocs might be less dense than smaller ones, i.e. contain less active cells per volume and more voids and dead material. This seems to be partially the case, as large flocs (> 1 mm) often enclose bigger particles which do not contribute to respiration. Furthermore, activated sludge flocs are fractal in their geometry, with fractal dimensions of 1.0 - 1.8 (27, 33, 48). As is typical of fractal aggregates, the porosity of flocs increases with increasing floc size (1), resulting in reduced mass and hence respiration rate per volume as the aggregates get larger. The same applies of course also under the lower oxygen concentrations but this weak correlation is covered by the more pronounced diffusion limitation. Fractal geometry of the activated sludge flocs might therefore provide an explanation why the volumetric respiration rates of most sludges have been too low to create anoxic conditions even in the larger flocs. Alternatively, this might be due to advective transport through pores and channel-like structures (32) since larger flocs often consist of dense subunits that are only loosely connected. Flow might have been detected in some of our oxygen profiles that showed a local increase in oxygen concentration (data points marked with an arrow in Fig. 3). Flow could substantially enhance oxygen transfer compared to diffusion. In this case, our calculations of volumetric respiration rates (and denitrification rates) based on diffusional transport underestimate R. If advection is important as transport mechanism in activated sludge flocs, a reduced oxygen bulk concentration does not necessarily result in anoxic zones and enhanced denitrification as discussed above.

Considering fractal geometry and advective transport might help to understand the differences between the flocs from the SBR and the other samples. SBR have been reported to form more compact (and larger) flocs (54) which would allow for higher volumetric respiration rates compared to conventional WWTP flocs and prevent advective transport of oxygen inside the floc. This hypothesis is supported by CLSM analysis of the 3D floc structure that demonstrated SBR flocs to be

more compact than WWTP flocs (Fig. 4). However, further research is needed to better understand the impact of floc structure, i.e. fractal geometry and advective transport, on the floc's function.

Sulfate reduction. Low numbers of SRB were detected by FISH in all samples, and the amplification of the DSR gene fragments indicated the presence of SRB in samples from WWTP Bremen and Prague. In contrast, no sulfate reduction was detected in any experiment by microsensor or radioisotope analysis. The sensitivity of the applied techniques was high ($1\mu M$ H_2S and 5 µmol S g^{-1} TSS·h^{-1}, respectively). Re-oxidation was excluded during anoxic incubations, and by the ^{35}S analysis even immediate precipitation of H_2S, e.g., as FeS (38), would have been detected. Consequently, sulfate reduction did not occur during oxic incubations and no sulfate reduction potential was apparent in the anaerobic incubations. However, a shortcoming of the approach was the use of acetate as sole carbon source in almost all experiments. Acetate is not utilized as electron donor by incompletely oxidizing SRB including *Desulfovibrio* sp. (55), which were detected by far as the main component of the SRB community in the analyzed samples. Most likely, sulfate reduction in our experiments had therefore to rely on endogenous electron donors of the activated sludge that were either produced from the acetate added or had been stored within the flocs. Whereas this assumption is doubtful for the microsensor experiments, due to the small volume of a single floc compared to incubation volume and time, it is well sound for the radiotracer and the test-tube incubations. Here, about one third of the reactor volume consisted of concentrated activated sludge, and only two third of the sludge bulk water had been replaced by the artificial medium. Essentially, the substrate spectrum was similar to the original activated sludge sample but slightly diluted. Therefore, we are convinced that we would have been able to detect sulfate reduction in the observed systems if it had occurred. The complete absence of sulfate reduction, and the detection of significantly lower numbers of SRB in the pilot plant and SBR compared to the WWTP samples most likely indicate unfavorable conditions for SRB in the investigated sludges. It might be possible that SRB are not able to grow and multiply in the aerated activated sludge but rely on the continuous re-inoculation via sewer, biofilm wall growth in the basin (46), or backwash from settler and anaerobic digester. The lack of these sources in the lab-scale SBR and the pilot plant might explain the low numbers of SRB detected there by FISH. This low amount of SRB might also explain the failure to detect the DSR gene fragment in samples from the SBR. Possibly, the same amount of DNA that resulted in reliable amplifications from the other samples might have been to low to yield PCR products from the SBR. Considering the reported occurrence of higher numbers of SRB in activated sludge (e.g. 26, 34, 58) in the light of our results, we would suggest that the actual function of these SRB in the aeration basins might not be sulfate reduction. For instance, oxygen (11) and nitrate (35) have been described as alternative electron acceptors. However, also plant-to-plant differences have to be kept in mind, and sulfate reduction may occur in other activated sludge systems.

Conclusion. We found that anoxic microniches and denitrification are possible and detectable in aerated activated sludge. The structure of the activated sludge flocs plays an important role for the occurrence of this phenomenon. However, anoxia seems to be rather the exception than the rule in conventional wastewater treatment plants, and sulfate reduction seems to be almost fully absent. The exact interrelations between structure and function of the activated sludge floc require further investigation, especially to describe on a quantitative basis the fractal geometry - respiration correlation.

REFERENCES

1. **Alldredge, A.** 1998. The carbon, nitrogen and mass content of marine snow as function of aggregate size. Deep Sea Res. **45:**529-541.

2. **Amann, R. I., B. J. Binder, R. J. Olson, S. W. Chisholm, R. Devereux, and D. A. Stahl.** 1990. Combination of 16S rRNA-targeted oligonucleotide probes with flow cytometry for analyzing mixed microbial populations. Appl.Environ.Microbiol. **56:**1919-1925.

3. **Amann, R. I., L. Krumholz, and D. A. Stahl.** 1990. Fluorescent-oligonucleotide probing of whole cells for determinative, phylogenetic, and environmental studies in microbiology. J.Bacteriol. **172:**762-770.

4. **Amann, R. I., W. Ludwig, and K. H. Schleifer.** 1995. Phylogenetic identification and in situ detection of individual microbial cells without cultivation. Microb.Rev. **59:**143-169.

5. **Broecker, W. S., and T.-H. Peng.** 1974. Gas exchange rates between air and sea. Tellus. **26:**21-35.

6. **Christensen, M. H., and P. Harremoes.** 1977. Biological denitrification of sewage: a literature review. Prog. Watet Technol. **8:**509-555.

7. **de Beer, D., V. O'Flaharty, J. Thaveesri, P. Lens, and W. Verstraete.** 1996. Distribution of extracellular polysaccharides and flotation of anaerobic sludge. Appl.Microbiol.Biotech. **46:**197-201.

8. **de Beer, D., A. Schramm, C. M. Santegoeds, and M. Kühl.** 1997. A nitrite microsensor for profiling environmental biofilms. Appl.Environ.Microbiol. **63:**973-977.

9. **de Beer, D., J. C. van den Heuvel, and S. P. P. Ottengraf.** 1993. Microelectrode measurements of the activity distribution in nitrifying bacterial aggregates. Appl.Environ.Microbiol. **59:**573-579.

10. **Devereux, R., M. D. Kane, J. Winfrey, and D. A. Stahl.** 1992. Genus- and group-specific hybridization probes for determinative and environmental studies of sulfate-reducing bacteria. Syst.Appl.Microbiol. **15:**601-609.

11. **Dilling, W., and H. Cypionka.** 1990. Aerobic respiration in sulfate reducing bacteria. FEMS Microbiol. Letters. **71:**123-128.

12. **Droppo, I. G., D. T. Flannigan, G. G. Leppard, C. Jaskot, and S. N. Liss.** 1996. Floc stabilization for multiple microscopic techniques. Appl.Environ.Microbiol. **62:**3508-3515.

13. **Eberl, L., R. Schulze, A. Ammendola, O. Geisenberger, R. Erhart, C. Sternberg, S. Molin, and R. Amann.** 1997. Use of green fluorescent protein as a marker for ecological studies of activated sludge communities. FEMS Microbiol. Letters. **149:**77-83.

14. **Epping, E. H. G., and B. B. Jørgensen.** 1996. Light enhanced oxygen respiration in benthic phototrophic communities. Mar.Ecol.Prog.Ser. **139:**193-203.

15. **Fossing, H., and B. B. Jørgensen.** 1989. Measurement of bacterial sulfate reduction in sediments: evaluation of a single-step chromium reduction method. Biogeochem. **8:**205-222.

16. **Goronszy, M. C., G. Demoulin, and M. Newland.** 1996. Aerated denitrification in full-scale activated sludge facilities. Wat.Sci.Tech. **34:**487-491.

17. **Goronszy, M. C., G. Demoulin, and M. Newland.** 1997. Aerated denitrification in full-scale activated sludge facilities. Wat.Sci.Tech. **35:**103-110.

18. **Gray, N. F.** 1990. Activated sludge. Theory and practice. Oxford University Press, Oxford.

19. **Griebe, T.** 1991. Ph.D. thesis, University of Hamburg, Hamburg, Germany.

20. **Hao, X., H. J. Doddema, and J. W. van Groenestijn.** 1997. Conditions and mechanisms affecting simultaneous nitrification and denitrification in a Pasveer oxidation ditch. Biores. Technol. **59:**207-215.

21. **Jørgensen, B. B., and D. J. Des Marais.** 1990. The diffusive boundary layer of sediments: oxygen microgradients over a microbial mat. Limnol.Oceanogr. **35:**1343-1355.

22. **Juretschko, S., G. Timmermann, M. Schmidt, K.-H. Schleifer, A. Pommerening-Röser, H.-P. Koops, and M. Wagner.** 1998. Combined molecular and conventional analysis of nitrifying bacterial diversity in activated sludge: *Nitrosococcus mobilis* and *Nitrospira*-like bacteria as dominant populations. Appl.Environ.Microbiol. **64:**3042-3051.

23. **Kühl, M., R. N. Glud, H. Ploug, and N. B. Ramsing.** 1996. Microenvironmental control of photosynthesis and photosynthesis-coupled respiration in an epilithic cyanobacterial biofilm. J.Phycol. **32:**799-812.

24. **Kühl, M., and B. B. Jørgensen.** 1992. Microsensor measurement of sulfate reduction and sulfide oxidation in compact microbial communities of aerobic biofilms. Appl.Environ.Microbiol. **58:**1164-1174.

25. **Kühl, M., C. Steuckart, G. Eickert, and P. Jeroschewski.** 1998. A H$_2$S microsensor for profiling biofilms and sediments: application in an acidic lake sediment. Aquat.Microb.Ecol. **15:**201-209.

26. **Lens, P. N., M.-P. De Poorter, C. C. Cronenberg, and W. H. Verstraete.** 1995. Sulfate reducing and methane producing bacteria in aerobic wastewater treatment systems. Wat.Res. **29:**871-880.

27. **Li, D., and J. J. Ganczaczyk.** 1989. Fractal geometry of particle aggregates generated in water and wastewater treatment process. Environ. Sci. Technol. **23:**1385-1389.

28. **Li, D., and J. Ganczarczyk.** 1991. Size distribution of activated sludge flocs. J.WPCF. **63:**806-814.

29. **Li, Y. H., and S. Gregory.** 1974. Diffusion of ions in sea water and in deep-sea sediments. Geochim.Cosm.Acta. **38:**703-714.

30. **Lide, D. R. (ed.).** 1992. CRC Handbook of chemistry and physics, 73 ed. CRC Press, Boca Raton.

31. **Lloyd, D., L. Boddy, and K. J. P. Davies.** 1987. Persistence of bacterial denitrification capacity under aerobic conditions: the rule rather than the exception. FEMS Microbiol.Ecol. **45.**

32. **Logan, B. E., and J. R. Hunt.** 1988. Bioflocculation as a microbial response to substrate limitations. Biotech.Bioeng. **31:**91-101.

33. **Logan, B. E., and D. B. Wilkinson.** 1990. Fractal geometry of marine snow and other biological aggregates. Limnol.Oceanogr. **35:**130-136.

34. **Manz, W., M. Eisenbrecher, T. R. Neu, and U. Szewzyk.** 1998. Abundance and spatial organization of Gram-negative sulfate-reducing bacteria in activated sludge investigated by in situ probing with specific 16S rRNA targeted oligonucleotides. FEMS Microbiol.Ecol. **25:**43-61.

35. **McCready, R. G. L., W. D. Gould, and F. D. Cook.** 1983. Respiratory nitrate reduction by *Desulfovibrio* sp. Arch.Microbiol. **135:**182-185.

36. **Muyzer, G., T. Brinkhoff, U. Nübel, C. M. Santegoeds, H. Schäfer, and C. Wawer.** 1998. Denaturing gradient gel electrophoresis (DGGE) in microbial ecology, p. 1-27. *In* A. D. L. Akkermans, J. D. van Elsas, and F. J. de Bruijn (ed.), Molecular microbial ecology manual, 3rd ed, vol. 3.4.4. Kluwer Academic Publishers, Dordrecht, The Netherlands.

37. **Nielsen, L. P.** 1992. Denitrification in sediment determined from nitrogen isotope pairing. FEMS Microbiol.Ecol. **86:**357-362.

38. **Nielsen, P. H., and K. Keiding.** 1998. Disintegration of activated sludge flocs in presence of sulfide. Wat.Res. **32:**313-320.

39. **Patureau, D., N. Bernet, and R. Moletta.** 1997. Combined nitrification and denitrification in a single aerated reactor using the aerobic denitrifier *Comamonas* sp. strain SGLY2. Wat.Res. **31:**1363-1370.

40. **Ploug, H., and B. B. Jørgensen.** 1999. A net-jet flow system for mass transfer and microsensor studies of sinking aggregates. Mar.Ecol.Prog.Ser.**176:**279-290.

41. **Ploug, H., M. Kühl, B. Buchholz-Cleven, and B. B. Jørgensen.** 1997. Anoxic aggregates - an ephemeral phenomenon in the pelagic environment? Aquat.Microb.Ecol. **13:**285-294.

42. **Revsbech, N. P.** 1989. An oxygen microelectrode with a guard cathode. Limnol.Oceanogr. **34:**474-478.

43. **Revsbech, N. P., B. Madsen, and B. B. Jørgensen.** 1986. Oxygen production and consumption in sediments determined at high spatial resolution by computer simulation of oxygen microelectrode data. Limnol.Oceanogr. **31:**293-304.

44. **Risgaard-Petersen, N., and S. Rysgaard.** 1995. Nitrate reduction in sediments and waterlogged soil measured by ^{15}N techniques, p. 287-295. *In* K. Alef and P. Namijaeri (ed.), Methods in Applied Soil Microbiology and Biochemistry. Academic Press.

45. **Robertson, L. A., R. Cornelisse, P. de Vos, R. Hadioetomo, and J. G. Kuenen.** 1989. Aerobic denitrification in various heterotrophic nitrifiers. Antonie van Leeuwenhoek. **56:**289-299.

46. **Santegoeds, C. M., T. G. Ferdelman, G. Muyzer, and D. de Beer.** 1998. Structural and functional dynamics of sulfate-reducing populations in bacterial biofilms. Appl.Environ.Microbiol. **64:**3731-3739.

47. **Sedlak, R.** 1991. Phosphorus and nitrogen removal from municipal wastewater. Principle and practice, 2nd ed. Lewis publishers, Boca Raton, FL.

48. **Tambo, N., and Y. Watanabe.** 1979. Physical characteristics of flocs 1: The floc density function and aluminum floc. Wat.Res. **13:**409-419.

49. **Teske, A., C. Wawer, G. Muyzer, and N. B. Ramsing.** 1996. Distribution of sulfate-reducing bacteria in a stratified fjord (Mariager Fjord, Denmark) as evaluated by most-probable-number counts and denaturing gradient gel electrophoresis of PCR-amplified ribosomal DNA fragments. Appl.Environ.Microbiol. **62:**1405-1415.

50. **Verstraete, W., and E. van Vaerenbergh.** 1986. Aerobic activated sludge, p. 43-112. *In* W. Schönborn (ed.), Microbial Degradations, 1st ed, vol. 8. VCH, Weinheim, Germany.

51. **von Münch, E., P. Lant, and J. Keller.** 1996. Simultaneous nitrification and denitrification in bench-scale sequencing batch reactors. Wat.Res. **30:**277-284.

52. **Wagner, M., R. Amann, H. Lemmer, and K.-H. Schleifer.** 1993. Probing activated sludge with oligonucleotides specific for proteobacteria: inadequacy of culture-dependent methods for describing microbial community structure. Appl.Environ.Microbiol. **59:**1520-1525.

53. **Wagner, M., A. M. Roger, J. L. Flax, G. A. Brusseau, and D. A. Stahl.** 1998. Phylogeny of dissimilatory sulfite reductases supports an early origin of sulfate respiration. J.Bacteriol. **180:**2975-2982.

54. **Wanner, J.** 1994. Activated slufge bulking and foaming control. Technomic Publishing Company, Lancaster.

55. **Widdel, F., and F. Bak.** 1992. Gram-negative mesophilic sulfate-reducing bacteria, p. 3352-3378. *In* A. Balows, H. G. Trüper, M. Dworkin, W. Harder, and K.-H. Schleifer (ed.), The Prokaryotes, 2nd ed. Springer Verlag, New York.

56. **Wimpenny, J. W.** 1969. Oxygen and carbon dioxide as regulators of microbial growth and metabolism, p. 161-198. *In* P. M. Meadow and S. J. Pirt (ed.), Microbial Growth. Cambridge University Press, Cambridge.

57. **Wistrom, A. O., and E. D. Schroeder.** 1996. Enhanced nutrient removal by limiting dissolved oxygen concentration in a continously fed, intermittently decanted, activated sludge plant. Environ. Technol. **17:**371-380.

58. **Zietz, U.** 1995. The formation of sludge bulking in the activated sludge process. Eur. Water Pollut.Contr. **5:**21-27.

SUMMARY

Biofilms are complex communities of immobilized microorganisms in which various processes occur in close spatial and functional coupling. In wastewater treatment, they are used, e.g., for nitrogen elimination. Ammonium is oxidized by nitrifying bacteria to nitrate, which is further converted by denitrifying bacteria into gaseous dinitrogen. In this thesis, activity, identity, and spatial distribution of nitrifying bacteria in biofilms were investigated by the combined application of microsensors and fluorescence *in situ* hybridization (FISH).

An initial study, performed with a nitrate/nitrite-biosensor, showed that nitrification was restricted to a narrow but highly active zone at the surface of a trickling filter biofilm. This correlated well with the detection of dense clusters of ammonia-oxidizing *Nitrosomonas* sp. in close vicinity to nitrite-oxidizing *Nitrobacter* sp. in the same layer.

The development of an ion-selective microsensor for nitrite and the improvement of sensors for ammonium and nitrate facilitated the subsequent, more detailed analyses regarding products and substrates of nitrification and the respective nitrifying populations in biofilms.

By means of the rRNA approach, yet uncultured relatives of *Nitrospira moscoviensis* were detected in nitrifying aggregates, and were identified as active nitrite oxidizers by the use of microsensors. Together with ammonia-oxidizing *Nitrosospira* sp. they dominated the nitrifying shell of these aggregates from a fluidized bed reactor. Abundance and volumetric activity of the ammonia- and nitrite-oxidizers were quantified along the decreasing ammonium concentration in the reactor column. From these data it was possible to calculate cell-specific *in situ* reaction rates and to estimate substrate affinities of uncultured nitrifiers for ammonium and nitrite. Comparing these values with literature data it was hypothesized that in habitats with high substrate concentrations *Nitrosomonas* sp. and *Nitrobacter* sp. dominated due to their higher maximum specific reaction rates. In contrast, in low-substrate environments *Nitrosospira* sp. and *Nitrospira* sp. might be better competitors due to their higher substrate affinity. This conclusion was supported by the abundance and distribution of *Nitrosomonas/Nitrosospira* and *Nitrobacter/Nitrospira* in a biofilm under high ammonium concentrations and with pronounced gradients of oxygen and nitrite.

Activated sludge flocs are in many features similar to biofilms. The occurrence of anoxic centers in flocs has been proposed. Therefore, in the last part of this thesis anoxic microniches, denitrification and sulfate reduction in single flocs were investigated using microsensors. These data were complemented by incubation experiments to reveal denitrification and sulfate reduction rates in sludge samples. Furthermore, the three-dimensional floc structure and the community structure of sulfate reducing bacteria in activated sludge were analyzed.

APPENDIX

ZUSAMMENFASSUNG

Biofilme sind komplexe Lebensgemeinschaften immobilisierter Mikroorganismen, in denen verschiedenste Prozesse auf engstem Raum gekoppelt sein können. Sie finden u.a. Verwendung zur Stickstoffeliminierung bei der Abwasserbehandlung. Dabei wird zunächst Ammonium von nitrifizierenden Bakterien zu Nitrat oxidiert. Denitrifizierende Bakterien können anschließend Nitrat zu gasförmigem Stickstoff umsetzten und dadurch aus dem System entfernen. Im Rahmen dieser Arbeit wurden Aktivität, Identität und räumliche Anordnung von Nitrifikanten in Biofilmen durch den kombinierten Einsatz von Mikrosensoren und Fluoreszenz-*in situ*-Hybridisierung (FISH) untersucht.

In einer ersten Studie wurde mit einem Nitrat/Nitrit-Biosensor die Nitrifikationszone als dünne, hochaktive Schicht an der Oberfläche eines Tropfkörper-Biofilms bestimmt. Im selben Bereich konnten durch FISH dichte Kolonien von Ammonium-Oxidierern der Gattung *Nitrosomonas* und Nitrit-Oxidierer der Gattung *Nitrobacter* in enger Nachbarschaft nachgewiesen werden.

Die Entwicklung eines ionenselektiven Mikrosensors für Nitrit und die Verbesserung der Sensoren für Ammonium und Nitrat ermöglichte in den folgenden Arbeiten eine genauere Analyse der Substrat- und Produkt-Konzentrationen der Nitrifikation in Biofilmen und der damit verbundenen Populationen nitrifizierender Bakterien.

Mit Hilfe des rRNA-Ansatzes konnten in nitrifizierenden Aggregaten bisher unkultivierte Vertreter der Gattung *Nitrospira* detektiert und durch Mikrosensor-Messungen als aktive Nitrit-Oxidierer identifiziert werden. Gemeinsam mit ammoniumoxidierenden *Nitrosospira* sp. bildeten sie den Hauptbestandteil der nitrifizierenden Schicht in diesen Aggregaten aus einem Flüssigbett-Reaktor. Anzahl und Aktivität der Ammonium- und Nitrit-Oxidierer wurden entlang der abnehmenden Ammoniumkonzentration im Reaktor quantifiziert, die *in situ* Reaktionsraten pro Zelle berechnet, und die Substrataffinität der unkultivierten Nitrifikanten für Ammonium und Nitrit abgeschätzt. Durch Vergleich mit Literaturwerten ergab sich die Hypothese, daß in Habitaten mit hohen Substratkonzentrationen *Nitrosomonas europaea* und *Nitrobacter* sp. aufgrund ihrer höheren maximalen Reaktionsraten dominieren müßten, während bei geringer Substratkonzentration *Nitrosospira* sp. und *Nitrospira* sp. aufgrund ihrer höheren Substrataffinitäten überlegen sein sollten. Diese Vermutung wurde durch Abundanz und Verteilung von *Nitrosomonas/Nitrosospira* bzw. *Nitrobacter/Nitrospira* in einem weiteren Biofilm mit hohen Ammoniumkonzentrationen und ausgeprägten Sauerstoff- und Nitritgradienten gestützt.

Belebtschlammflocken ähneln in vieler Hinsicht Biofilmen, und das Auftreten anoxischer Kernbereiche in Flocken war postuliert worden. Im letzten Teil dieser Arbeit wurde das Vorkommen von anoxischen Mikro-Nischen, Denitrifikation und Sulfatreduktion in einzelnen Flocken mit Mikrosensoren untersucht. Diese Daten wurden durch die Bestimmung von Denitrifikations- und Sulfatreduktionsraten in Inkubationsexperimenten ergänzt. Zusätzlich wurde die dreidimensionale Flockenstruktur und die Populationsstruktur von sulfatreduzierenden Bakterien im Belebtschlamm analysiert.

RESUME

Les biofilms sont des communautés complexes de microorganismes au sein desquelles plusieurs processus sont couplés d'un point de vue spatial et fonctionnel. Dans le traitement des eaux usées, ils sont utilisés, par exemple, pour l'élimination de l'azote. L'ammonium est oxydé, par les bactéries nitrifiantes en nitrate, puis converti en azote gazeux par les bactéries dénitrifiantes. Cette thèse présente une étude de l'activité, de l'identité et de la distribution spatiale des bactéries nitrifiantes au sein de biofilms, à l'aide de l'application combinée de microsondes et de techniques d'hybridation *in situ* par fluorescence (FISH).

Une étude initiale, obtenue avec une biosonde nitrate/nitrite, a montré que la nitrification était restreinte à une zone étroite mais très active à la surface d'un biofilm formé dans un filtre à écoulement. Parallèlement, des groupes importants d'ammonium oxydantes type *Nitrosomonas* sp. en relation étroite avec des nitrites oxydantes type *Nitrobacter* sp. ont été détectés au sein de la même zone.

Le dévelopement d'une microsonde à nitrite et l'amélioration des sondes pour l'ammonium et le nitrate, ont facilité une analyse plus détaillée des produits et substrats de la nitrification ainsi que des populations bactériennes nitrifiantes dans les biofilms.

A l'aide de techniques utilisant les ARNr, une bactérie, encore non isolée, se rapprochant de *Nitrospira muscoviensis*, a été détectée dans des aggrégats nitrifiants, puis identifiée à l'aide de microsensors comme étant une nitrite oxydante active. Avec *Nitrosopira* sp., elles dominent la paroi de ces aggrégats formés dans un réacteur à fond fluidifiant. L' abondance et l'activité des ammonium et nitrites oxydantes ont été quantifiées le long du gradient de concentration en ammonium. Les activités spécifiques par cellule et les affinités en ammonium et nitrite ont été calculées pour des nitrifiantes non-cultivées. Il est supposé qu'en environnement à forte teneurs en substrats, *Nitrosomonas* sp. et *Nitrobacter* sp. seraient les espèces dominantes grâce à leur forte activités spécifiques. Au contraire, en milieus pauvres en substrats, *Nitrosospira* sp. et *Nitrospira* sp. sembleraient être de meilleur compétiteurs grâce à leurs fortes affinités. Cette conclusion est confirmée par la distribution de ces bactéries dans un biofilm soumis à de hautes teneurs en ammonium et de forts gradient en oxygène et nitrite.

Les boues flocculentes et les biofilms présentent des caractéristiques communes. La possible apparition de conditions d'anoxie aux centres des flocculents a été suggérée. Ainsi, la dernière partie de cette thèse a été consacrée à l'étude, à l'aide de microsensors, de la dénitrification et de la sulfato-réduction dans des flocculents isolés. Parallèlement, la dénitrification et la sulfato-réduction on été estimée dans des échantillons de boues. De plus, la structure tridimensionelle du floculent et les communautés de bacteries sulfato-réductrices ont été analysées dans une boue active.

RESUMEN

Las biopelículas están constitutidas por comunidades de microorganismos inmobilizadas, en las cuales se desarrollan varios procesos intimamente conectados tanto espacial como funcionalmente. En tratamiento de aguas residuales estas biopelículas se usan, por ejemplo, en la eliminación de nitrógeno. El amonio se ve oxidado a nitrato por las bacterias nitrificantes, y éste se ve convertido posteriormente en nitrógeno gas por las bacterias desnitrificantes. En la presente Tesis se investigó la actividad, identidad y la distribución espacial de bacterias nitrificantes mediante la aplicación combinada de microsensores e hibridación *in situ* por fluorescencia (FISH).

En un primer estudio, en el cual se utilizó un biosensor de nitrato/nitrito, se observó que la nitrificación estaba restringida a una capa fina y con elevada actividad en la superficie de la biopelícula del filtro percolador. Estos resultados se correlacionaban con la detección, en la misma zona, de agrupaciones densas de bacterias oxidadoras de amonio (*Nitrosomonas* sp.) en las cercanías de organismos oxidadores de nitritos (*Nitrobacter* sp.).

El desarrollo de un microsensor selectivo para el ion nitrato y la mejora de los sensores para amonio y nitrato, facilitaron tanto el estudio en mayor detalle de los sustratos y productos de la nitrificación como el análisis de las poblaciones nitrificantes en biopelículas.

El uso combinado de la técnica FISH y los microsensores permitió la detección de el microorganismo aun no cultivado *Nitrospira moscoviensis* en el interior de agregados nitrificantes, así como demostrar su participación activa en la oxidación de nitrito. Este organismo, juntamente con el oxidador de amonio *Nitrosospira* sp. se encontraban dominando la corteza nitrificante de los agregados en un reactor de lecho fluidizado. Se cuantificó la abundancia y la actividad por volumen de los oxidadores de amonio y de nitrito paralelamente a la disminución en concentración de amonio en la columna del reactor. A partir de estos datos fue posible calcular las tasas de reacción *in situ* por célula, así como estimar la afinidad por los sustratos amonio y nitrito de organismos nitrificantes no cultivados. De la comparación de nuestros valores con los citados en la literatura se pudo hipotetizar que en los hábitats con elevada concentración de sustrato, *Nitrosomonas* sp. y *Nitrobacter* sp. dominan debido a la elevada tasa máxima de catálisis específica. Al contrario, en ambientes con baja concentración de sustrato *Nitrosospira* sp. y *Nitrospira* sp. deben competir más eficazmente debido a su elevada afinidad por el sustrato. Esta conclusion estuvo apoyada por la abundancia y distribución de *Nitrosomonas/Nitrosospira* y *Nitrobacter/Nitrospira* en un biofilm sometido a elevadas concentraciones de amonio y con gradientes de oxígeno y nitrito pronunciadas.

Las partículas que conforman los lodos activos se parecen en muchos aspectos a biopelículas. Se ha propuesto la existencia de núcleos anóxicos en estas partículas, por tanto en la última parte de la tesis se ha estudiado, con el uso de microsensores, la presencia de micronichos anóxicos, desnitrificación y reducción de sulfatos en partículas aisladas. Los resultados obtenidos se compaginaron con experimentos donde se pudo poner de manifiesto las tasas de reducción de sulfato y desnitrificación mediante incubaciones de lodos activos. Además, se analizó la estructura tridimensional de las partículas, así como la estructura de la comunidad de bacterias sulfato reductoras en lodos activos.

РЕЗЮМЕ

Биофильмы являются комплексными сообществами микроорганизмов, тесно связанных пространственно и функционально. Одной из функций биологических пленок, применяемых для очистки сточных вод, является продукция газообразного азота. Аммоний, используемый нитрификаторами, окисляется до нитрата, который в дальнейшем восстанавливается до газообразного азота денитрифицирующими бактериями. Исследование активности, состава и пространственной организации сообщества нитрифицирующих бактерий в биофильмах с использованием микросенсоров и флуоресцентной in situ гибридизации (FISH) были предметом настоящего исследования.

Предварительное исследование с использованием нитратно-нитритного биосенсора показало, что процесс нитрификации происходит в узкой, но достаточно активной зоне на поверхности фильтра, где была локализована пленка. В том же слое наблюдаются плотные кластеры аммоний-окисляющих *Nitrosomonas* sp., ассоциированных с нитрит-окисляющими бактериями *Nitrobacter* sp.

Разработка ионно-селективного микросенсора для измерения нитрита, а также ряд усовершенствований аммоний- и нитрат-сенсоров позволили провести более детальное исследование субстратов и продуктов нитрификации, а также соответствующих популяций нитрифицирующих бактерий в биофильмах.

С помощью rRNA метода в агрегатах нитрификаторов была обнаружена некультивируемая *Nitrospira moscoviensis*, являющаяся активным нитрит-окислителем, что в свою очередь показали микросенсорные измерения. Вместе с аммоний-окисляющими *Nitrosospira* sp. они представляют «нитрифицирующий барьер», отделяющий эти агрегаты от собственно раствора в реакторе. Количество и волюметрическая активность аммоний- и нитрит-окислителей оценивались в ходе уменьшения концентрации аммония в колонке реактора. Эти данные позволили оценить специфические скорости реакций *in situ*, а также субстратную избирательность некультивируемых нитрификаторов для аммония и нитрита. Сравнительный анализ полученных данных с литературными источниками показал, что в местах с высокой концентрацией субстрата популяции *Nitrosomonas* sp. *Nitrobacter* sp. доминируют за счет большей специфической скорости реакции. В свою очередь *Nitrosospira* sp. и *Nitrospira* sp. являются доминантными формами в условиях низкой концентрации субстрата за счет их повышенной субстратной избирательности.Этот вывод подтверждается количеством и характером распределения *Nitrosomonas/Nitrosospira* и *Nitrobacter/Nitrospira* пар в биологической пленке при повышенных концентрациях аммония и градиентах кислорода и нитрита.

Хлопья в канализационных стоках во многих чертах схожи с биологическими пленками. Предполагается, что центральные части хлопьев лишены кислорода. Исследование анаэробных микрониш, процессов денитрификации и нитратредукции в отдельных хлопьях с использованием микросенсорных методов обсуждается в заключительной части работы. Эти данные были дополнены натурными измерениями скоростей денитрификации и сульфатредукции в образцах из канализационных стоков. Анализировалась трехмерная структура хлопьев и структурная организация сообщества сульфатредукторов.

SAMENVATTING

Biofilms zijn ingewikkelde gemeenschappen van geimmobiliseerde microorganismen, waarin verschillende processen dicht bijeen plaatsvinden en vaak onderling gekoppeld zijn. Zij worden o.m. toegepast in de stikstofverwijdering bij afvalwaterzuivering. Hierbij wordt eerst ammonium door nitrificerende bacteriën tot nitraat geoxideerd. Vervolgens wordt door denitrificerende bacteriën nitraat tot stikstofgas omgezet waardoor stikstof uit het ecosysteem verdwijnt. In deze studie zijn activiteit, identiteit en ruimtelijke verdeling van nitrificeerders in biofilms onderzocht door een combinatie van microsensor metingen en fluorescente-*in situ*-hybridisatie (FISH).

In eerste studie werd met een nitraat/nitriet biosensor vastgesteld dat nitrificatie plaatsvindt in een dunne, uiterst actieve zone aan het oppervlak van een trickling-filter biofilm. In deze zone werden met FISH kolonies met hoge celdichtheden van ammonium oxiderende *Nitrosomonas* en nitriet oxiderende *Nitrobacter* in elkaars dichte nabijheid gevonden.

De ontwikkeling van een ion-selectieve microsensor voor nitriet en de verbetering van sensoren voor ammonium en nitraat maakten een nadere studie mogelijk van substraat- en product concentraties in nitrificerende biofilms, in relatie tot de aanwezige nitrificerende bacterie populaties.

In nitrificerende aggregaten uit een gefluidiseerd bed reactor werden, met behulp van de rRNA benadering, tot nu toe oncultiveerbare vertegenwoordigers van het geslacht *Nitrospira* ontdekt. Met microelectrodes werd aangetoond dat zij nitriet oxideerders zijn, die samen met ammonium oxiderende *Nitrosospira* sp. de nitrificerende buitenlaag van deze aggregaten vormen. Het aantal en de celspecifieke- en volumetrische activiteit van ammonium- en nitriet oxideerders werd gemeten over de lengteas van de reactor, waarlangs de ammonium concentratie geleidelijk afneemt. Tevens werden schattingen gemaakt van de ammonium- en nitriet affiniteiten van de uncultiveerbare nitrificeerders. Na vergelijking met literatuur gegevens werd de hypothese opgesteld dat in een milieu met hoge substraat concentraties *Nitrosomonas europea* en *Nitrobacter* sp. domineren door hun hoge groeisnelheid, terwijl bij lagere substraat concentraties *Nitrosospira* sp. en *Nitrospira* sp. beter concurreren door hun hogere substraat affiniteit. Deze hypothese werd bevestigd door de verdeling van *Nitrosomonas/Nitrosospira,* dan wel *Nitrobacter/Nitrospira* in een andere biofilm met hoge ammonium belading en steile zuurstof en nitriet profielen.

Actief slib vlokken zijn in vele opzichten vergelijkbaar met biofilmen. Het voorkomen van anoxische zones in thet midden van de vlokken werd mogelijk geacht. In de laatste studie van deze thesis werd de aanwezigheid van anoxische microzones, denitrificatie en sulfaatreductie in aparte vlokken onderzocht met microsensoren. Deze gegevens werden vergeleken met denitrificatie en sulfaatreductie metingen m.b.v. incubatie experimenten. Tenslotte werd ook de 3-dimensionale vlokstructuur en populatie opbouw van sulfaat reducerende bacteriën in actief slib geanalyseerd.

SAMMENFATNING

Biofilm er komplekse samfund af immobiliserede mikroorganismer, hvori diverse processer foregår i tæt rumligt og funktionelt kobling. Ved spildevandsrensning udnyttes sådanne processer til blandt andet fjernelse af nitrogen. Af nitrificerende organismer bliver ammonium oxideret til nitrat og dette bliver af denitrificerende bakterier reduceret til gasformigt dinitrogen. I denne Ph.D. afhandling er aktiviteten, den rummelige fordeling samt typen af nitrificerende bakterier undersøgt med en kombination af mikrosensorer og "fluoroscence in situ hybridization" (FISH).

Et indledende studie udført med nitrat/nitrit biosensor viste at nitrifikations processen var begrænset til en tynd men meget aktiv zone ved overfladen af en biofilm fra et overrislingsrensningsanlæg. Dette korrelerede med tilstedeværelsen af tætte klynger af ammoniumoxiderende Nitrosomonas sp. sammen med nitritoxiderende Nitrobacter sp. i det samme lag.

Udviklingen af en ionselektiv mikrosensor til bestemmelse af nitrit samt forbedring af sensorer til ammonium og nitrat bestemmelse muliggjorde den efterfølgende detaljerede analyse af produkter og substrater for nitrification og de respektive populationer af nitrificerende bakterier i biofilmene.

Ved hjælp af rRNA teknikker kunne foreløbig ikke kultiverede slægtninge til Nitrospira moscoviensis identificeres i nitrifierende aggregater og samtidig kunne disse med mikrosensorer påvises at oxidere nitrit. Sammen med ammonium oxiderende Nitrosospira sp. dominerede de ikke kultiverede Nitrospira sp. i den nitrificerende skal omkring aggregater fra en fluid-bed reaktor. Hyppigheden og volumen specifik aktivitet af ammonium og nitrit oxiderere blev kvantificeret langs den faldende ammonium koncentrationsgradient i reaktorkolonnen. Fra disse data var det muligt at udregne *in situ* reaktionshastigheden per celle samt at estimere substrat affiniteten for de ikke kultiverede nitrificerene bakterier for ammonium og nitrit. Fra sammenligning med tidligere publicerede data opstilledes følgende hypotese: I omgivelser med høje substrat koncentrationer dominerer Nitrosomonas sp. og Nitrobacter sp. på grund af deres højere specifikke reaktions hastigheder. I omgivelser med lave substrat koncentrationer kan Nitrosospira sp. og Nitrosomonas sp. bedre konkurrere på grund af deres højere substrat affinitet. Denne konklusion blev støttet af den observerede hyppighed og fordeling af Nitrosomonas/Nitrosospira samt Nitrobacter/Nitrospira i en biofilm under høje ammonium koncentrationer og stærke gradienter af ilt og nitrit.

Aggregater fra aktiveret slam ligner på mange måder biofilm og tilstedeværelse af anoxiske centre i aggregaterne er tidligere blevet foreslået. Derfor blev anoxiske mikronicher, denitrification og sulfatreduktion i enkelte aggregater undersøgt med mikrosensorer i den sidste del af Ph.D. studiet. Disse resultater blev støttet med inkubations eksperimenter med henblik på at belyse denitrifications og sulfat reduktions hastigheder i slamprøver. Yderligere blev den tredimensionale struktur af aggregaterne samt strukturen af det bakterielle samfund af sulfat reducerende bakterier i aktiveret slam undersøgt.

ZAMMAGFASST

A Biofilm is a recht a komplexe Gschicht aus Bakteria und andera kloina Viechln, auf boarisch a Schlaaz, der wo auf irgendoana Oberflächn drobsitzt. Hernemma kamma des z.B. für d'Abwasser-Reinigung zur Schtickschtoffentfernung. As Ammonium werd dann von nitrifizierende Bakterien zu Nitrat oxidiert, und des kann nachad von denitrifizierende Bakterien zum Stickstoff umgsetzt wern, der as System verlasst. In meiner Dokterarbad hab i d'Aktivität, d'Identität und d'räumliche Verteilung von soichane Nitrifikanten in Biofilmen mitra Kombination aus Mikrosensoren und Fluoreszenz-*in situ*-Hybridisierung (FISH) ogschaut.

In am erschten Schritt isch mitram Nitrat/Nitrit-Biosensor die Nitrifikationsschicht als a dünne, mordsaktive Schicht glei an der Oberflächen von am Tropfkörper-Biofilm beschtimmt worra. Grad a do ham mir mit FISH dicke Klumpen von Ammonium-Oxidierern von der Gattung *Nitrosomonas* und Nitrit-Oxidierer von der Gattung *Nitrobacter* glei nebenanander gfund'n.

Als nexschtes isch a ionenselektiver Nitrit-Mikrosensor entwickelt worra, und dia Sensora für Ammonium und Nitrat hamma vabessert. Dadurch hamma im Anschluß Subschtrat- und Produkt-Konzentrationa von da Nitrifikation in Biofilmen genauer messen kenna.

In nitrifizierende Aggregate hab i mitram rRNA-Ansatz neie Bakterien vom Typ *Nitrospira* gfunden, und hab mit die Mikrosensora zoigt, daß dia im Biofilm Nitrit oxidiera. Mit die ammonium-oxidierende *Nitrosospira* sp. mitanand warn dia die gröschte Population in da nitrifizierenda Schicht in dene Aggregate. I hab dene ihra Zahl üba da ganza Reaktor quantifiziert, *in situ* Aktivitäta pro Zelle ausgrechnet und eahna Subschtrat-Affinität für Ammonium odr Nitrit abgschätzt. Wamma des mit da Literatur vagleicht, na schaugts so aus, daß da *Nitrosomonas europaea* und da *Nitrobacter* sp. die mehreren sei miassten, wanns vui zum Fressen gibt, indem dass se nämlich die höheren Reaktionsraten zammabringan. Wanns aber niedrige Subschtrat-Konzentrationa hat, nachern soittan da *Nitrosospira* sp. und da *Nitrospira* sp. die andre überlegn sei, wei se as Subschtrat vui besser binden kenna. Dia Vermutung isch schpätr inram andara Biofilm no gschtützt worra.

A Belebtschlammflockn isch im Prinzip ganz ähnlich wiara Biofilm. Drum hot ma se scho manchmol denkt, daß in soichene Flocken in da Mittn da Sauerstoff scho vabraucht isch. Im letschten Deil von meiner Arbad hab i nacherd probiert, soiche anoxische Stelln in Flockn mit Mikrosensorn zum findn, und hab gschaut, ob da vielleicht Denitrifikation oder Sulfatreduktion schtattfind. Außerdem hab i die dreidimensionale Flockenstruktur untersucht, und gschaut, wieviele und welche Sulfatreduzierer in die untersuachten Belebtschlämmer dringwesen sind.

List of Publications

A) Contributions to the Manuscripts Presented in this Dissertation

1) **Schramm, A., and R. Amann.** 1998. *In situ* structure and function analysis of biofilms. p. 45-54 *in:* Technik anaerober Prozesse, (Eds.) H. Märkl, R. Stegmann, DECHEMA-Fachgespräche Umweltschutz, DECHEMA e.V., Frankfurt am Main, Germany

   literature review and writing by A.S., editorial help by R.A.

2) **Schramm, A., L.H. Larsen, N.P. Revsbech, N.B. Ramsing, R. Amann, and K.-H. Schleifer.** 1996. Structure and function of a nitrifying biofilm as determined by in situ hybridization and the use of microelectrodes. Appl. Environ. Microbiol. **62**: 4641-4647

   outline of the project by R. A. and K.-H.S., concept by A.S.,L.H.L. and N.B.R., microelectrode construction and measurements by L.H.L., N.P.R. and A.S., in situ hybridization by A.S., writing by A.S. with help of the co-authors

3) **De Beer, D., A. Schramm, C.M. Santegoeds, and M. Kühl.** 1997. A nitrite microsensor for profiling environmental biofilms. Appl. Environ. Microbiol. **63**: 973-977

   concept and sensor development by D.d.B., construction, testing and application of sensors by A.S. writing by D.d.B. with help of the co-authors

4) **Schramm, A., D. de Beer, M. Wagner, and R. Amann.** 1998. Identification and activity in situ of *Nitrosospira* and *Nitrospira* spp. as dominant populations in a nitrifying fluidized bed reactor. Appl. Environ. Microbiol. **64**: 3480-3485

   concept and experimental by A.S., help with measurements and CLSM by D.d.B. and M.W., respectively, writing by A.S. with editorial help of the co-authors

5) **Schramm, A., D. de Beer, J.C. van den Heuvel, S. Ottengraf and R. Amann.** 1999. Microscale distribution of populations and activities of *Nitrosospira* and *Nitrospira* spp. along a macroscale gradient in a nitrifying bioreactor: quantification by in situ hybridization and the use of microsensors. Appl. Environ. Microbiol. **65**: 3690-3696

   concept, experimental and writing by A.S., editorial help by the co-authors

6) **Schramm, A., D. de Beer, A. Gieseke, and R. Amann.** Microenvironments and distribution of nitrifying bacteria in a membrane-bound biofilm.

   concept, experimental and writing by A.S., editorial help by the co-authors

7) **Schramm, A., C. M. Santegoeds, H. K. Nielsen, H. Ploug, M. Wagner, M. Pribyl, J. Wanner, R. Amann, and D. de Beer.** An interdisciplinary approach to the existence of anoxic microniches, denitrification, and sulfate reduction in aerated activated sludge. Appl. Environ. Microbiol. **65** (9)

   concept by D.d.B., microsensor work by A.S. and C.M.S., calculations by A.S. and H.P., incubation experiments by H.K.N. and D.d.B., CLSM by A.S. and M.W., SRB screening by A.S. and C.M.S., writing by A.S. with help of the co-authors

101

B) Further Publications

Schramm, A. and R. Amann. 1999. Nucleic acid based techniques for analyzing the diversity, structure, and dynamics of microbial communities in wastewater treatment. *In*: Environmental Processes - Wastewater and Waste Treatment. Vol. 11a of the Series: Biotechnology, 2nd Edition, (Eds.) H.-J. Rehm, G. Reed, A. Pühler, P. Stadler. Wiley-VCH, Weinheim.

De Beer, D. and A. Schramm. 1999. Microenvironments and mass transfer phenomena in biofilms studied with microsensors. Wat.Sci.Technol.**39** (7): 173-178

Rabus, R., H. Wilkes, A. Schramm, G. Harms, A. Behrends, R. Amann, and F. Widdel. 1999. Anaerobic utilization of alkylbenzenes and *n*-alkanes from crude oil in an enrichment culture of denitrifying bacteria affiliated with the *Azoarcus/Thauera* cluster. Environ. Microbiol.**1** (2): 145-157

Santegoeds, C.M., A. Schramm, and D. de Beer. 1998. Microsensors as a tool to determine chemical microgradients and bacterial activity in wastewater biofilms and flocs. Biodegradation **9**: 159-167

Schramm, A., D. De Beer, H. van den Heuvel, S. Ottengraf and R. Amann. 1998. *In situ* structure/function studies in wastewater treatment systems. Wat.Sci.Technol. **37** (4-5): 413-416

De Beer, D., A. Schramm, C.M. Santegoeds, and H.K. Nielsen. 1998. Anaerobic processes in activated sludge. Wat.Sci.Technol. **37** (4-5): 605-608

Schramm, A., L.H.Larsen, N.P. Revsbech, and R.I. Amann. 1997. Structure and function of a nitrifying biofilm as determined by microelectrodes and fluorescent oligonucleotide probes. Wat.Sci.Technol. **36** (1): 263-270

C) Manuscripts in Preparation

Von Keitz, V., A. Schramm, K. Altendorf, and A. Lipski. Characterization of microbial communities of biofilters by phospholipid fatty acid analysis and rRNA targeted oligonucleotide probes. submitted to Syst.Appl.Microbiol.

Böttcher, M.E., B. Hespenheide, C. Beardsley, E. Llobet-Brossa, A. Schramm, A. Wieland, G. Böttcher, R. Amann, U.-G. Berninger, and O. Larsen. Biogeochemistry, stable isotope geochemistry, and microbial community structure of a temperate intertidal mudflat: an integrated study. in preparation for Cont. Shelf Research

Gieseke, A., P. Arnz, A. Schramm, R. Amann, and P. Wilderer. Nutrient removal with a sequencing batch biofilm reactor: process parameters and microscale investigations. in preparation for Wat.Sci.Technol.

Oerther, D.B., J. Pernthaler, A. Schramm, R. Amann, and L. Raskin. Monitoring precursor 16S rRNA of *Acinetobacter* sp. in activated sludge wastewater treatment systems. in preparation for Appl.Environ.Microbiol.

Lebenslauf

14.7. 1970	geboren in Augsburg
1976 - 1980	Grundschule Stadtbergen
1980 - 1989	Humanistisches Gymnasium bei St.Stephan in Augsburg, Abitur 1989
1989/90	Zivildienst im Pflegedienst der Urologischen Klinik, Augsburg
1990 -1995	Studium der Biologie (Diplom) an der Technischen Universität München
November 1992	Vordiplom
März/April 1995	Diplomprüfungen in Botanik, Mikrobiologie, Ökologie und Biochemie
Juni-Dezember 1995	Diplomarbeit am Department of Microbial Ecology, University of Aarhus, Dänemark, sowie am Lehrstuhl für Mikrobiologie der TU München.
1.1.-31.12. 1996	wissenschaftlicher Angestellter am Lehrstuhl für Mikrobiologie, TU München
5.6. 1996	Heirat der Krankenschwester Doris Elisabeth Hafner
1997-1999	wissenschaftlicher Angestellter am Max-Planck-Institut für Marine Mikrobiologie, Bremen.
10.10. 1997	Geburt der Tochter Anne Magdalena

Sonstige Tätigkeiten:

April/August 1992	Mitarbeit bei der Ökosystemforschung im Sylter Wattenmeer (SWAP) als wissenschaftliche Hilfskraft für das Fraunhofer-Institut für atmosphärische Umweltforschung, Garmisch-Partenkirchen
1.3. - 14.9. 1993	Ausbildung zum Forschungstaucher
Sommer 1994	Mitarbeit an Makrophytenkartierungen zur Gewässergütebestimmung verschiedener Seen in Deutschland und Österreich und erneut am SWAP
Oktober 1994	Studentische Hilfskraft bei Michael Wagner und Rudolf Amann, Lehrstuhl für Mikrobiologie, TU München: *In situ* Hybridisierung und Inhibierung von ammonium-oxidierenden Bakterien
Juli 1998	Mitarbeit an der Makrophytenkartierung des Chiemsees